Investigating the Transport and Fate of Nitrogen from Farms to River in the Lower Rangitikei Catchment

A thesis presented in partial fulfilment of the requirements for the degree of

Master of Science

in

Earth Science

at Massey University, Manawatu, New Zealand

MASSEY
UNIVERSITY

Stephen Brian Collins

2015

Abstract

A sound understanding of the transport and fate of leached nitrate-nitrogen (NO_3^--N) in shallow groundwater is key to understanding the impacts of land use intensification on the quality of groundwater and surface water bodies. However, these are not well understood in the Lower Rangitikei catchment. This study was undertaken to assess the groundwater flow pattern and its interactions with the Rangitikei River; the redox conditions of the groundwater; and the extent of NO_3^--N attenuation in shallow groundwater in the Lower Rangitikei catchment.

Groundwater depths were collected from more than 100 wells to map the piezometric surface to inform the groundwater flow pattern within the study area. Groundwater interactions with the Rangitikei River were estimated qualitatively from two longitudinal river flow and water quality surveys (on 6th and 20th January 2015) under low-flow conditions. Fifteen wells were sampled and analysed in the study area during December 2014 to characterise the groundwater redox condition. A total of nine piezometers were installed at a range of depths (3 m and 6 m) on two dairy farms (sand country and river terrace) and one cropping farm (sand country). In these piezometers, NO_3^--N, dissolved oxygen (DO) and other parameters were monitored over March, April and May 2015. Single-well push-pull tests were used to measure NO_3^--N attenuation in shallow groundwater during May 2015.

Groundwater flow was largely influenced by the regional topography, particularly shallow groundwater (<30 m), where it flows from elevated areas such as Marton in a southerly direction towards the Rangitikei River. The longitudinal river flow and water quality surveys revealed a dynamic relationship between the river and the underlying aquifer. The surveys suggested groundwater discharges into the river both upstream and downstream of Bulls. The groundwater redox characterisation showed generally anoxic/reduced groundwater across the lower Rangitikei catchment area. Groundwater typically has a low DO concentration (<1 mg/L) with elevated levels of available electron donors, particularly dissolved organic carbon and Fe^{2+}. These groundwater characteristics provide for generally favourable conditions for NO_3^--N reduction. Monitoring at the installed piezometers

showed a generally low NO_3^--N concentration at these sites. The push-pull tests revealed NO_3^--N reduction occurring at all three sites, with the rate of reduction varying between 0.04 mg N L^{-1} hr^{-1} to 1.57 mg N L^{-1} hr^{-1}.

These results suggest that groundwater is likely to be connected with the Lower Rangitikei River. However, NO_3^--N concentrations in the river and groundwater were generally low, especially for the river at low flows. This suggests NO_3^--N may be undergoing reduction within shallow groundwater before it has a chance to seep into the river. Further evidence for appreciable levels of NO_3^--N reduction in the shallow groundwater is provided by the redox characterisation of reduced groundwater and the push-pull tests. However, more spatial and temporal surveys and *in-situ* measurements of denitrification occurrence in the shallow groundwater of the study area are required.

Acknowledgements

I would like to acknowledge the help and efforts of many people who have made this research possible.

First of all, I would like to thank my supervisors Dr Ranvir Singh and Dr Alan Palmer for not only providing me with this research topic, but also for their guidance and intellectual input.

I would also like to thank Horizons Regional Council, and in particular Ms Abby Matthews and Dr Jon Roygard, whose generous support with field surveys and related expenses, and resource consent applications, has made this work so much easier.

Thanks also go to the many land owners who have allowed me access to their properties and those who allowed me to install piezometers on their properties. Also to Denis Hocking who made himself available to show me the local sand country geomorphology.

To my colleague Aldrin Rivas who helped me with so many of the finer details of this study, as well as the many lab hours that he contributed to. I will also thank other Massey students and staff including David Feek, Ahmed Elwan and Andrew Neverman for their assistance in the field.

I would also like to thank Massey University for the generous Masterate Scholarship provided to me, as well as the Helen E Akers, Hurley Fraser and DG Bowler Postgraduate Scholarships that were awarded to me.

Finally, I would like to thank my family, friends and office colleagues who not only encouraged me, but who made this experience so enjoyable.

Contents

Abstract i
Acknowledgements iii
List of Figures vi
List of Tables viii
1 Introduction 1
1.1 Background 1
1.2 Study Objectives 2
1.3 Thesis Outline 2
2 Literature Review 4
2.1 Groundwater – Surface Water Interactions 4
2.2 Sources and Consequences of Nitrate in Groundwater 9
2.3 Nitrate Attenuation via Denitrification in Groundwater 14
2.4 Previous Studies on the Transport and Transformation of Nitrate in New Zealand Agricultural Catchments 18
2.5 Conclusions 20
3 The Study Area – Lower Rangitikei Catchment 21
3.1 Climate and Land Use 21
3.2 Soils 23
3.3 Geology 27
3.3.1 Wanganui Basin Development 27
3.3.2 Main Geological Units 30
3.4 Well Log Interpretation 35
3.5 Conclusions 43
4 Groundwater Flow and its Interactions with Surface Water 45
4.1 Introduction and Objectives 45
4.2 Methods and Materials 45
4.2.1 Groundwater Level Survey 45
4.2.2 Groundwater – Surface Water Interactions 48
4.3 Results and Discussion 52
4.3.1 Groundwater Flow Direction 52

4.3.2 Groundwater – Surface Water Interactions 56
4.3.3 River Water Quality 59
4.4 Conclusions 62
5 Groundwater Chemistry and Redox Conditions 63
5.1 Introduction and Objectives 63
5.2 Methods and Materials 63
5.3 Results and Discussion 65
5.3.1 Groundwater Chemistry 65
5.3.2 Hydrochemical Facies and Groundwater Classification 76
5.3.3 Groundwater Redox Conditions 80
5.4 Conclusions 85
6 Measuring Shallow Groundwater Denitrification 86
6.1 Introduction and Objectives 86
6.2 Methods and Materials 86
6.2.1 Site Selection and Piezometer Installation 86
6.2.2 Shallow Groundwater Monitoring 90
6.2.3 Push-Pull Tests 90
6.2.4 Analytical Methods 92
6.3 Results and Discussion 93
6.3.1 Shallow Groundwater Chemistry and Redox Conditions 93
6.3.2 Shallow Groundwater Denitrification 97
6.4 Conclusions 104
7 Summary and Conclusions 106
References 113
Appendix: Well Log Descriptions 122

List of Figures

Figure 1: The study area shaded green is the coastal Groundwater Management Zone of the Rangitikei River, approximately 850 km^2. 3
Figure 2: Components of total catchment runoff contributing to streamflow. In (a) the directions of overland flow, interflow and baseflow are shown; and (b) the river hydrograph from a rainfall event (Hiscock & Bense, 2005). 5
Figure 3: Stream-aquifer interactions: (a) gaining stream; (b) losing stream; (c) losing stream; (d) flow-through stream (Hantush et al., 2011). 6
Figure 4: Low flow survey of the Rangitikei River on 25 March 2003 (Roygard & Carlyon, 2004). 7
Figure 5: Gaining stream (A) where groundwater seeps to surface water and a losing stream (B) where surface water leaks to groundwater. Where contour lines point in the upstream direction (C) the river is gaining, and where contour lines point downstream it is losing (Winter et al., 1998). 8
Figure 6: Schematic diagram of the entire N-cycle including N-fixation, ammonification, nitrification, and denitrification (van der Perk, 2012). 10
Figure 7: Thermodynamic sequence of electron acceptors for oxidation of organic carbon in the saturated zone (Rivett et al., 2008). 15
Figure 8: Average air temperatures 1971-2000 recorded at Ohakea Aerodrome (NIWA, 2015). 22
Figure 9: Average monthly potential evapotranspiration for 1954-1990, and average monthly rainfall 1981-2010 recorded at Ohakea Aerodrome (NIWA, 2015). 23
Figure 10: Soils of the Coastal Rangitikei as characterised by Cowie et al. (1967). Joint names are soil associations where soils exist in a topographically repeating and predictable pattern (McLaren & Cameron, 1994). 24
Figure 11: Relation of soil series to topography of the river flats (Cowie et al., 1967). 26
Figure 12: Locality map and geological setting of the Wanganui Basin (Carter et al., 1999). 28
Figure 13: Fold axes of the Manawatu anticlines overlaid on an Enhanced Thematic Mapper satellite image of the Wanganui Basin (Jackson, et al., 1998). 30
Figure 14: Simplified geological map showing the Q2 (Ohakean) and Q1 (Holocene) deposits with regional fault lines shown with their sense of direction. Well logs shown in blue are used to create subsequent cross sections while red ones were previously used for carbon dating (Figure 19). The nickpoint is the estimated former extent of Ohakean deposits which were subsequently eroded or covered by later deposits. 36
Figure 15: Cross Section A-B Santoft to Bulls with interpreted locations of various gravel units and fault lines. Orange units are reworked gravels; green units are Ohakean or later gravels. F = fault; U = up; D = down. Well legends can be seen in the Appendix. 37
Figure 16: Cross Section C-B Scott's Ferry to Bulls with interpreted locations of various gravel units and fault lines. Orange units are reworked gravels; green units are Ohakean or later gravels. F = fault; U = up; D = down. Well legends can be seen in the Appendix. 38

Figure 17: Cross Section A-C Santoft to Scott's Ferry with interpreted locations of various gravel units and fault lines. Orange units are reworked gravels; green units are Ohakean or later gravels. F = fault; U = up; D = down. Well legends can be seen in the Appendix. 39
Figure 18: Ohakean gravels outcropping near 322041. A centre pivot irrigator can be seen in the background. 41
Figure 19: Cross section through the Holocene marine wedge south of Tangimoana (Clement, 2011 after Shepherd et al., 1986). Shells from T1 – T5 were used for radiocarbon dating and their locations are shown in Figure 14. 44
Figure 20: Location and depth of wells used in piezometric survey. 47
Figure 21: Sites used for longitudinal river flow and water quality survey, 6 January 2015. 50
Figure 22: Sites used for longitudinal river flow and water quality survey, 20 January 2015. 51
Figure 23: Shallow groundwater flow from wells screened less than 30 m deep. Contours are masl. 53
Figure 24: Deep groundwater flow from wells screened greater than 30 m deep. Contours are masl. 54
Figure 25: Total oxidised nitrogen (mg/L) at the Onepuhi site. 60
Figure 26: Total oxidised nitrogen (mg/L) at the Bulls Bridge site. 61
Figure 27: Total oxidised nitrogen (mg/L) at the McKelvies site. 61
Figure 28: Location of groundwater sampling sites in the Lower Rangitikei catchment area, December 2014. 64
Figure 29: Distribution of major cations in groundwater in the Lower Rangitikei catchment, December 2014. 70
Figure 30: Distribution of major anions in groundwater in the Lower Rangitikei catchment, December 2014. 71
Figure 31: Distribution of NO_3^--N in groundwater in the Lower Rangitikei catchment, December 2014. 75
Figure 32: Piper diagram with results of the December 2014 groundwater survey. Colours are only for differentiation. 76
Figure 33: Piper diagram of major cation and anion data. Blue area indicates Group 1 water type and brown area indicates Group 2 water type (PDP, 2013). 78
Figure 34: Concentration of selected chemical constituents relative to well depth of groundwater in the Lower Rangitikei catchment, December 2014. 79
Figure 35: Iron pan about 30 cm from the surface, though the depth can vary. The pan shows evidence of ferrous iron being oxidised at the oxic/anoxic interface. 84
Figure 36: Sanson Site. 89
Figure 37: Bulls Site. 89
Figure 38: Santoft Site. 90
Figure 39: Shallow groundwater monitoring results over early 2015 for NO_3^--N, NH_4^+-N and dissolved oxygen at piezometers installed at Sanson, Bulls and Santoft. 95
Figure 40: Shallow groundwater monitoring results over early 2015 for redox potential, pH, electrical conductivity and groundwater level at piezometers installed at Sanson, Bulls and Santoft. 96
Figure 41: Results of push-pull tests showing Bromide and Nitrate-N concentrations, the dilution corrected Nitrate-N concentration and the Nitrate-N/Bromide ratio. The denitrification rate is shown in red. 100
Figure 42: Accumulation of N_2O-N during the push-pull test. 101

List of Tables

Table 1: Changes in farm livestock numbers in New Zealand between 1990 and 2007 (Quinn et al., 2009). 9
Table 2: Main subunits of the Middle and Late Pleistocene in stratigraphic order, youngest to oldest (Begg et al., 2005). 33
Table 3: Longitudinal river flow and water quality survey results for 6 January 2015. 56
Table 4: Longitudinal river flow and water quality survey results for 20 January 2015. 56
Table 5: Ion concentrations in mg/L of wells sampled in the Lower Rangitikei catchment, December 2014. 66
Table 6: Ion concentrations in meq/L with CBE results of wells sampled in the Lower Rangitikei catchment, December 2014. 67
Table 7: Water classification based on Total Dissolved Solids (Younger, 2007). 72
Table 8: Actual and estimated TDS of wells sampled in the Lower Rangitikei catchment, December 2014. 72
Table 9: Concentration of minor ions collected from groundwater in the Lower Rangitikei catchment, December 2014. 74
Table 10: Threshold concentrations for identifying redox processes in aquifer systems (McMahon & Chapelle, 2008). 81
Table 11: Redox assignment of 15 groundwater wells surveyed in December 2014 in the Lower Rangitikei catchment. 82
Table 12: Details of the piezometers installed at sites around the study area. 88
Table 13: Test solution and background concentrations for Sanson-A (3 m) 97
Table 14: Test solution and background concentrations for Sanson-B (6 m) 97
Table 15: Test solution and background concentrations for Bulls-A (3 m) 97
Table 16: Test solution and background concentrations for Bulls-B (6 m) 98
Table 17: Test solution and background concentrations for Santoft-A (3 m) 98

1 Introduction

1.1 Background

In recent decades New Zealand has undergone a period of agricultural intensification with dairy being a major contributor (MacLeod & Moller, 2006). Suitable land is being converted into dairy farms, often at the expense of sheep and beef, and a higher stocking ratio is being used compared with previous land uses (Quinn et al., 2009). A greater demand for water has also occurred for irrigation, feeding stock and cleaning dairy sheds after milking. Although many of these changes and demands can be managed, the presence of agricultural chemicals has proven to be one of the more difficult consequences to manage (Harter et al., 2014). As dairy intensification has increased, so have the flux of agricultural chemicals in the pastoral environment.

Nitrogen is a major nutrient in the farming system, which, in New Zealand, has been traditionally supplied through the root nodules of nitrogen-fixing clover (Parfitt et al., 2006). Nitrate-nitrogen (NO_3^--N) is the most plant-available form of nitrogen and the one that is readily taken up by plants. Its high solubility also means it is readily leached from the soil if it is not taken up by plants. Though nitrogen-based fertilisers have increased in use over this period of dairy intensification, the main source of NO_3^--N leaching in New Zealand is from cow urine patches (Di & Cameron, 2002). Cow urine is primarily in the form of ammonium (NH_4^+), but is easily converted to NO_3^--N by soil bacteria. The high concentration of NO_3^--N in the urine patch means it cannot all be taken up by the grass and is instead leached to groundwater. Rainfall or irrigation will increase the rate at which NO_3^--N is leached downward through the soil profile (Silva et al., 1999).

Once the NO_3^--N is leached to groundwater it is transported with the movement of groundwater flow where it may eventually interact with streams, rivers and lakes (Harter et al., 2014). Depending on the type of interaction, rivers can increase their NO_3^--N load from the groundwater contribution of their total flow. This can have a harmful effect on the water quality and cause eutrophication, especially at times of low flow (Smith et al., 1999).

Though NO_3^--N is transported with groundwater, it can also be attenuated through a natural process known as denitrification (Korom, 1992). Microbes in the subsurface can reduce NO_3^--N to N_2 (molecular nitrogen) if suitable conditions exist in the groundwater. This reaction can remove NO_3^--N from groundwater before it reaches surface water bodies, and improve the quality of groundwater. This thesis investigates the transport and fate of NO_3^--N from farms to river in the Lower Rangitikei catchment (Figure 1).

1.2 Study Objectives

The main objectives of this study are to understand the groundwater flow pattern, including its interactions with streams and rivers, and determine the extent to which NO_3^--N is attenuated in shallow groundwaters in the Lower Rangitikei catchment. Specifically, the objectives of this research are to:

- Model and characterise the hydrogeology of the coastal Rangitikei groundwater management zone;
- Survey and map groundwater flow direction and its interactions with the Rangitikei River; and
- Assess the transport and transformation 'denitrification' potential in shallow groundwaters.

1.3 Thesis Outline

A total of seven chapters constitute this thesis. Chapter 1 gives a brief background and introduction to the study aims and specific objectives. Chapter 2 reviews the literature relevant to NO_3^--N in groundwater, denitrification in the subsurface and previous studies on the transport and fate of NO_3^--N in the New Zealand context. Chapter 3 collates the existing information of climate, soils, and geology to model and characterise the hydrogeology of the study area. Chapter 4 presents the results of a groundwater level survey and longitudinal river flow gauging to map groundwater flow patterns and potential groundwater – surface water interactions. Chapter 5 presents the results of a groundwater quality survey, explains the local hydrochemistry, the redox condition of the groundwater and the potential for denitrification in the subsurface environment. Chapter 6 presents the

results of a field study into the rate of denitrification in shallow groundwater, covering a range of land uses and soil types. Finally, Chapter 7 provides a synthesis of the results obtained and a discussion on the transport and fate of NO_3^--N in the Lower Rangitikei catchment, along with suggested potential areas of further investigation.

Figure 1: The study area shaded green is the coastal Groundwater Management Zone of the Rangitikei River, approximately 850 km^2.

2 Literature Review

The main aim of this study is to understand the transport pathways of groundwater and the fate of NO_3^--N as it moves from farms to river in the Lower Rangitikei River catchment. There are several components that need to be reviewed in order to give context to this study. This chapter, therefore, reviews and summarises the current knowledge about groundwater – surface water interactions; the sources and consequences of NO_3^--N in groundwater; NO_3^--N attenuation via denitrification in the subsurface environment; and previous studies on the transport and fate of NO_3^--N in New Zealand agricultural catchments. A critical review of various measurements and analysis methods and techniques is also presented to inform and develop the methodology employed in this study.

2.1 Groundwater – Surface Water Interactions

Surface water is known to have various interactions with underlying aquifers, the nature of which is dynamic across the length of a river and its catchment. The implication when considering water quality is that any contamination present in a single body of water is therefore a threat to the other. As precipitation falls in a catchment, the movement of that water is then considered to partition between overland flow, interflow and baseflow (Figure 2). Overland flow occurs where the rainfall intensity is higher than the infiltration capacity of the soil and it causes water to move across the surface. This can be due to high intensity rainfall or a heavy soil texture, such as clay. Interflow is the lateral movement of water in the soil zone in the general direction of topographic slope (Hiscock & Bense, 2005). Overland flow and interflow together represent the quickflow or surface runoff from a stream catchment. Baseflow is the component of total runoff contributed by groundwater discharge to surface water and supports flow during dry periods of little or no rain (Hiscock & Bense, 2005). The hydrograph in Figure 2 shows quickflow surging after a rainfall event with baseflow contributing more slowly but for a longer period of time after rainfall eases. Baseflow is likely to increase as the water table rises (Hiscock & Bense, 2005).

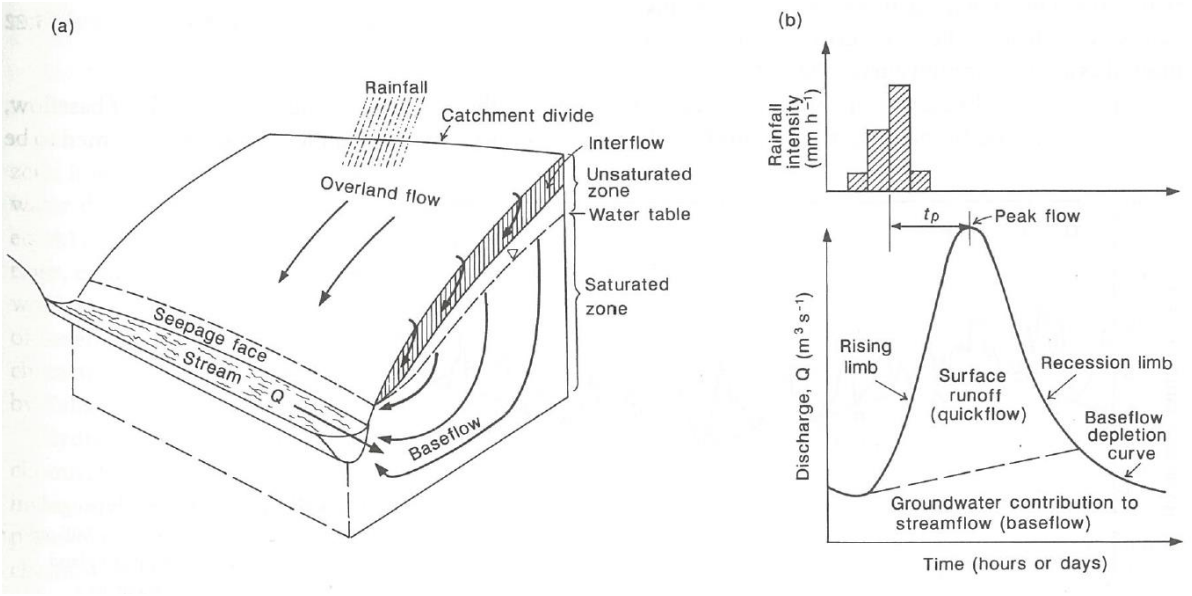

Figure 2: Components of total catchment runoff contributing to streamflow. In (a) the directions of overland flow, interflow and baseflow are shown; and (b) the river hydrograph from a rainfall event (Hiscock & Bense, 2005).

Baseflow implies interaction of groundwater with the surface water, where some proportion of the stream flow has arrived via groundwater. Often though, the nature of the water table can vary over space and time and the level of interaction that groundwater has with surface water can vary. Along a river, a range of scenarios is likely resulting in a river reach either gaining from groundwater or losing to groundwater. Streams with water levels lower than the water table receive water from the aquifer and are called gaining streams (Figure 3a). Alternatively, streams with water levels higher than the water table lose water to groundwater and are called losing streams (Figure 3b, c). Where a stream gains water from one side, but loses water from the other side, it is called a flow-through stream (Figure 3d) (Hantush et al. , 2011).

There are a number of methods and techniques available to determine groundwater-surface water interactions. A complete review of these methods is provided by Kalbus et al. (2006). It summarises the common methods under direct measurements of water flux; heat tracer methods; methods based on Darcy's Law; and mass balance approaches. This study will use a survey of groundwater levels and longitudinal river flow monitoring to estimate the degree of interactions between groundwater and surface water. It relies on a combination of flow gauging and chemical analysis from the river and nearby wells.

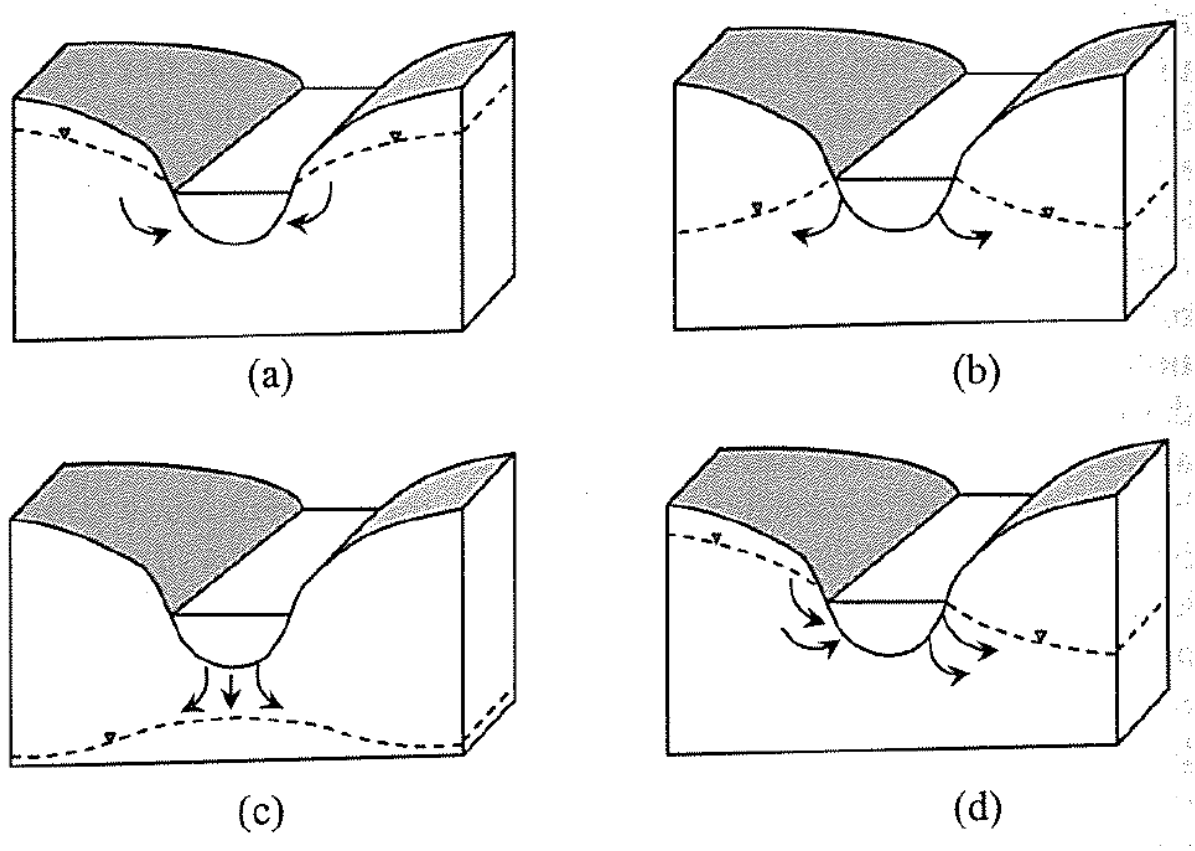

Figure 3: Stream-aquifer interactions: (a) gaining stream; (b) losing stream; (c) losing stream; (d) flow-through stream (Hantush et al., 2011).

Three previous stream gauging surveys have been carried out on the Rangitikei River since 1978 (Roygard & Carlyon, 2004). These cover much of the river's length, from headwaters to near the coast at the Bulls Bridge. They show the river has a dynamic relationship with the underlying aquifer, with various reaches showing a constant flow, gaining flow or losing flow (Figure 4). The main tributaries within the catchment, such as the Hautapu River, Moawhango River, Kawhatau River and Mangawhararikі River, merge with the Rangitikei River between Pukeokahu and Mangaweka. During low flows the Rangitikei River has very little inflow from the tributaries downstream of Mangaweka. This area of the catchment has shown reductions in flow by 9% during 1983 and 2% during 2003 between the Mangaweka and Vinegar Hill gauging sites. The same reach gained 1.4 m^3/s (about 10%) in 1978. The 2003 survey included more sites and showed a loss of about 4% between the Mangaweka and Otara sites. The losses are assumed to be groundwater recharge as there are no consented abstractions in this area. Some reaches of the river south of Vinegar Hill are considered constant flow and reflect low inflow from

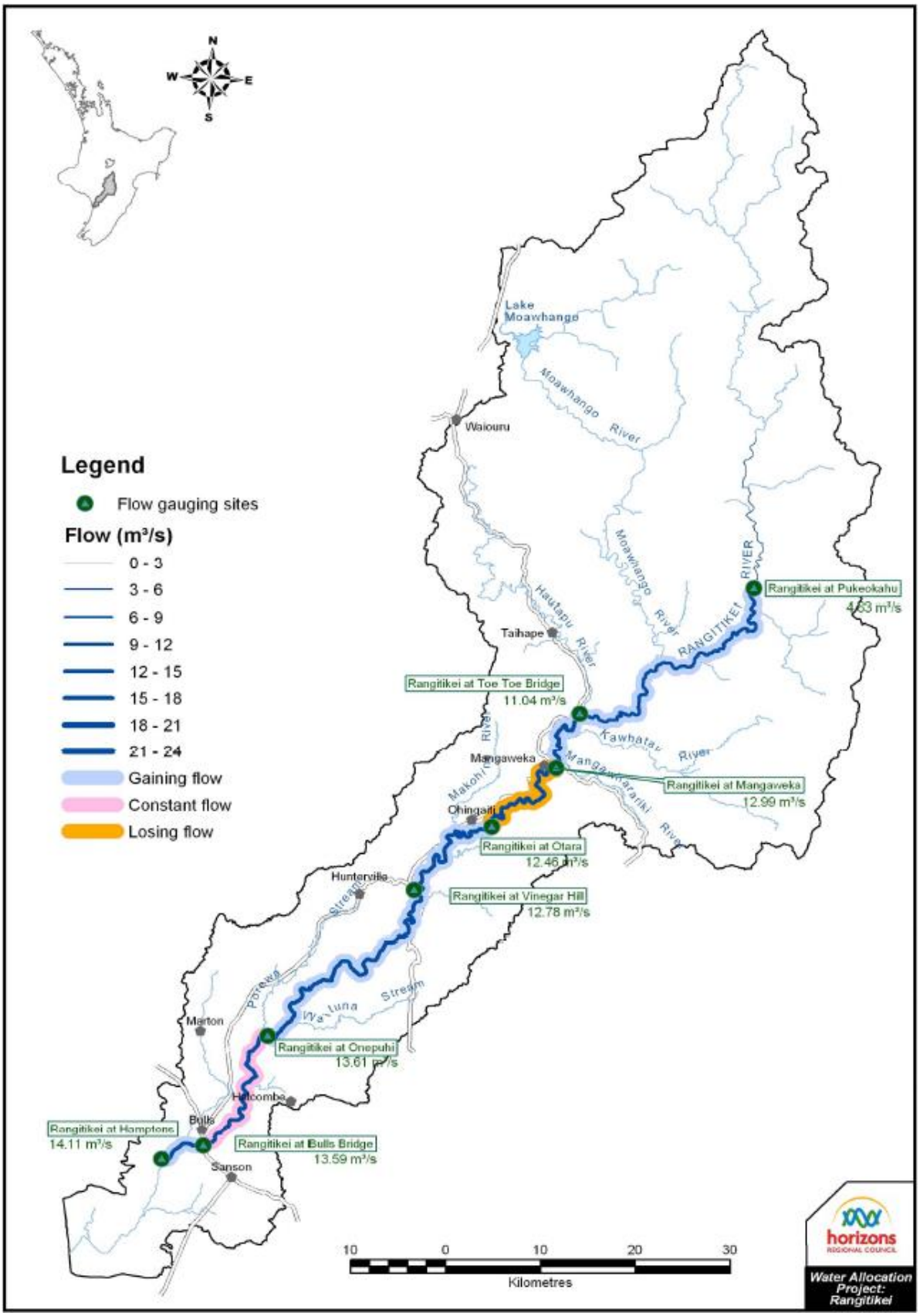

Figure 4: Low flow survey of the Rangitikei River on 25 March 2003 (Roygard & Carlyon, 2004)**.**

tributaries and the low level of abstraction here (Roygard & Carlyon, 2004). However, there is no information available about groundwater and river water interactions in the lower coastal reaches of the river. This study will consider part of the lower reaches of the river, from approximately Halcombe to the coast (Figure 4).

Groundwater – surface water interactions can also be observed where water table contours cross surface water paths (Winter et al., 1998). The shape of groundwater contours mapped in the vicinity of a stream can identify where groundwater flow is directed to the stream (gaining reach, Figure 5C); and also where groundwater flow is directed away from the stream (losing reach, Figure 5D). Alternatively, if groundwater contours plot perpendicular to the stream, then it suggests no interaction.

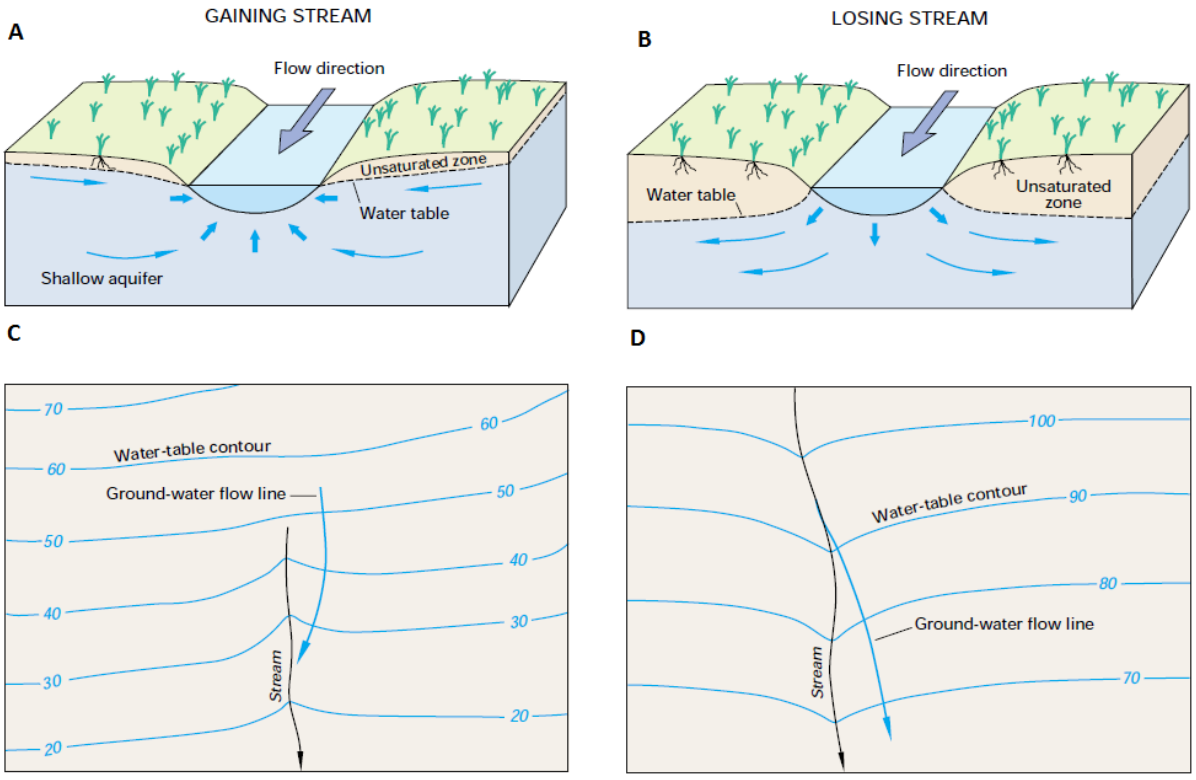

Figure 5: Gaining stream (A) where groundwater seeps to surface water and a losing stream (B) where surface water leaks to groundwater. Where contour lines point in the upstream direction (C) the river is gaining, and where contour lines point downstream it is losing (Winter et al., 1998).

2.2 Sources and Consequences of Nitrate in Groundwater

There is a general consensus that agricultural activities constitute the greatest source of NO_3^--N to groundwater (Harter et al., 2014). The main agricultural activities are nitrogen fertiliser use, cow urine patches, irrigated agriculture and effluent spreading. These activities have the potential to leach NO_3^--N over a large area and are therefore considered a diffuse source of contamination. In the New Zealand context, the increased use of some of these practices has occurred in tandem with a change in land use over the past two or three decades. New Zealand has a long history of sheep and beef farming, but as market demands have changed over time there has been a trend toward dairy farming and other land uses, usually at the expense of sheep and beef. From 1990-2007, the area occupied by sheep and beef farming contracted 2.2 M ha as lowlands were converted to dairying, arable cropping and horticulture, and steeper hill country areas were planted into forestry (Table 1). Over this time there had been a major expansion in the dairy industry, with 515,000 hectares of sheep and beef farms converted to dairy farming and a 17% increase in the stocking rate (Table 1) (Quinn et al., 2009). The more intensive nature of dairy farming has meant a greater potential for NO_3^--N leaching to groundwater (Verloop et al., 2006).

Table 1: Changes in farm livestock numbers in New Zealand between 1990 and 2007 (Quinn et al., 2009).

Dairy	**Number of Farms**	**Milking Cows/Farm**	**Effective Area/Farm (ha)**	**Cows/Ha**	**Total Area of Pasture in Dairying (ha)**
1990	13,357	160	67	2.4	894,919
2007	11,630	337	121	2.81	1,407,230
Sheep and Beef	**Number of Farms**	**Total Stock Units/Farm**	**Effective Area/Farm (ha)**	**Stock Units/Ha**	**Total Area of Pasture in Sheep and Beef farming (ha)**
1990	21,300	3,155	516	6.5	10,990,800
2007	13,600	4,268	645	6.2	8,772,000

While the atmosphere is made up of approximately 78% nitrogen (as N_2), it is not reactive toward oxidation or reduction because of its strong triple bond and therefore plants and animals are not able to metabolise this source (Howard & Rees, 1996). To make nitrogen biologically available, some groups of bacteria, together with various plant species, are able to assimilate atmospheric nitrogen in a process known as nitrogen fixation (Bouchard et al., 1992) (Figure 6). In agricultural areas, legumes are commonly included in crop rotations on poorly fertile soils to increase the amount of soil nitrogen and reduce the reliance on fertilisers (van der Perk, 2012). In New Zealand, nitrogen fixation by legumes is one of the

largest inputs of nitrogen, with white clover fixing between 29 and 75 kg N ha^{-1} yr^{-1} (Parfitt et al., 2006). Organic nitrogen is made available to the soil system by the decomposition and mineralisation of organic matter by heterotrophic bacteria and fungi. Organic nitrogen is first oxidised to amino acids and finally to NH_4^+ in the process known as ammonification (van der Perk, 2012) (Figure 6).

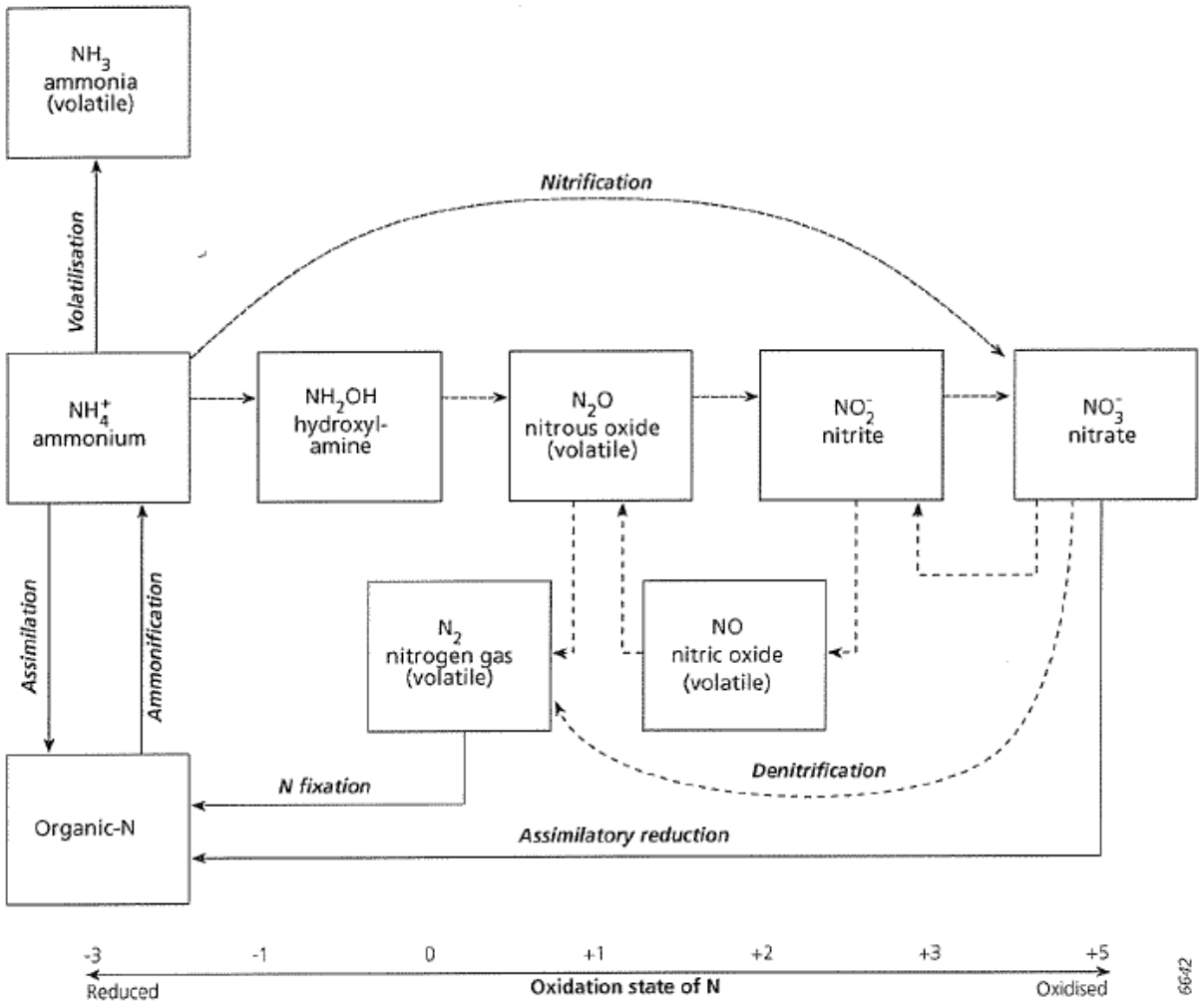

Figure 6: Schematic diagram of the entire N-cycle including N-fixation, ammonification, nitrification, and denitrification (van der Perk, 2012).

Next in the cycle is nitrification (Figure 6), where under aerobic conditions, autotrophic bacteria oxidise NH_4^+ (3- oxidation state) to NO_3^- (5+ oxidation state) in several steps. The overall nitrification process can be summarised as a two-step process (van der Perk, 2012):

$$2NH_4^+ + 3O_2 \rightarrow 2NO_2^- + 4H^+ + 2H_2O$$

$$2NO_2^- + O_2 \rightarrow 2NO_3^-$$

Industrial nitrogen fixation began in the early 20th century with the discovery of the reaction between nitrogen gas and hydrogen gas to produce ammonia. Ammonia is then synthesised to produce a range of fertilisers including urea ($CO(NH_2)_2$), ammonium nitrate (NH_4NO_3), and ammonium sulphate ($(NH_4)_2SO_4$). In the mid-20th century, nitrogen-based fertilisers started to be used on a much larger scale to increase agricultural output (Erisman et al., 2008). The recognition that nitrogen-based fertilisers have the potential to harm groundwater bodies from leaching has been known for several decades (Bourodim & Michna, 1972; Michna & Bourodim, 1973; Singh, 1976, 1979). Until the late 1980s, the primary source of nitrogen in agriculture was from biological nitrogen fixation, arising mainly from white clover in pasture grazed for 12 months of the year (Parfitt et al., 2006). Since then, nitrogen fertiliser use has changed rapidly, increasing from 50,000 t in 1989 to 342,000 t in 2003, with most of the increased use being applied to flat to rolling land (Parfitt et al., 2006). The average rate of application to pasture in New Zealand varies from 3 kg N ha^{-1} yr^{-1} to 34 kg N ha^{-1} yr^{-1} with the highest rates used for intensive dairying (Parfitt et al., 2006).

Though fertiliser use in New Zealand has increased in recent decades, the biggest source of NO_3^--N leaching is from cow urine patches (Di & Cameron, 2002). Only a small amount of nitrogen ingested by a grazing animal is actually removed from the pasture in animal products. A large proportion (between 60-90%) of the nitrogen ingested is returned to the soil in the form of urine and manure (Haynes & Williams, 1993; Jarvis et al., 1995). More than 70% of the nitrogen returned to the pasture is in the urine, and of this, between 70-90% of the urine is in the form of urea (Haynes & Williams, 1993). A cow may urinate 10-12 times per day, with each patch covering about 0.5-0.7 m^2 (Jarvis et al., 1995). The nitrogen-loading rate under a cow urine patch is equivalent to approximately 1000 kg N ha^{-1} (Di & Cameron, 2002). Some of this nitrogen gets lost through volatilisation, but most of it gets nitrified, resulting in the accumulation of NO_3^--N in the soil. Because of the high loading rate under the urine patch, and it being well above the biological needs of the plant, there is a high potential for the NO_3^--N to leach (Di & Cameron, 2002). The leaching potential is particularly high during the autumn-winter-spring period in New Zealand (May to September), when the soil is wet and excess water drains from the root zone (Di & Cameron, 2002).

Along with increased use of fertilisers in recent decades, irrigation has also provided the means by which agricultural production has been able to keep pace with population growth. The results shown in Table 1 have been made possible with an increase in irrigated agriculture, which has allowed for higher stocking rates. However, an inevitable consequence of this is an increase in nutrient leakages from the farm system (Quinn et al., 2009). Average nitrogen leaching losses are considerably greater for dairy farms (38 kg N/ha/yr), compared to sheep and beef farms (8 kg N/ha/yr) (Quinn et al., 2009). In the Canterbury region, irrigation has increased over the past 25 years, allowing more intensive cropping and pastoral farming. This has also coincided with increased concentrations of NO_3^--N in groundwaters, particularly in seaward areas where most of the irrigation has occurred (Wilcock et al., 2011). Studies have revealed groundwater in irrigated areas of Canterbury have high NO_3^--N concentrations (15-20 mg/L) because of intensive agriculture exacerbated by irrigation (Wilcock et al., 2011).

Another recent concern for groundwater quality in New Zealand is the application to land of dairy shed effluent (DSE). DSE is a mixture of faeces, urine and water washed into a pond from the dairy milking parlour at the end of a milking session. It is rich in nutrients (particularly nitrogen) and is applied back to land as a useful source of nutrients into the farm system. The concern is that excessive application of DSE may cause NO_3^--N leaching and groundwater contamination (Di et al., 1998a). Di et al. (1998a) assessed NO_3^--N leaching of DSE and NH_4^+ fertiliser applied to a free-draining pasture soil in Canterbury receiving spray (50 mm $month^{-1}$) or border-check irrigation (100 mm $month^{-1}$) in a lysimeter trial. The concentration of NO_3^- in the leachate reached 5 mg N l^{-1} under both flood and spray irrigation following the first fertiliser application, but did not increase above control values (<1 mg N l^{-1}) after the first DSE application. After the second DSE/fertiliser application, the NO_3^--N concentration in the leachate increased significantly during the winter/spring period. Under spray irrigation, the NO_3^--N concentration peaked at 40 and 17 mg N l^{-1} for the N fertiliser and DSE, respectively. Under flood irrigation, NO_3^--N reached 25 and 10 mg N l^{-1} for the N fertiliser and DSE, respectively. The lower NO_3^--N concentrations in the leachate were attributed to the greater loss of nitrogen by denitrification and the greater dilution of soil solution NO_3^--N by the larger volume of irrigation water applied, typical of a flood irrigation system. These results and others (Di et al., 1998a; Silva et al.,

1999) show DSE application to land can be a concern, especially when combined with fertiliser applications and irrigation.

The human health concern of excess NO_3^--N in drinking water primarily has to do with the occurrence of methemoglobinemia, which affects the oxygen-carrying capacity of blood, mostly in infants. To protect human health, national and world agencies have set standards for the maximum allowable NO_3^--N in drinking water. These are commonly reported as two limits: for the concentration of the NO_3^- ion, or as the nitrogen portion of the NO_3^--N ion. In New Zealand, the maximum acceptable value (MAV) is 50 mg/L NO_3^- or equivalent 11.3 mg/L NO_3^--N (Ministry of Health, 2005).

Besides the human health concerns of NO_3^--N, it can also lead to eutrophication of streams and lakes where groundwater contributes to surface waters. Like terrestrial plants, inorganic nitrogen and phosphorus are the two principal nutrients found to limit the growth of algae and vascular plants in freshwater and marine ecosystems (Smith et al., 1999). Ecosystems can be described using terms referring to their supplies of growth-limiting nutrients. Waters with a relatively large supply of nutrients are termed eutrophic (well-nourished), and eutrophication is the process by which water bodies are made more eutrophic through an increase in their nutrient supply (Smith et al., 1999). Groundwater can contribute to the eutrophication of surface waters where they have some degree of connection and the groundwater is nutrient rich. Once the excess nutrients reach surface water bodies, aquatic plants overcome their nutrient limitations and induce a sudden growth of plants and algae. The impacts of eutrophication can include noxious and toxic algal blooms, increased turbidity with a subsequent loss of submerged aquatic vegetation, oxygen deficiency, disruption of ecosystem functioning, loss of habitat, loss of biodiversity, shifts in food webs and loss of harvestable fisheries (Rabalais, 2002). The Australian and New Zealand Environment Conservation Council has determined the trigger value for eutrophication of surface water to be just 0.44 mg/L NO_3^--N (Stenger et al., 2008).

The relatively slow nature of groundwater movement means any effects of land use decisions are likely to be delayed in many regions as contaminated groundwater replaces older, higher quality groundwater. Groundwater moves at a much slower rate than surface

waters, commonly at centimetres per day, though often slower (Weight, 2008). Currently, the water quality of Lake Taupo is considered very good, though it has begun to deteriorate, largely due to farming in its catchment (Hadfield et al., 2007). Groundwater investigations were undertaken to estimate the potential future land use impacts and the lag in effects. Mean residence times of groundwater contributing to the lake ranged from 20 to 75 years, with higher nitrogen concentrations occurring in groundwater recharged since farm development some 40 years ago. Modelling predicts nitrogen mass loading to the lake from current land use will continue to increase for a substantial period of time (>100 years) (Hadfield et al., 2007).

2.3 Nitrate Attenuation via Denitrification in Groundwater

The leached NO_3^--N in groundwater may potentially flow to surface waters where groundwater – surface water interactions occur. However, this also depends on potential attenuation of NO_3^--N in groundwater. Under reducing conditions, the process of denitrification breaks down NO_3^- (5+ oxidation state) to N_2 (0 oxidation state) through intermediate compounds, including NO_2^-, NO, and N_2O (van der Perk, 2012):

$$2NO_3^- + 10e^- + 12H^+ \rightarrow$$
$$2NO_2^- + 6e^- + 8H^+ + H_2O \rightarrow$$
$$2NO + 4e^- + 6H^+ + 4H_2O \rightarrow$$
$$N_2O + 2e^- + 2H^+ + 5H_2O \rightarrow$$
$$N_2 + 6H_2O$$

Though it is a similar process, denitrification is not the opposite of nitrification. The intermediate products, NO and N_2O, are gases that can volatise from the system before the denitrification reaction has been completed with the synthesis of N_2. Both NO and N_2O are greenhouse gases and their emissions contribute to global warming (van der Perk, 2012). Nitrate is the most plant-available form of nitrogen and is considered inert in most aerobic soils (Prado et al., 2006). Because of its soluble nature, it will either be assimilated back into plants or leached through the soil to groundwater.

In the saturated zone, denitrification is the main attenuation process that may remove NO_3^--N from the groundwater system. In groundwater aquifers, microbial bacteria are responsible for facilitating the reduction of NO_3^--N to other forms. They obtain their energy from the oxidation of organic and inorganic compounds. Bacteria that use organic carbons as their energy source are heterotrophs, while those using inorganic compounds for cell construction are autotrophs. In the saturated zone, organic carbon is the most common electron donor available for oxidation (Korom, 1992). It also tends to be oxidised preferentially with free oxygen (O_2), as it supplies most energy to micro-organisms during metabolic electron transfer (Rivett et al., 2008). As O_2 is depleted, the reduction of other electron acceptors becomes energetically favourable. Figure 7 shows the procession of electron acceptors for oxidation of organic carbon starting with O_2. Facultative anaerobes (bacteria capable of growing with or without oxygen) alternatively consume NO_3^--N as O_2 levels decrease. As NO_3^--N becomes depleted, reduction reactions subsequently favour manganese, iron oxides and sulphates (Rivett et al., 2008).

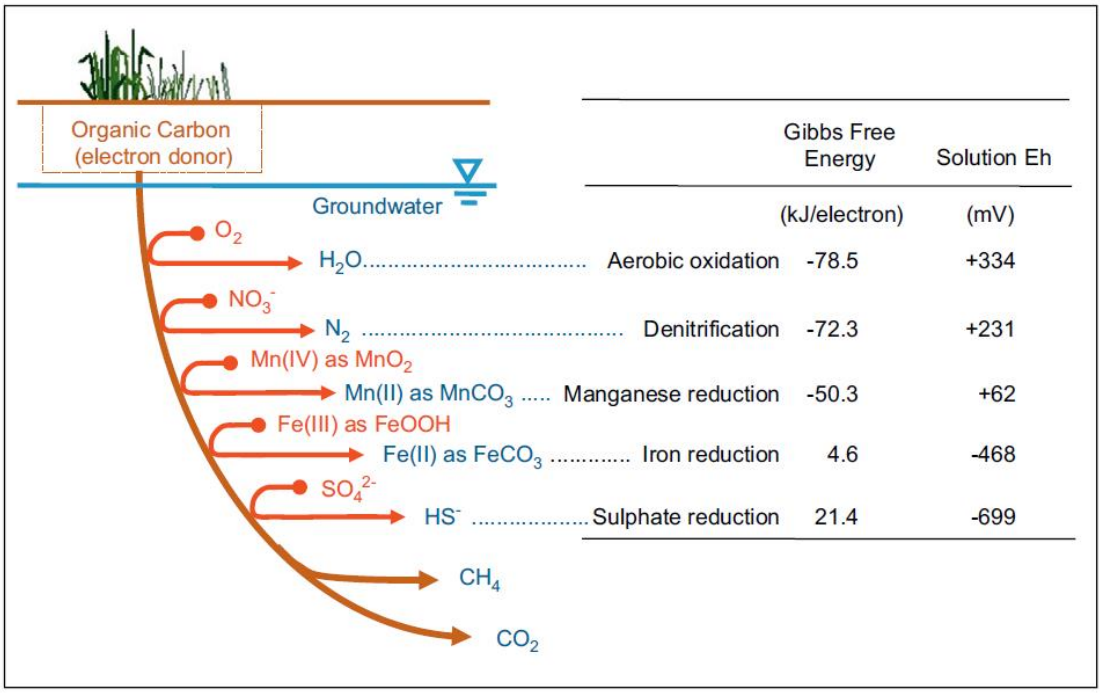

Figure 7: Thermodynamic sequence of electron acceptors for oxidation of organic carbon in the saturated zone (Rivett et al., 2008).

The rate of denitrification is most often related to the amount of dissolved organic carbon (DOC) in groundwater. DOC levels in most aquifers are relatively low, but sufficient for

denitrification, at <5 mg/L (Rivett et al., 2007). If DOC is too low and becomes a limiting factor, other electron donors can take the place of DOC for electron transfer. In these cases, reduced inorganic species such as Mn^{2+}, Fe^{2+} and HS^- can serve as electron donors and denitrification is carried out by autotrophic microbes (Korom, 1992). Reduction of NO_3^--N by Fe^{2+} can proceed either abiotically or biotically. In abiotic reduction, it is thought Fe^{2+} acts to promote denitrification where Fe^{2+} reduces NO_3^- to NO_2^- and is subsequently regenerated by the oxidation of organic carbon. NO_2^- can then be abiotically reduced in DOC-poor environments by the further oxidation of iron (Rivett et al., 2008). Examples of reaction equations for abiotic denitrification are given by Ottley et al. (1997):

$$10Fe^{2+} + 2NO_3^- + 14H_2O \rightarrow 10FeOOH + N_2 + 18H^+$$
$$15Fe^{2+} + NO_3^- + 13H_2O \rightarrow 5Fe_3O_4 + N_2 + 28H^+$$

The biotic reduction of NO_3^--N by Fe^{2+} can take place by a common bacteria *Gallionella ferruginea* under anaerobic conditions (Korom, 1992). In this situation, NO_3^--N is reduced to NO_2^-, which can be then further reduced abiotically. A small amount of DO is required for growth, so the likely ecological niche for *G. ferruginea* is at the oxic/anoxic interface where Fe^{2+} and DO meet in opposed diffusion gradients (Korom, 1992). Alternatively, autotrophic denitrification can take place by reduced sulphur. In groundwater, this is typically provided by iron sulphide (pyrite), described in the following equation by (Korom, 1992):

$$5FeS_2 + 14NO_3^- + 4H^+ = 7N_2 + 10SO_4^- + 5Fe^{2+} + 2H_2O$$

As well as electron donors available, there are several other environmental conditions that must be reached for denitrification to take place. There firstly must be N oxides (NO_3^-, NO_2^-, NO, and N_20) present as terminal electron accepters. The DO level must also be sufficiently low for NO_3^--N to proceed as the electron acceptor. A concentration of <2 mg/L DO is generally thought to be the limit where denitrification begins to take place (Bates & Spalding, 1998; Christensen et al., 2000; Stenger et al., 2013). Denitrifying bacteria also require a number of nutrients to support their metabolic activities. As well as a source of N, they also require C, P, S and other micro nutrients (including B, Cu, Fe, Mn, Mo, Zn and Co) for effective metabolism. *pH* also exerts a controlling influence on the denitrification rate.

The *pH* range preferred by most heterotrophic denitrifiers is considered to be between 5.5 and 8.0, with denitrification arrested at >8.3 (Rust et al., 2000). Denitrification may also increase *pH* as NO_3^--N is consumed and OH^- and CO_2 are produced. These would normally combine to produce HCO_3^- but if the production of OH^- exceeds that of CO_2, the *pH* can rise (Rivett et al., 2008). Previous studies have tested the capacity of shallow groundwater to attenuate NO_3^--N with varying results (e.g. Trudell et al., 1986; Tesoriero et al., 2000; Sánchez-Pérez et al., 2003; and Clague et al., 2013).

The primary method of measuring denitrification potential in groundwater is through the 'push-pull' test. This method provides quantitative information on a range of subsurface characteristics, but is most useful for measuring rates of chemical or microbial reactions (Istok, 2013). The test involves the injection (push) of a prepared test solution into the subsurface via a single injection point (e.g. a piezometer), followed by an extraction phase (pull) of the test solution from the same location (Istok, 2013). The test solution would normally be spiked with a nonreactive tracer (e.g. Br^-) to assess the rate of dilution of the test solution, and one or more reactive tracers aimed at a particular biogeochemical process (Istok, 2013).

A number of variations exist on this method. Although the basic principle has been used and repeated for a number of denitrification tests, there are usually some differences among the published literature. The earliest use of this test for measuring denitrification was by Trudell et al. (1986), while investigating nitrate attenuation in a sand aquifer. The test solution was monitored and sampled over 450 hours, or 2 – 3 weeks. Others ranged from 120 hours (Clague, 2013) to 100 minutes (Sánchez-Pérez et al., 2003). In order to ensure NO_3^--N reduction is observed and captured, the test solution for this study will be monitored over 360 minutes. The reduced nature of the groundwater indicated that the denitrification was likely to be rapid.

Other differences in the method include the volume of the test solution used and the preparation of the test solution itself. Istok (2013) suggests between 100 and 400 L for the test solution. Trudell et al. (1986) used 200 L while Clague (2013) used 40 L and Sánchez-Pérez et al. (2003) used only 20 L. Likewise, the concentration of the tracers within the test

solution also varied among published data. Clague (2013) used concentrations of 100 mg/L^{-1} Br^- and 40 mg/L^{-1} NO_3^--N in the test solution. Concentrations of 10 mg/L^{-1} will be used for each of Br^- and NO_3^--N in the test solutions for this study with 100 L injection volumes in most cases. Push-pull tests are usually performed through the use of shallow piezometers (3 – 8 m) using a packer system to inject the test solution into the formation. The same system, or a very similar one, will be used to perform the tests for this study. Sites were selected based on the results of a groundwater survey, with piezometers installed at 3 and 6 m around the study area.

2.4 Previous Studies on the Transport and Transformation of Nitrate in New Zealand Agricultural Catchments

The increasing use of nitrogen fertilisers over the 20th century means NO_3^--N concentrations have increased in some agricultural catchments. Concern for the harmful effects excess NO_3^--N concentrations can have to human and ecological health has stimulated interest in tracking the movement of NO_3^--N through the environment, and their eventual sink or transformation. Knowing the transport pathways of NO_3^--N and its attenuation somewhere in the system can promote better management of land and water resources. Most of the research in this area involves investigating how NO_3^--N moves from one environmental compartment to the next, in particular the groundwater – surface water interactions (Capel et al., 2008). In New Zealand, there is now a growing body of literature on nitrate attenuation in the subsurface of agricultural catchments. Much of this work has taken place under the Groundwater Assimilative Capacity programme, a partnership between ESR, Lincoln Ventures and AquaLinc Research. This has been complemented by the work Massey University and Horizons Regional Council have done in recent years on NO_3^--N attenuation in shallow groundwater in the Horizons region.

Barkle et al. (2007) quantified the denitrification capacity in the vadose zone at three sites in the Lake Taupo catchment. Soil profiles were sampled from the soil surface down to the water table in 0.5 m increments. Texture, allophanic content, *pH*, NO_3^--N and NH_4^+-N and DOC were all determined. Vadose zone materials were amended with NO_3^--N, incubated and maintained under anaerobic conditions. Down to 1.2 m, the denitrification capacity

ranged from 0.03 to 9.18 kg N/ha/day. Below 1.2 m it ranged from <0.01 to 0.09 kg N/ha/day. Results from the study found denitrification capacities low in comparison to other studies (Barkle et al., 2007). In the Toenepi catchment in nearby Waikato, Stenger et al. (2008) investigated why NO_3^--N was low in shallow groundwater in spite of intensive dairying. The effect of reducing conditions in groundwater was thought to be responsible, so the vadose zone NO_3^--N concentrations were monitored, as well as dissolved oxygen and Mn and Fe. Results suggested NO_3^--N reduction through heterotrophic and/or autotrophic denitrification is widespread in the catchment, either in the vadose zone or the shallow groundwater.

In-situ testing for denitrification within shallow groundwater was tested by Burbery & Wang (2010), based on a modified push-pull test. A two-well recirculating tracer well test method had been developed to measure natural attenuation in fast-flowing alluvial aquifers. The method ensures the injected test solution can be sampled over a longer period of time without it being diluted and moved with the general groundwater flow. This method was used in a range of aquifer conditions at several locations across New Zealand to evaluate NO_3^--N reaction rates *in-situ* (Burbery et al., 2013). Under anoxic, electrochemically reduced, NO_3^--N -free aquifers of volcanic lithology, Burbery et al. (2013) measured a denitrification rate of between 0.09 to 0.26 kg N/ha/day. However, the method performed poorly under a fast-flowing, NO_3^--N -impacted fluvio-gravel aquifer, likely because of aerobic conditions within the aquifer (Burbery et al., 2013).

Work by Stenger et al. (2012) and Stenger et al. (2013) has investigated the assimilative capacity of groundwater as a means of estimating the proportion of nitrogen either denitrified or diluted as it moves from agricultural catchments to surface waters. A key part of this is to use single-well push-pull tests in order to define the extent of denitrification. Tests undertaken within the Toenepi catchment failed to show any denitrification unless glucose was added to the injection solution (Clague, 2013). Massey University is currently working a similar work-stream focussed on the Manawatu catchment, including its assimilative capacity and denitrification capacity. An experimental site was established at Massey University's No.1 Dairy Farm to determine the appropriate procedures for measuring denitrification in the subsurface (Rivas et al., 2014), while the NO_3^--N attenuation

factor of a sub-catchment of the Manawatu River was also estimated and linked to catchment characteristics (Elwan et al., 2015). As yet, no such studies have been carried out on the Lower Rangitikei catchment to estimate the denitrification capacity of the shallow groundwater.

2.5 Conclusions

This chapter has provided an overview of the theoretical and current knowledge about groundwater – surface water interactions in the Rangitikei catchment; the sources and consequences of NO_3^--N in groundwater; NO_3^--N attenuation via denitrification and methods to measure denitrification; and previous studies on the transport and transformation of NO_3^--N in NZ agricultural catchments. This review has highlighted a lack of studies on the coastal Rangitikei catchment. In particular, a lack of knowledge exists on the nature of interaction the river has with groundwater in the Lower Rangitikei River; and the denitrification capacity in the coastal Rangitikei catchment, an area that has become more agriculturally intensive over recent years.

3 The Study Area – Lower Rangitikei Catchment

This thesis considers the Lower Rangitikei River Catchment, an area comprising the townships of Marton in the north, Sanson in the east, Tangimoana in the south and the Santoft area in the west (Figure 1). For management purposes, Horizons Regional Council has assigned this area as the Coastal Rangitikei Groundwater Management Zone (RGMZ) which principally represents the surface water catchment, though it is thought the aquifer boundary is wider than these limits. This chapter outlines the climate conditions of the study area, land uses and a description of soils in the region and their diversity. The local geology is also examined and is assisted by an interpretation of well logs drilled in the area.

3.1 Climate and Land Use

The Manawatu-Rangitikei plains are characterised by moderate temperatures without great extremes, with warm summers and mild winters (Cowie et al., 1967). The climate supports a range of land uses, though the threat of drought is present during some summers, particularly towards the coast where it can be drier. The Ohakea Aerodrome has hosted a climate station for decades and is located centrally in the study area. This station will be used to describe climate features with data supplied by NIWA's National Climate Database. The purpose is to give a general picture of the climate of the study area, though it may differ more towards the coast, e.g. slightly lower rainfall in coastal areas.

Average temperatures range from a high of around 18°C in February to a low of around 9°C in July. Average daily maximums and minimums are within a few degrees of the average (Figure 8). On an average basis, rainfall does not show a strong seasonal trend. Figure 9 shows the average monthly rainfall for the 30-year period 1981-2010 against the average monthly potential evapotranspiration 1954-1990. Rainfall is around 900 mm per year in this region, slightly lower than Palmerston North, with about 1000 mm per year. Evapotranspiration follows a seasonal pattern leading to potential soil moisture deficits in summer, depending on the soil type and water retention. Soil moisture deficits occur on average 10-15 days in both January and February (Burgess, 1988) and commonly into March and April, with irrigation used to offset the difference.

The prevailing wind is westerly to north-westerly occurring 30 to 50 percent of the time (Burgess, 1988). The coastal sand dunes common in this area have been aligned in response to this prevalent wind direction. The average wind speed is usually about 5 m/s, with wind speeds generally lower in winter and higher in spring (Burgess, 1988). The region also receives about 2000 sunshine hours per year, with approximately 250 hours received in January and as low as 80 hours in June (NIWA, 2015).

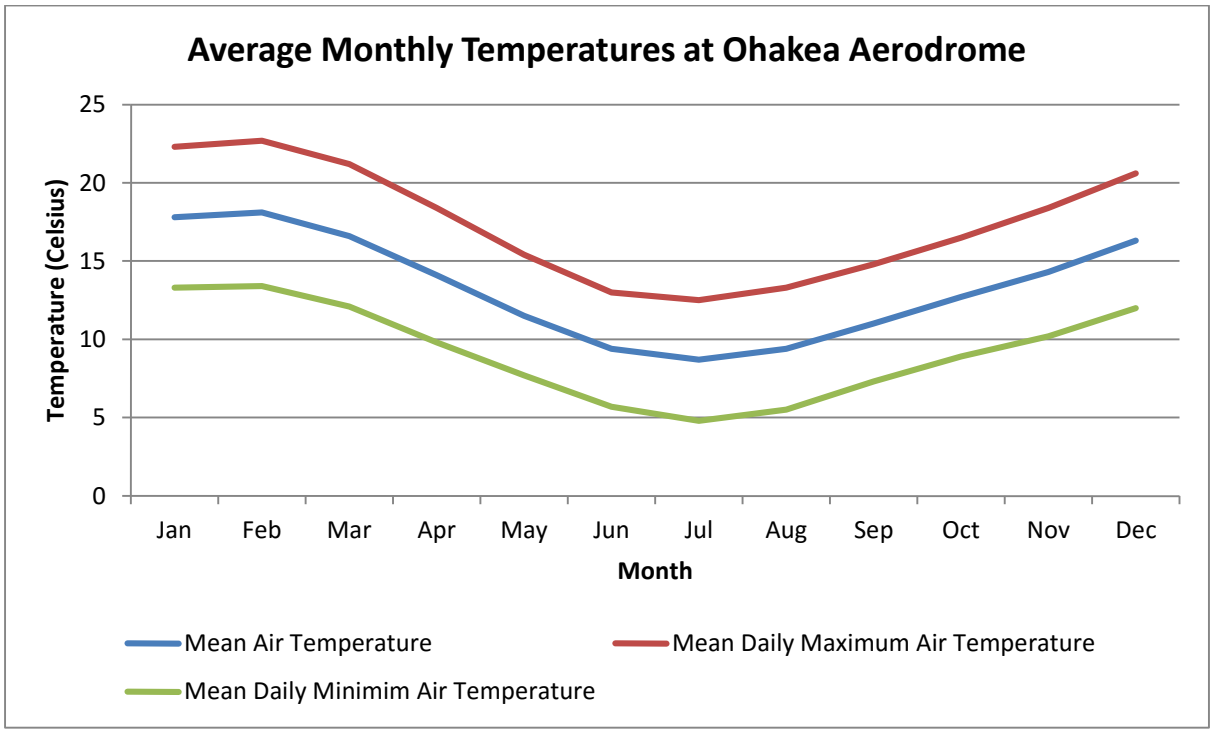

Figure 8: Average air temperatures 1971-2000 recorded at Ohakea Aerodrome (NIWA, 2015).

The climate is able to support a range of land uses, though there are a few that make up the majority. Land used for sheep and beef production covers approximately 350 km^2, or about 42% of total land use. Dairy makes up approximately 200 km^2 (24%); exotic forestry occupies approximately 123 km^2 of land (15%), though this is most densely located in the coastal area. High producing exotic grassland occupies approximately 70 km^2 (8%) and cropping makes up about 13 km^2 (1.5%). These figures were estimated in 2008 for a report into the land use and land use capability in the Manawatu-Wanganui Region (Clark & Roygard, 2008). In the succeeding seven years, some changes to land use could be expected, especially toward dairy, but the overall picture would still be similar.

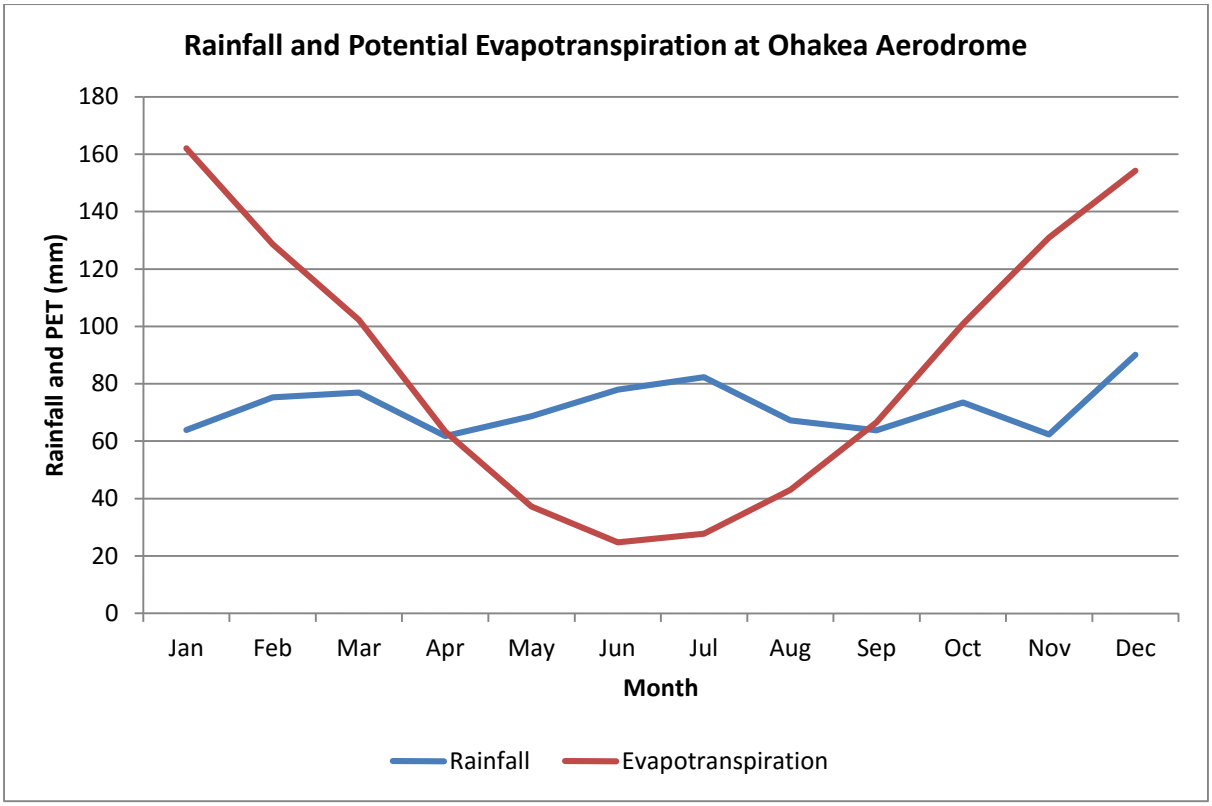

Figure 9: Average monthly potential evapotranspiration for 1954-1990, and average monthly rainfall 1981-2010 recorded at Ohakea Aerodrome (NIWA, 2015).

3.2 Soils

The soils of the Rangitikei area have been studied and mapped in detail by Cowie et al. (1967) and Campbell (1978). These were published in the form of bulletins and emphasised the land use capabilities of the soil in terms of qualitative descriptions. Mostly concerned with the genesis, texture and drainage characteristics of the soils and their development in a range of landscapes, these reports have been useful in identifying soil moisture characteristics and determining where irrigation would be most effective. The qualitative soil descriptions also describe how the soil type can affect the infiltration rate and rainfall recharge. Cowie et al. (1967) described the soils under two primary landscape types: soils of the sand country and soils of the river flats and terraces. In New Zealand, traditional soil mapping, such as those by Cowie et al. (1967), have been superseded by S-Map, the national soils database. The study area is partially covered by S-Map, though soil names are different to the ones characterised by Cowie et al. (1967). To be consistent with the established names outlined below, Figure 10 provides a map of the coastal Rangitikei sand country, river flats and terrace soils.

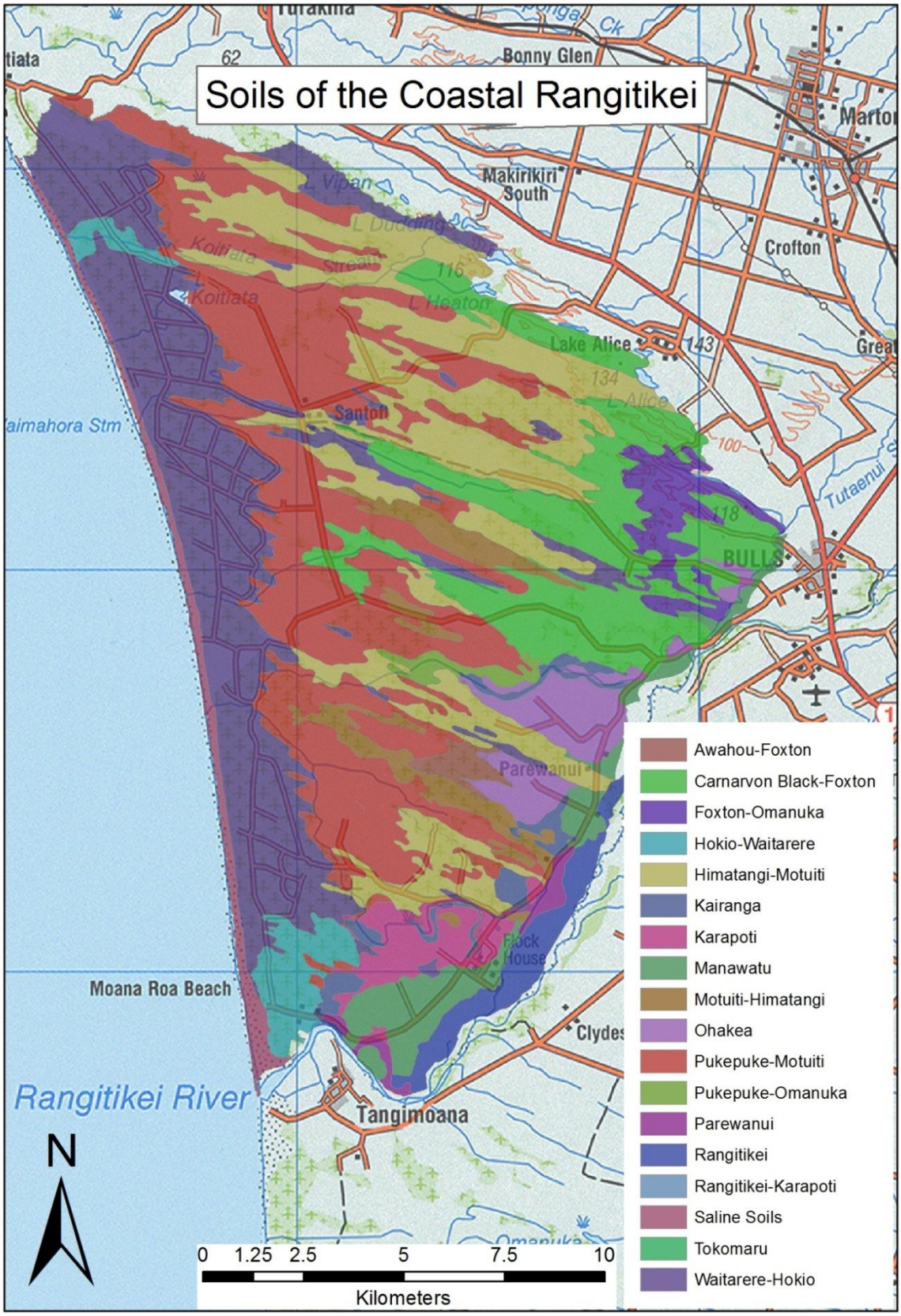

Figure 10: Soils of the Coastal Rangitikei as characterised by Cowie et al. (1967). Joint names are soil associations where soils exist in a topographically repeating and predictable pattern (McLaren & Cameron, 1994).

The soils of the sand country occur on the dunes, sand plains and peaty swamps. The accumulation of wind-blown sand takes place not just in the Rangitikei district, but a wide area stretching from southern Wanganui down to Hokio in the Horowhenua. As the sand accumulates on the beaches it is simultaneously built into dunes by the wind as the shoreline progrades so that the youngest dunes and associated sand plains are nearest the coast. There have been four major dune building phases. The Koputaroa Phase is restricted to small areas at the north and south, while three other phases – the Foxton, Motuiti, and Waitarere – form belts parallel to the coast, the oldest being farthest inland. The Koputaroa Phase is 25,500 to 10,000 years old based on the presence of Kawakawa Tephra. The Foxton Phase is about 4,000 to 2,000 years old and does not contain c. 233 AD Taupo eruption tephra. Sands of the Motuiti Phase, which do contain Taupo ash and pumice, and overlie traces of Maori occupation, are therefore 1,800 to 500 years old. The Waitarere Phase started about 150 years ago (BP) and is still accumulating (Cowie, 1963).

The Waitarere sand formed on the unconsolidated dunes of the youngest phase (Waitarere). These are excessively drained soils and have minimal soil profile development and are susceptible to wind erosion, especially when disturbed. Motuiti sand (previously mapped as Foxton dark grey sand) is the next older soil, formed on the less consolidated dunes of the older dune complex (Motuiti Phase) and is excessively drained with a thin topsoil. Foxton black sand, on the Foxton Phase sand dunes, is the most consolidated and has a greater level of profile development but is still considered excessively drained.

Soils of the river flats and terraces are derived from material brought down from rivers and reworked sand from dunes during floods. Additions of alluvium deposited by flooding events have interrupted the soil-forming process, leading to a lack of distinct horizon often found in non-accumulating soils. As the river moves through the landscape over time, a range of sediments is deposited in different positions, creating various soil characteristics as they develop. A former river channel's levees limit drainage and produce a high water table on the adjacent low-lying river flats, creating comparatively poorly drained soils. Five soils have been identified by Cowie et al. (1967), separated on the basis of drainage and rate of accumulation of alluvium. Figure 11 shows these soil series in relation to their topographic position.

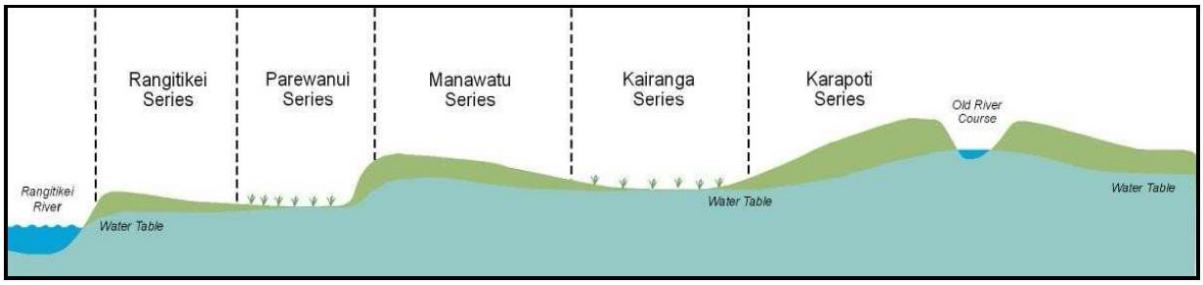

Figure 11: Relation of soil series to topography of the river flats (Cowie et al., 1967).

The Rangitikei soil series has formed on the low, frequently-flooded river flats bordering the main rivers where alluvium accumulates rapidly. Topsoils are indistinct and often thin, and textures are sandy, but many of the soils receive seepage from higher ground and rarely dry out excessively. The Rangitikei loamy sand is a characteristic type within this series. The Parewanui silt loam is alone in representing the Parewanui series, which is formed on the low lying frequently-flooded river flats where seepage from higher ground tends to keep the water table high and therefore poorly drained. It typically has a finer alluvium than the Rangitikei series because of its greater distance from the river. The Manawatu soil series is formed on slightly higher flats than the Rangitikei series, where flooding is less frequent and accumulation of alluvium is slower. These soils have a greater degree of soil development, with deeper topsoils and a yellow subsoil more distinct than the Rangitikei series. Manawatu fine sandy loam is a typical member of this series and is moderately well drained, like others in this series. The Kairanga series is formed on low-lying parts of the river flats, where seepage from neighbouring higher areas keeps the water table high, particularly in winter. These soils differ from the Parewanui series by a slower accumulation rate of alluvium, resulting in a deeper and more distinct topsoil. The Kairanga silt loam is the most extensive of the series. The Karapoti soil series is on the higher parts of the river flats, which now do not regularly receive fresh alluvium from flooding. The topsoil is shallower and the subsoil is more developed and compact than the Manawatu series.

Soils of the terraces are formed from old sediments, which are now sufficiently above river level to be free from flooding, and the accumulation of fresh alluvium. They have commonly received additions of windblown material known as loess, layers of which are thicker eastward from the coast. These were classed as moderately to strongly gleyed yellow-grey earths at the time, but would be reclassified as Pallic Soils under the New

Zealand Soil Classification (Hewitt, 1998). The soils of the terrace land include the Ohakea, Tokomaru, Halcombe, Milson, and Marton series (Cowie & Rijkse, 1977).

The Ohakea series occur on the low terraces and is formed from loess, colluvium and alluvium, and is composed of imperfectly to poorly drained soils. Stony gravels are present 90 to 150 cm from the surface. The Tokomaru series occurs on the intermediate and high terraces bordering the eastern bank of the Rangitikei River. It is formed from thick deposits of silty loess and is imperfectly to poorly drained. The Milson series occurs where the loess is thinner and finer textured, farther away from the rivers than the Tokomaru series. Drainage is poor as well. The Marton series occurs on the flat to rolling tops of the dissected high terraces, from clay-rich thin deposits of fine loess. The Halcombe series occurs on the rolling to moderately steep sides of the valleys dissecting the terraces. It is formed from loess on underlying sandstone and gravels.

3.3 Geology

3.3.1 Wanganui Basin Development

The Coastal Rangitikei catchment exists as part of the Wanganui Basin (Figure 12), one of the most studied Plio-Pleistocene shallow marine stratigraphic sequences in the world. The basin is approximately 200 x 200 km, situated in a proto-back-arc position (Proust et al., 2005) in the western North Island and recording glacio-eustatic sea level fluctuations back to Marine Isotope Stage (MIS) 100. Beds deposited during periods of high sea level are called the highstand systems tracts (HST). They show either an aggradational or progradational pattern as the shoreline shifts seaward across the shelf. Sediment is supplied by rivers and mostly settles on the shelf (Carter & Naish, 1998). As the sea-level begins to fall, erosion of the shelf occurs as rivers erode deposits of the previous cycle and cut valleys. Sometimes deposits of this period create a regressive systems tract (RST) (Naish & Kamp, 1997), though more often an unconformity is created by this sequence boundary and marks the end of the previous depositional cycle and the beginning of a new one. As the sea-level reaches its lowest point, the shoreline stops moving seaward and becomes stationary. Deposits of this period are called lowstand systems tract (LST) and often show a shellbed associated with this stage. The inner part of the ramp is no longer erosional and

river levels rise in incised valleys. As sea-levels begin to rise again, deposits on the shelf show a retrogradational pattern within the beds as the shoreline moves landwards. Estuarine sedimentation is characteristic of this systems tract as incised valleys are flooded with seawater. Sediments deposited at this stage are referred to as transgressive systems tract (TST). The sea-level again reaches its maximum extent during a highstand period (Nichols, 2009). Each cycle is known as a cyclothem. This process of alternating high and low sea levels has been the main depositional influence in the Wanganui Basin during the Pleistocene.

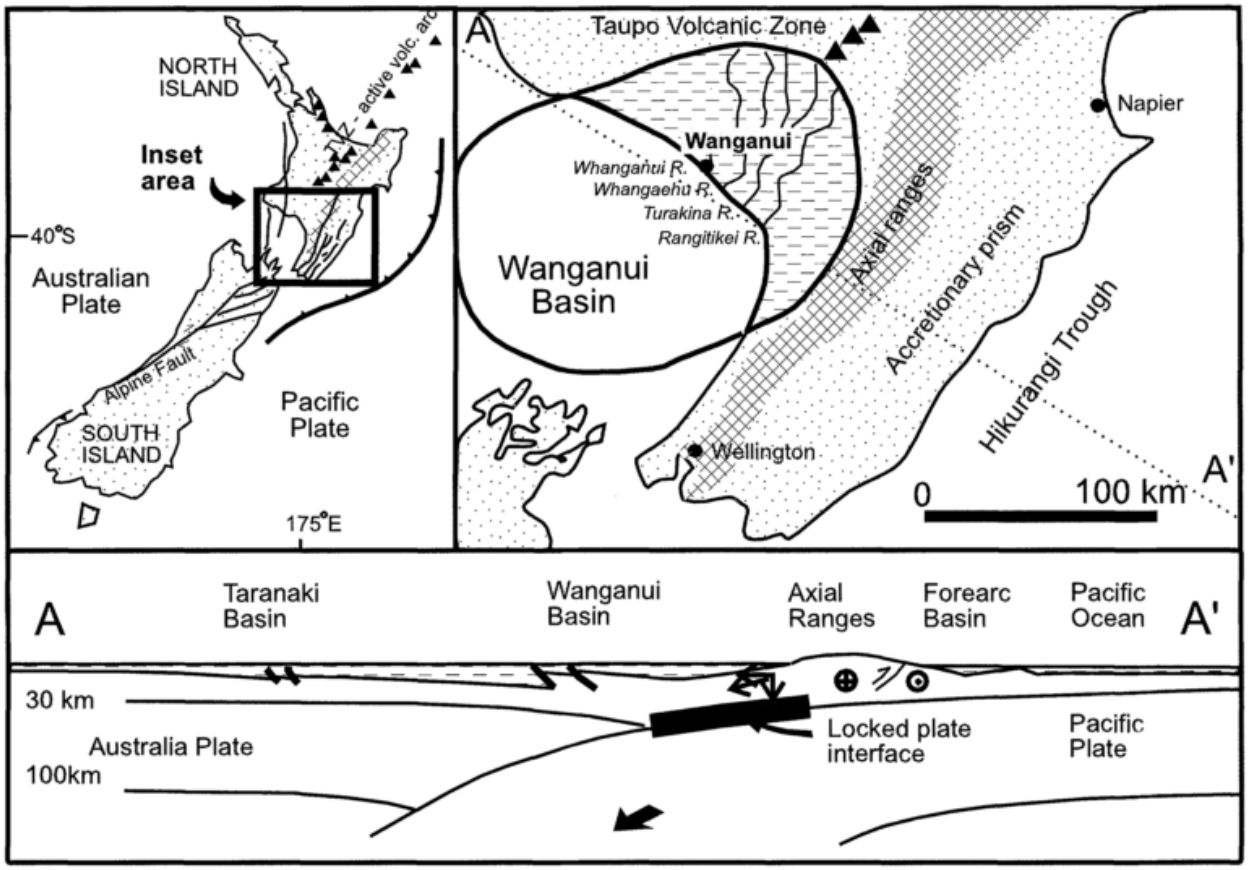

Figure 12: Locality map and geological setting of the Wanganui Basin (Carter et al., 1999).

Development of the basin commenced in the Late Miocene-Early Pliocene age (c. 5.5 – 4.7 Ma) with the Matemateaonga Formation in eastern Taranaki (Vonk & Kamp, 2004). This was followed in the Late Pliocene (3.6 – 2.59 Ma) with a subsidence event known as the Tangahoe pull-down, which represents the base of the Rangitikei Supergroup (Kamp et al., 2004). Seismic and well data analysed by Anderton (1981) show that during the Late Pliocene-Early Pleistocene, a series of NNE trending faults was active along the eastern

margin of the basin, with basement block movements controlling the sedimentation. Sedimentation kept pace with basin subsidence, although the depocentre shifted several times as regional tilting progressively moved subsidence to the south and emergence to the north (Anderton, 1981). Several anticline structures are present in the area, which can act as boundaries for the flow of deeper groundwater, but they also confine river channels to the synclines between them. These anticlines are named after their respective localities: the Pohangina, Mt Stewart-Halcombe, Feilding, Marton and Levin anticlines (Figure 13).

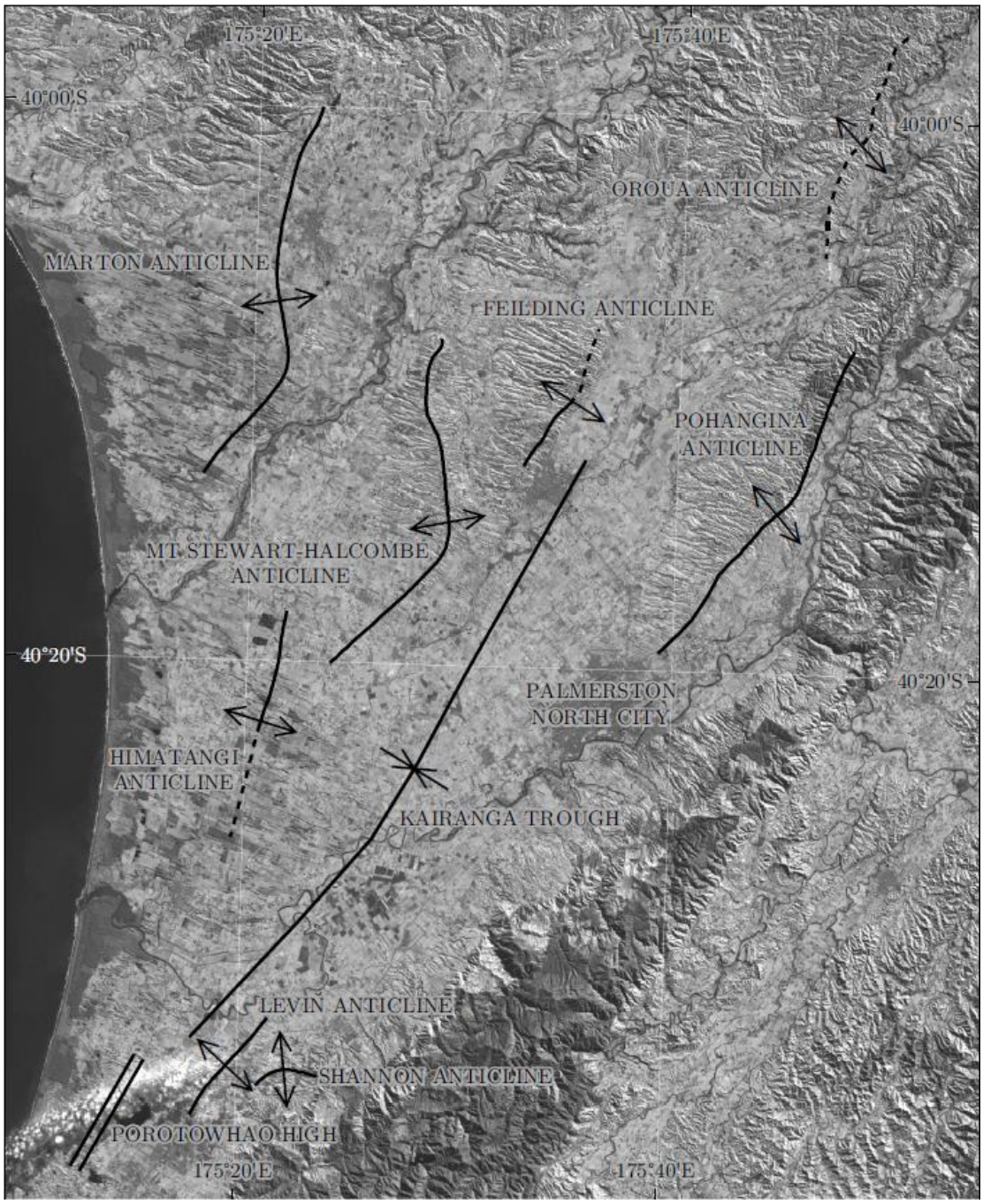

Figure 13: Fold axes of the Manawatu anticlines overlaid on an Enhanced Thematic Mapper satellite image of the Wanganui Basin (Jackson, et al., 1998).

3.3.2 Main Geological Units

At the same as time the basin depocentre was migrating southwards, the northern margin of the basin was being uplifted. The result of this pattern is that younger sediments still accumulated to the south of the basin, while progressively older strata were being exposed along the northern margin of the basin. Plio-Pleistocene strata are generally tilted to the south so the Rangitikei River valley (and other river valleys in the Wanganui Basin) has exposed most of the geological history and development of the basin. The following

sections summarise the main geological units in the area according to their age from oldest to youngest. The main groups are based on a review by Begg et al. (2005), with unit descriptions summarised by Townsend et al. (2008).

Unit 1: Torlesse Terrane "greywacke basement" (260 – 150 Ma)

The greywacke basement rocks underlie all other sediments, but outcrop only far to the east forming the Ruahine and Tararua Ranges. The greywacke is primarily composed of hard quartzo-feldspathic sandstone with interbedded mudstone. These rocks have experienced deformation from several episodes of folding and faulting, creating large blocks of greywacke with a sheared mudstone matrix. Rocks in this group typically lack porosity, with a mineralised cement often filling the intergranular spaces (Begg et al., 2005). As a consequence, fluid storage capability of this group is typically low, with most storage being provided by joints and non-mineralised shear planes within the rock (Begg et al., 2005). Three exploration wells intersect basement rocks between approximately 2600 m and 1000 m. Deep petrographic analysis of samples taken from these wells show the basement rocks have undergone a low grade of metamorphism (Mortimer et al., 1997).

Unit 2: Pliocene – Early Pleistocene deposits (3.6 – 0.7 Ma)

This unit marks the beginning of sedimentation within the southern Wanganui Basin, and approximately the first half of the Rangitikei Supergroup. The oldest formation described here marks the onset of regional subsidence and is therefore composed primarily of marine mudstone. With successive younger formations, the unit is characterised by increasing amounts of sandstone and lithologically diverse cyclothems. Sediments of this unit consist mostly of marine mudstone, siltstone, and limestone; shallow marine sand and estuarine silt; non-marine lignite and clay; silts and pumiceous sand (Bekele & Rawlinson, 2014).

The lower part of the Rangitikei Supergroup comprises the Tangahoe Mudstone, a massive to faintly parallel laminated, blue-grey, variably bioturbated mudstone ranging from 360-450 m thick. The Utiku Group unconformably overlies the Tangahoe Mudstone and is 350 m thick. This group consists of several siltstone, sandstone and silty sandstone members and is also moderately fossiliferous and bioturbated. The Mangaweka Mudstone succeeds the Utiku Group and is 440 m thick, though it is thicker farther west in the Wanganui Basin. It

comprises a thinner basal sandstone member and a thicker massive siltstone member with occasional sandy beds (Journeaux et al., 1996). It contains the silicic Eagle Hill Tephra, dated at 2.85 +/- 0.2 Ma, which confirms its age as late Pliocene (Townsend et al., 2008). The Mangarere Formation is c. 200 m thick, composed primarily of siliclastic sandstone and siltstone and is of Mangapanian age. Succeeding this is the 65 m Tikapu Formation, the base of which includes the Hautawa Shellbed.

The Hautawa Shellbed is a mollusc- and brachiopod-rich coquina shellbed containing the age-diagnostic bivalve *Zygochlamys delicatula*. The arrival of this species has been dated at 2.59 Ma (Beu, 1999) and is a useful indicator species in the New Zealand context, as it is roughly coincident with the beginning of the Pleistocene Epoch, now formally ratified at 2.58 Ma (Gibbard et al., 2010). The overlying Makohine Formation (Naish & Kamp, 1995) is a 165 m thick formation containing four cyclothems, with each typically consisting of sandstone, siltstone and shellbed members. The Orangipongo, Mangaonoho and Vinegar Hill formations contain 13 cyclothems, with an overall thickness of about 440 m. The lithology of these formations is very similar to the Makohine Formation of repeating siltstone, sandstone and shellbed cycles (Naish & Kamp, 1995).

The Maxwell Group represents a change in sedimentation that occurred as the Wanganui Basin was migrating southwards and includes more sediments of terrestrial origin, including lignite layers and estuarine deposits. The Okehu Group lies above an unconformity spanning approximately 500,000 years and is cut into the top of the Maxwell Group (Townsend et al., 2008). The top of the group is represented by the Potaka tephra which has an estimated age of 1.05 Ma with fission track dating (Pillans et al., 2005). The Kai-iwi Group overlies the Okehu Group and includes pumice sand overlain by successions of silt and sand (Fleming, 1953).

Unit 3: Middle Pleistocene Deposits (700 – 128 ka)

This unit represents the latest portion of the Rangitikei Supergroup and includes the Shakespeare Group and Pouakai Group. The Shakespeare Group comprises conglomerate, sandstone, siltstone, shellbeds and marginal marine deposits that can be observed outcropping in a band between Feilding and Wanganui (Townsend et al., 2008). This group

contains marine terrace deposits (Q15-Q9) described by Pillans (1990). The Pouakai Group includes middle to late Pleistocene alluvial and marine deposits and is defined by sediments Q7 and younger (Townsend et al., 2008).

Table 2: Main subunits of the Middle and Late Pleistocene in stratigraphic order, youngest to oldest (Begg et al., 2005).

Age	Relative age	Material/Lithology	Name	Depositional Environment	Relative Sea level	Absolute age (Ka)
Late Pleistocene (<128 ka)	Holocene (Q1)	Mud, silt & peat; gravel & sand		Estuarine, lacustrine, dunes, alluvial	High	0-15
	Late Otiran (Q2)	Gravel & sand	Ohakea	Alluvial	Low	15-30
	Middle Otiran (Q3)	Gravel & sand; 1 loess	Rata	Alluvial	Low-moderate	30-60
	Early Otiran (Q4)	Gravel & sand; 2 loess	Porewa	Alluvial	Low-moderate	60-71
	Kaihinu Interglacial (Q5)	Sand, silt & minor gravel; 3 loesses	Rapanui (Tokomaru, Otaki sst)	Marginal marine to marine	High	71-128
Middle Pleistocene (700 – 128 ka)	Waimea Glacial (Q6)	Gravel & sand; 3 loesses	Greatford, Marton	Alluvial	Low	128-186
	Karoro Interglacial (Q7)	Sand, silt, 4 loesses, tephra	Rapanui	Marginal marine to marine	High	186-245
	Waimaunga Glacial (Q8)	Gravel & sand; 4 loesses	Burnand	Alluvial	Low	245-303
	Brunswick, Braemore Interglacial (Q9)	Sand, silt, 5 loesses, tephra	Brunswick, Braemore	Marginal marine to marine	High	303-339
	Unnamed (Q10)	Gravel & sand, 5 loesses	Aldworth, Waituna	Alluvial	Low	339-362
	Ararat, Rangitatau Interglacial (Q11)	Sand, silt, 6 loesses, tephra	Ararata, Rangitatau	Marginal marine to marine	High	362-423
	Ball Interglacial (Q13)	Sand, silt, 7 loesses, tephra	Ball	Marginal marine to marine	High	478-524
	Piri Interglacial (Q15)	Sand, silt, 8 loesses, tephra	Piri	Marginal marine to marine	High	565-620

The Middle Pleistocene represents a major geological change where the northern region of the Wanganui Basin started to emerge from the sea (Begg et al., 2005). A series of marine terraces is preserved in the Wanganui area, extending several kilometres inland. These indicate the high sea-level stand shoreline at a particular point in time and reflect the relative and (often) absolute age of the land surfaces, with higher terraces being older. The oldest marine terrace, Marorau, is c. 670 Ka, though the Palmerston North to Foxton area

did not emerge until possibly as late as 400 Ka (Begg et al., 2005). The period between 670 Ka and the start of the Last Interglacial (c. 128 Ka BP) represents alternating warm, high level stand marine terraces and cool climate and low sea-level stand alluvial aggradational fans. Table 2 shows the marine isotope stages (Q15-Q1) and their associated glacial and interglacial deposits.

Unit 4: Post-glacial deposits (<128 ka)

The latest Quaternary deposits represent all marine and terrestrial sediments deposited since the Last Interglacial Maximum (128 – 80 ka). These deposits comprise the largest shallow groundwater resource in the study area. Last Glacial deposits and Holocene deposits (Q2 to Q1 respectively) are dominated by alluvial gravel deposits, and marine sand and silts laid down during this period. With each relative cool cycle since the Last Interglacial (Ohakea, Rata, Porewa; Table 2), there has been a period of extensive terrace formation associated with the deposition of alluvium. As the climate recovers and becomes warmer in the intervening interstadial period, river downcutting occurred as sediment supply was restricted. A steady regional uplift rate formed river terraces at successively lower levels with each succeeding stadial. This process has produced a series of river terraces, with each covered by a veneer of gravelly alluvium topped by loess units up to several metres thick (Te Punga, 1953).

Towards the coast, aggradation gravels are covered by Holocene silt, peat and wind-blown sand deposits. These gravel-poor areas have a lower permeability compared with the aggradation gravels described above. In other locations, some gravel deposits are clay-bound and deposited with fine grained overbank, swamp or lacustrine deposits. Alluvial gravels found farther inland tend to be clast supported, though sand and silt can be significant components. Where loess separates the clast-supported alluvial layers, the aquifer is likely to become locally confined (Begg et al., 2005).

Several attempts have been made to model the post-glacial deposits in the Manawatu region, though there seems to be a lack of consensus on the exact hydrogeological nature of the Late Pleistocene water-bearing sediments of the region. As part of a review of the groundwater resources of the Manawatu-Wanganui region, Zarour (2008) has provided a

summary of the hydrogeology of the area. While only some of this material relates specifically to the Rangitikei catchment, much of his discussion is broad enough to relate to the region as a whole. Zarour's review particularly highlights how thinking about the hydrostratigraphy of the region has changed over the years and how different interpretations are favoured by different researchers. While several authors have favoured a stratified hydrostratigraphy (e.g. Petricevich (1970); Lieffering (1990); Martley (2001)), others (e.g. Begg et al. (2005); Wilson (2007); Zarour (2008)) have rejected this approach and consider the entire late Pleistocene deposits as a single open aquifer.

3.4 Well Log Interpretation

Well logs were used to model the Late Pleistocene deposits and provide an interpretation of the development of Recent Q2 and Q1 sediments. These are the most recent deposits and are represented extensively, especially in the coastal margin of the study area. This was achieved by creating three cross sections; one parallel to the coast and another two inland from the coast to Bulls. The cross sections were drawn using Hydro GeoAnalyst 2014.2, with a 1000 m buffer. The cross sections (Figure 14) cover the areas from Santoft to Bulls (A-B; Figure 15); Scott's Ferry to Bulls (C-B; Figure 16); and Santoft to Scott's Ferry (A-C; Figure 17). These locations were selected for the availability of suitably deep wells and for surface outcrops. More detailed information on the individual wells used in this analysis can be found in the Appendix.

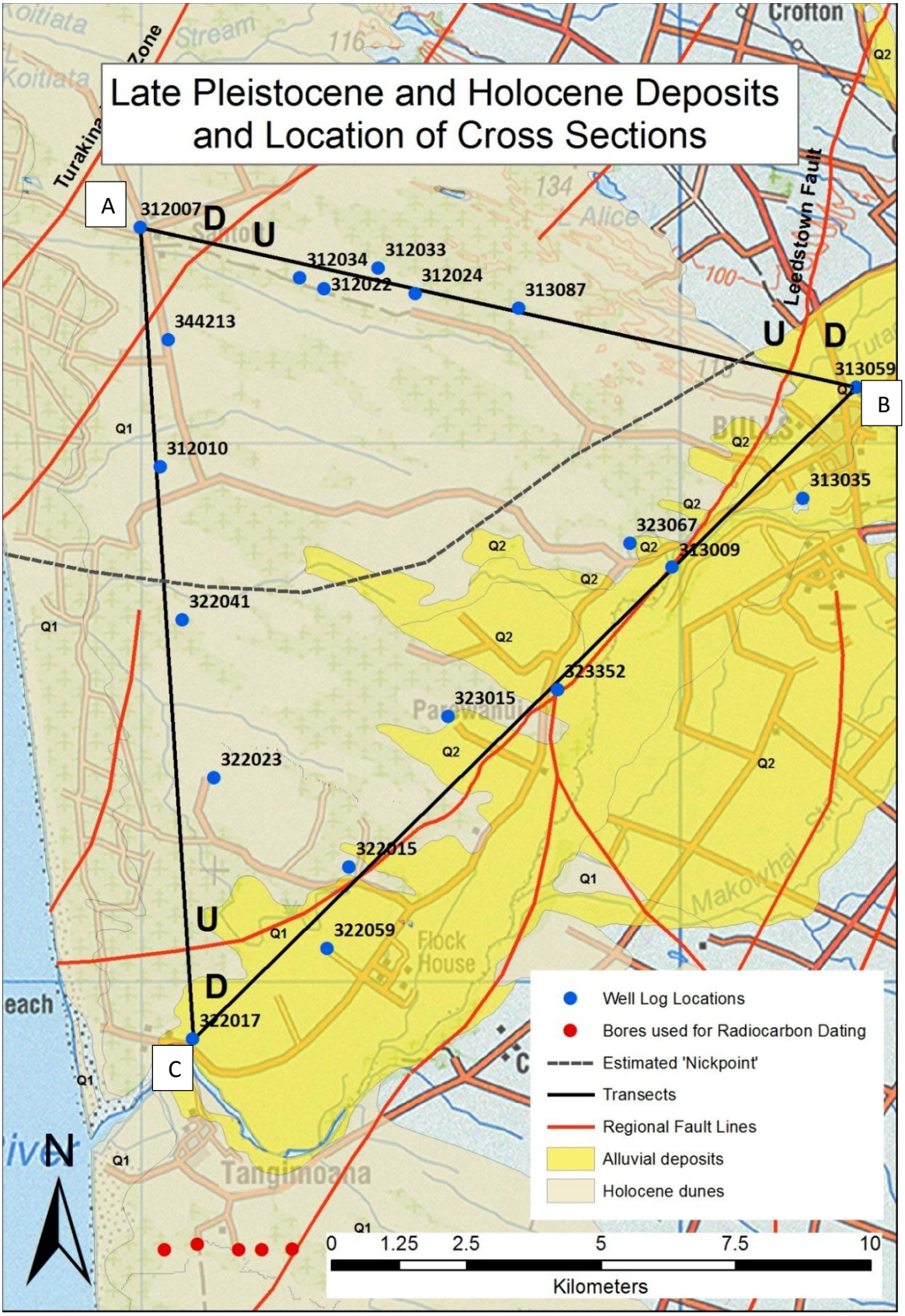

Figure 14: Simplified geological map showing the Q2 (Ohakean) and Q1 (Holocene) deposits with regional fault lines shown with their sense of direction. Well logs shown in blue are used to create subsequent cross sections while red ones were previously used for carbon dating (Figure 19). The nickpoint is the estimated former extent of Ohakean deposits which were subsequently eroded or covered by later deposits.

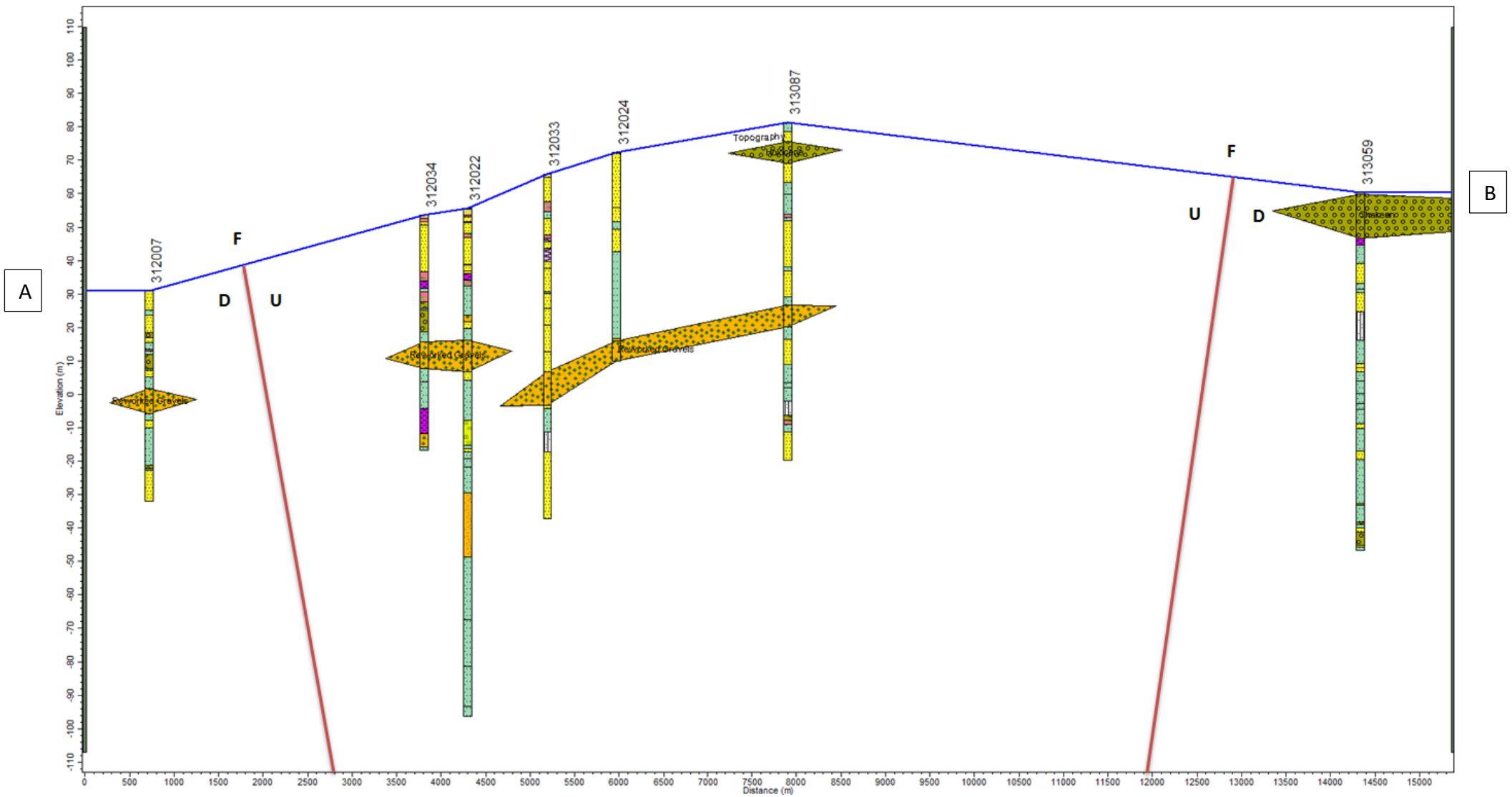

Figure 15: Cross Section A-B Santoft to Bulls with interpreted locations of various gravel units and fault lines. Orange units are reworked gravels; green units are Ohakean or later gravels. F = fault; U = up; D = down. Well legends can be found in the Appendix.

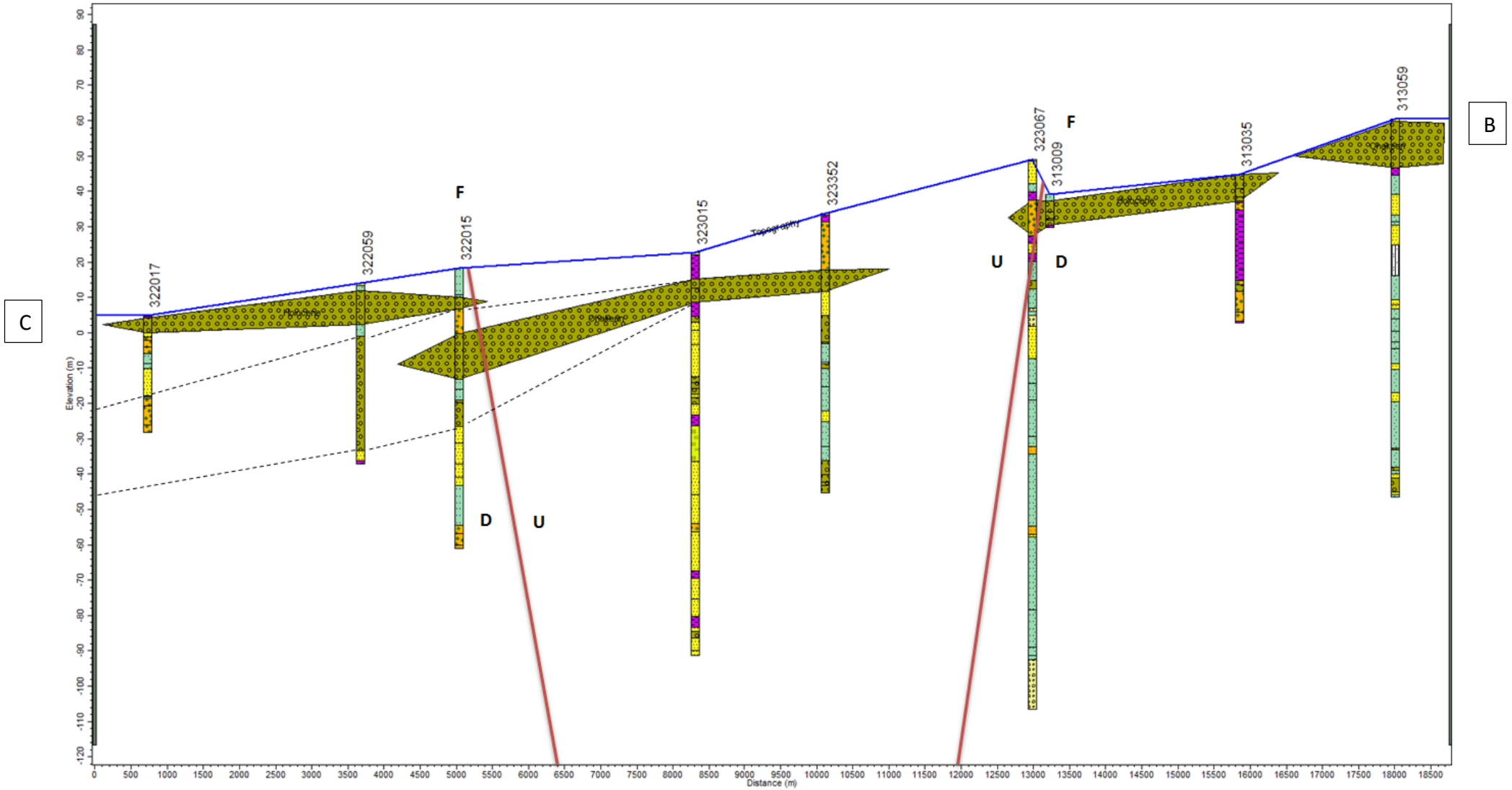

Figure 16: Cross Section C-B Scott's Ferry to Bulls with interpreted locations of various gravel units and fault lines. Orange units are reworked gravels; green units are Ohakean or later gravels. F = fault; U = up; D = down. Well legends can be found in the Appendix.

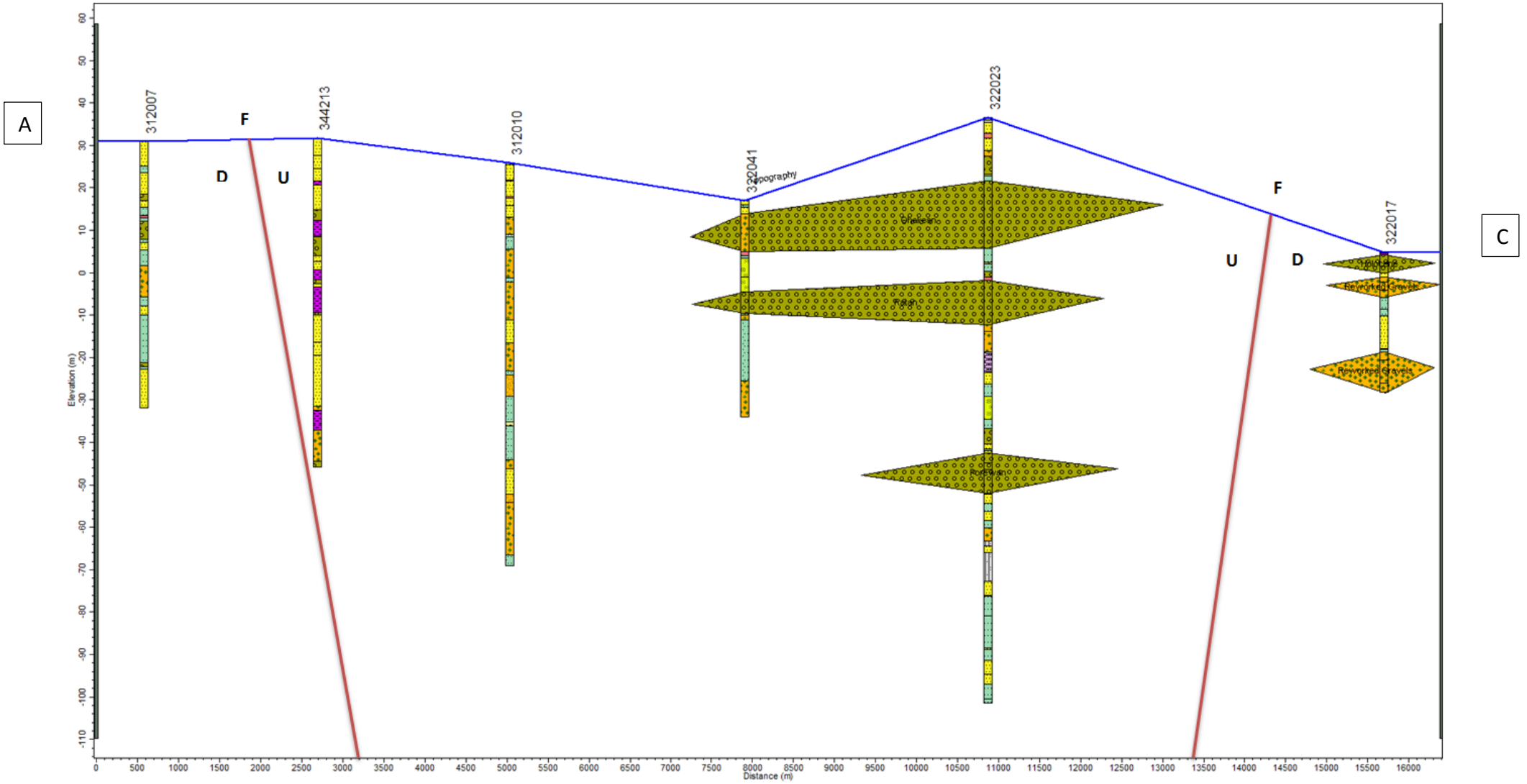

Figure 17: Cross Section A-C Santoft to Scott's Ferry with interpreted locations of various gravel units and fault lines. Orange units are reworked gravels; green units are Ohakean or later gravels. F = fault; U = up; D = down. Well legends can be found in the Appendix.

Cross section A-B (Figure 15), drawn from Santoft to Bulls, contains seven well logs and covers 15 km. At the western edge ('A' on the cross section; coastal side) surface soils are of the Pukepuke – Motuiti association, while farther inland wells (312034, 312022, 312033 and 312024) are located on soils of the Himatangi – Motuiti association. Farther east, at well 313087, the soil is of the Carnarvon Black – Foxton association. Approximately 6 km separates 313087 and 313059 at the end of the cross section, with no other wells close enough to the line of cross section. This well is located on the Ohakean terrace (Q2; 15 – 30 ka) outcrop near Bulls. The Ohakean gravels here are 10 m or so thick with the sequence below consisting of silt and sand. Several gravel units are indicated in the cross section, which are most likely all reworked gravel rather than part of the Q2 Ohakean terrace formation. It is unlikely the river extended this far, as described later. Several faults are present in the area and are indicated on the cross sections with their sense of throw. Between A-B the faults have created a horst feature creating a peak at 313087.

Cross section C-B (Figure 16) from Scott's Ferry to Bulls, contains nine well logs and covers 18 km. This line of cross section is unfortunate as it roughly overlaps with the Leedstown Fault, making interpretation unnecessarily difficult, though this line was chosen for the availability of wells logs and surface outcrops. From the west, well 322017 occurs on Holocene alluvium with approximately 5 m of Recent gravel deposits and only several kilometres from the present river mouth. To the east, at 322059, Holocene gravel deposits dominate the top 10 or so metres (Q1), with overbank silt deposits nearest the surface. Another large gravel package makes up most of the rest of the well log, and this is possibly Q2 deposits (as shown on the cross section). The Leedstown Fault separates this well and the next, 322015, with the downthrown side to the SE (Figure 14). 322015 is situated on the Himatangi – Motuiti association, with layers of silt built up beneath the surface. 323015 is located on the Ohakean terrace, though it borders sand dunes of Motuiti age. Ohakean gravels make up the first 20 metres or so of deposits, though some of these layers contain high clay fractions. Well 323352 is located on the Ohakean terrace, though located very close to later Holocene deposits. Near the top of the well is a thick (c. 13 metres) deposit of sand and gravel. The gravel would most likely be Ohakean (Q2) age, though if it is, it is not known why there would be such a component of sand through it. Farther NW, well 323067 is located on the Carnarvon Black – Foxton association, with several metres of (aeolian) sand

at the top of the well log. Continuing NW, the remaining wells 313009, 313035 and 313059 are all located on the Q2 Ohakean terrace gravels.

Cross section A-C (Figure 17) is 16 km long from Santoft to Scott's Ferry parallel to the coast and contains six well logs. From the north, wells 312007, 344213 and 312010 all occur on the Pukepuke – Motuiti association. 322041 is in a low point in the topography where the sand layer is thin, revealing an Ohakean gravel outcrop nearby (Figure 18).

Figure 18: Ohakean gravels outcropping near 322041. A centre pivot irrigator can be seen in the background.

These are likely to be Ohakean gravel deposits because of their short distance from other known Ohakean outcrops in the region (e.g. at Parewanui Road). This outcrop is evidence the Rangitikei River extended this far north and most probably continued even farther to the north. Farther south, towards the current Rangitikei River, well 322023 occurs on the Pukepuke – Motuiti sand-dune association but also contains volcanic material likely to be water-borne Taupo Pumice. The cross section finishes at 322017 on a Holocene river deposit.

In interpreting the development of the Q2 and Q1 deposits around the Rangitikei River, other sources will be used in addition to well logs and cross sections. First, a map by Milne (1973), with details of the river terraces of the Rangitikei River and the inferred extent of these terraces, known as the 'nickpoint', will be used. Second, age information collected by Mike Shepherd (c. 1986) in drill cores around the Tangimoana area will also be employed.

Ohakean deposits were laid down during the Last Glacial Maximum (Q2; 30 – 15 ka; Table 2), of which many outcrops can still be identified, especially around the Rangitikei River. Their total visible extent has been reduced since deposition, either through erosion, or subsequent concealment by later Holocene (Q1) deposits. Starting at 313059 ('B' on Figure 14), the Rangitikei River is likely to have coursed westwards, from approximately 313009, and drained into the sea somewhere between 322041 and 312010 (cross section A-C). This is the approximate location of the nickpoint Milne (1973) gave in his examination of the Rangitikei River terraces. Cross sections of A-B and A-C support Milne's nickpoint by showing the approximate extents of the Ohakean deposits based on well log data. The proposed path is shown in Figure 14, which is roughly coincident with the nickpoint given by Milne (1973). The river was likely flowing along the nickpoint sometime between 30 – 15 ka, though it is difficult to be sure. The Q1 sediments in the study area are primarily made up of sand-dune sequences, the oldest of which is the Foxton Phase, being 2000 to 4000 years old. Dunes of this age imply the river has not flowed along the nickpoint for at least 4000 years. Moreover, cross section A-B reveals a subtle peak at well 313087, created by the two faults at either side of the cross section. The peak is likely related to the Marton Anticline (Figure 13) and its growth over the last several thousand years has possibly been responsible for gradually shifting the Rangitikei River south to its current position.

On the south side of the river, at Tangimoana, a series of drill cores was taken to radiocarbon date the shell fragments recovered from the cores. The location of these drill cores is shown in Figure 14 and the cross section is shown in Figure 19. An examination of the drill cores reveals Ohakean gravels deposited at least 5000 years ago to at least 1 km from the coast. Fine marine sand succeeds the gravels, indicating a rising sea level around 3000 to 4000 years ago. Later, gravelly marine sand was deposited as the sea level retreated. The cross section (Figure 19) shows the unconsolidated sediments dipping

toward the coast as is also inferred in cross section C-B (Figure 16), which may reflect uplift in the Northern and Eastern areas of the Wanganui Basin. Finally, dune sands were deposited along the coast from approximately 4000 years ago, with deposition of the Foxton Phase sand dunes, followed by the Motuiti and Waitarere Phases.

3.5 Conclusions

Since the end of the Last Interglacial (c. 128 ka), the Wanganui Basin has filled with a range of marine and terrestrial sediments deposited in response to the interaction between a rising and falling sea levels and in conjunction with fluvial degradation and aggradation. To understand more about the nature of the water-bearing deposits, well logs were used to interpret the geological structure and Recent geological history. The well logs and associated cross sections suggest definite bands of gravels exist, but the cross sections do not support an overall trend of stratified/layered subsurface geology. Instead, they reflect a process where the sea has encroached to some degree, followed by a regression and a subsequent dominance of terrestrial, gravel deposits. This would again be followed by an advancing sea, but instead of completely covering the preceding deposited material, it would either mix with or erode it. The process repeated over many cycles, but to a different extent with each cycle. It is likely repeated cyclical sedimentation is more responsible for the characteristics seen in the cross sections, rather than a highly stratified nature of the subsurface geology.

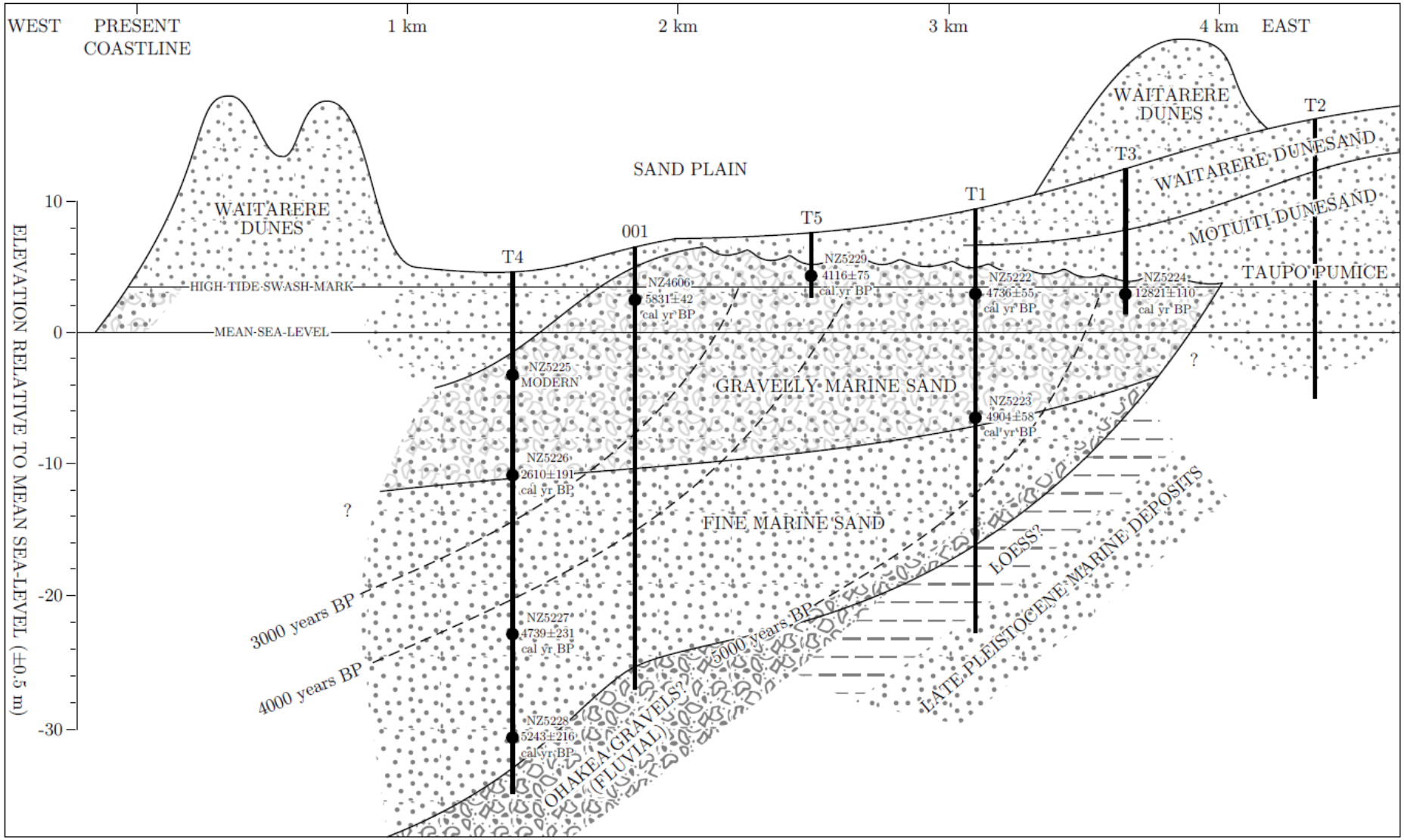

Figure 19: Cross section through the Holocene marine wedge south of Tangimoana (Clement, 2011 after Shepherd et al., 1986). Shells from T1 – T5 were used for radiocarbon dating and their locations are shown in Figure 14.

4 Groundwater Flow and its Interactions with Surface Water

4.1 Introduction and Objectives

Groundwater flow is mainly determined by the difference in hydraulic head across an area, but also depends on the geological material it passes through and local landforms. Chapter 4 presents the results of a groundwater survey undertaken to understand the general direction of groundwater flow in the Lower Rangitikei catchment. Aligned closely with groundwater flow is the interaction surface water bodies have with groundwater. These interactions include those scenarios where rivers are gaining or losing water to groundwater. Surface water-groundwater interaction can be dynamic and will change over the length of a river and may also change seasonally as the water table rises and falls (Younger, 2007). Any interaction groundwater has with surface water is also likely to impact water quality and the concentration of nutrients or pollutants present in a river. Therefore, the NO_3^--N concentration of a river can depend on the level of interaction groundwater has with a river, as NO_3^--N is mainly generated in the soil profile, it percolates and flows through the subsurface environment. This chapter also presents the results of a longitudinal river flow and water quality survey carried out on the Lower Rangitikei River to gain a better understanding of the surface water-groundwater interactions, and the effect it may have on NO_3^--N concentrations in the river.

4.2 Methods and Materials

4.2.1 Groundwater Level Survey

Depth to water level measured in wells tapping an unconfined aquifer can be used to construct a water table contour map, analogous to a topographic map, but representing the slope of the groundwater surface instead of the land surface. In an unconfined aquifer, groundwater is by definition at hydrostatic pressure. Where wells tap a confined aquifer,

groundwater is considered to be under pressure, causing the water level to rise within the well and in some cases rise above the land surface, becoming artesian.

In this study, approximately 200 wells were identified from the Horizons Regional Council's wells database to survey groundwater levels and map the groundwater flow direction. These wells were selected based on their spatial and depth distribution. The well owners were notified prior to a site visit, which took place over a two-week period in October 2014. Once at the site a visual inspection of the well was done as to whether it could be easily accessed for dipping. Groundwater depth was measured using an electrical tape and accurate location data was gathered by GPS. Groundwater depth information was gathered from just over half of the wells visited (Figure 20). The other half of the wells were not able to be dipped for several reasons, usually to do with a sealed well casing, or the pump running at the time. Groundwater depths were corrected to a common datum (Wellington datum) to be expressed as metres above sea level. These measured depths to groundwater were later visualised and analysed in ArcGIS 10.2.1. Data points were converted into a raster file using the Inverse Distance Weighted function, then converted into a topographic map with the contour function. Contour intervals were set at 10 m (see Figure 23 and Figure 24).

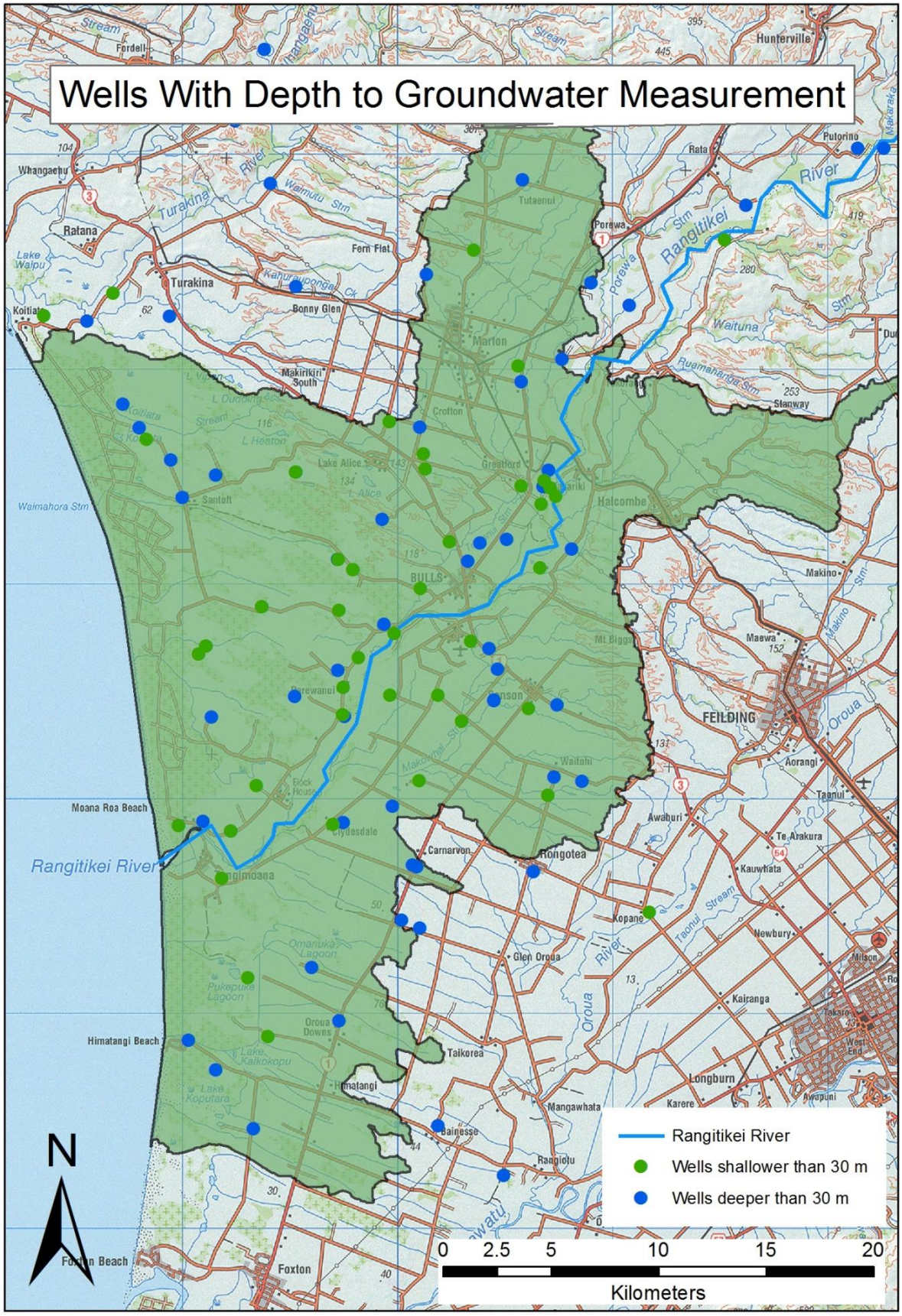

Figure 20: Location and depth of wells used in piezometric survey.

4.2.2 Groundwater – Surface Water Interactions

There are many ways of measuring surface water – groundwater interactions with varying data requirements (see Section 2.1). For practical reasons, groundwater – surface water interactions were measured using a longitudinal river flow and water quality survey. This method estimates the flux of groundwater into and out of a stream by measuring flow at several points along the stream. Several water quality parameters were also used to further interpret groundwater influx. The groundwater contour lines will also be used to provide some indication where groundwater is likely to be discharging to the river.

The study covered approximately 25 km of the Lower Rangitikei River, from Kakariki Bridge near Halcombe to a permanent river flow recording station 4 km from the coast. River discharge measurements were conducted across several points along the river in order to infer gaining and losing reaches. The selection of locations for river discharge measurements depended on the ability to safely cross or access the full width of the river. Therefore shallow reaches and bridges were considered first, but some deeper stretches were paddled across. These locations were assessed in the days before any measurement and permission was gained from land owners if required. Finally, six sites were selected for the river flow discharge measurements.

The longitudinal river flow and water quality surveys were conducted twice (6 January 2015 and 20 January 2015) at low flow conditions when no substantial rain had occurred recently. In the first survey (6 January 2015), river discharge and water quality measurements were taken at four locations (Figure 21): the Kakariki Bridge, the Bulls Bridge, a quarry near McDonnell Road and another quarry at Campion Road. In the second survey (20 January 2015), river discharge and water quality measurements were taken at the same locations in addition to another between the Kakariki Bridge and Bulls Bridge (Figure 22). Because of tidal influences on both these survey days, the most downstream flow measurements were taken from the permanent river flow monitoring station in Tangimoana (McKelvie's). This river flow station is operated by Horizons Regional Council.

River discharge measurements

River discharge measurements were made using the Sontek River Surveyor M9. The Sontek was traversed across the channel at least six times with data being transferred to a computer in real time as it was being collected. The river discharge measurements for the most downstream locations were taken from the permanent river flow recording station at McKelvie's, as the tide was incoming at the time of surveying.

River water quality

River water quality samples were collected from each selected location where river discharge measurements were taken. Water samples were taken directly from the river and filtered through a 45-micron filter into a 50 mL sample container. The samples were stored frozen until further analysis in the laboratory. The collected water samples were analysed using ion chromatography (IC) for chloride (Cl^-), sulphate (SO_4^{2-}) and NO_3^--N concentrations. In addition, specific conductivity was measured. These are common tracers used in longitudinal studies (Barthold et al., 2011).

Groundwater quality

Groundwater samples were taken during a survey in December 2014. More details of this survey will be discussed in Chapter 5 but results from that survey will be used in this analysis.

Figure 21: Sites used for longitudinal river flow and water quality survey, 6 January 2015.

Figure 22: Sites used for longitudinal river flow and water quality survey, 20 January 2015.

4.3 Results and Discussion

4.3.1 Groundwater Flow Direction

As outlined in Chapter 3, there is unlikely to be set layers of highly productive aquifers in the geological sequence throughout the entire catchment/study area. Instead, the groundwater resource in general could be thought of as a large leaky system, where it is locally confined, semi-confined and unconfined (Wilson, 2007). This probably reflects why there is such a variance in the depth of wells around the area. The depths of surveyed wells ranged from 3 m to 268 m ($\overline{x}$ 62.8 m, median 43.2 m) for the purpose of this analysis. It is also a zone of discharge for groundwater, where potential energy increases with depth, resulting in an upward movement of groundwater, particularly towards the coast (Weight, 2008). In practice, this means hydraulic head varies vertically as well as laterally. The vertical distribution of hydraulic head can be determined by wells drilled near each other, but screened at different depths. Where the hydraulic head increases with increasing depth, groundwater flow is upward and in general indicates an area of discharge (Moore, 2012). This phenomenon is seen in the study area, as well as other places around coastal Manawatu. Zarour (2008) made a point of this observation when examining the groundwater resources of the Manawatu-Wanganui region.

For the reasons mentioned above, it was considered appropriate to separate the water levels for contouring/flow analysis into two depth ranges: wells screened at less than 30 m (shallow) and wells screened at greater than 30 m depth (deep). This is expected to help separate the groundwater flow systems if there is any difference between the shallow and deep aquifers (Weight, 2008). A total of 44 wells screened at less than 30 m and 67 wells screened at greater than 30 m were dipped for this groundwater flow direction analysis (Figure 23). The measured depths to groundwater levels were converted to metres above sea level (masl) by subtracting the elevation of the well from the depth to groundwater level reading. Figure 23 and Figure 24 show the groundwater flow direction for the shallow and deep wells, respectively.

Figure 23: Shallow groundwater flow from wells screened less than 30 m deep. Contours are masl.

Figure 24: Deep groundwater flow from wells screened greater than 30 m deep. Contours are masl.

For shallow groundwater wells (Figure 23), the water table elevation ranged from 1.58 m to 168.7 m above sea level. The highest water table elevations (masl) are found in the northern part of the catchment in the Marton area. The highest contour elevations can be found in Marton. They are roughly concordant with the Marton Anticline (Figure 13). Groundwater flows from this topographical high down mostly in a southerly direction towards the Rangitikei River, suggesting some part of the groundwater flow interacts with surface water, most likely just upstream of Bulls. From Marton to Turakina, groundwater flows in a westerly direction, directly to the sea. From Marton to Bulls, the groundwater flows in a southerly direction, before gradually flowing to the south-west, reflecting the general topography of the area. As the topography flattens out from Bulls and Sanson, the groundwater flow gradient also flattens out (indicated by the increasing gap between the flow lines) and groundwater flows towards the sea. Where the groundwater flows beneath the Rangitikei River, the contour lines appear to refract, possibly indicating some sort of interaction between river water and groundwater.

For deep groundwater flow (Figure 24), the water table elevation ranged from 1.32 m to 167.1 m above sea level. The highest water table elevation (masl) is found further inland near Rewa, where groundwater is 160 masl. From here the trend shows a reasonably consistent south-west flow direction, where groundwater appears eventually discharging to the sea. Topographic influences are much gentler in the deep groundwater flow system (Figure 24), compared with the shallow groundwater flow (Figure 23). Groundwater flow gradients are also more consistent and evenly spaced in the deeper groundwater than the shallow groundwater, reflecting less influence from the surface topography.

Figure 23 and Figure 24 demonstrate the difference between the shallow and deep groundwater flow in the study area. Shallow groundwater is more strongly influenced by the local topography and is more likely to have some interaction with streams and rivers under which it flows.

4.3.2 Groundwater – Surface Water Interactions

A longitudinal river flow and water quality survey was used to infer groundwater – surface water interactions along the Lower Rangitikei River from Kakariki Bridge to Tangimoana (almost to the coast), a distance of approximately 25 km. The results of the river flow measurements, river water sampling and groundwater sampling are presented in Table 3 and Table 4. Groundwater sampling was done in December 2014.

Table 3: Longitudinal river flow and water quality survey results for 6 January 2015 with nearby groundwater quality data collected December 2014.

Surface Water Site	Discharge (m^3/s) (Std dev)	Specific Conductivity µS/cm	NO_3^- -N mg/L	Cl^- mg/L	SO_4^{2-} mg/L
1	20.45 (0.16)	172.8	0.03	6.22	10.60
2	22.59 (0.90)	177.1	0.03	7.11	11.65
3	22.13 (0.62)	183.4	0.03	6.99	11.29
4	22.61 (0.35)	185.8	0.02	7.44	11.83
5	16.81				
Groundwater Sites	**Depth (m)**	**Specific Conductivity µS/cm**	**NO_3^- -N mg/L**	**Cl^- mg/L**	**SO_4^{2-} mg/L**
314065	10.00	1098.0	0.001	93.57	124.07
313009	8.60	515.3	0.35	47.29	20.69
323097	21.00	211.2	0.16	9.83	12.24

Table 4: Longitudinal river flow and water quality survey results for 20 January 2015 with nearby groundwater quality data collected December 2014.

Surface Water Site	Flow (m^3/s) (Std dev)	Specific Conductivity µS/cm	NO_3^- -N mg/L	Cl^- mg/L	SO_4^{2-} mg/L
1	14.41 (0.22)	205.9	0.02	8.81	14.49
1.5	13.49 (0.08)	212.8	0.02	9.70	15.40
2	17.92 (0.14)	215.1	0.03	10.01	15.78
3	13.98 (0.10)	215.5	0.03	10.21	15.79
4	14.82 (0.14)	215.8	0.01	10.42	16.23
5	14.51				
Groundwater Sites	**Depth (m)**	**Specific Conductivity µS/cm**	**NO_3^- -N mg/L**	**Cl^- mg/L**	**SO_4^{2-} mg/L**
314065	10.00	1098.0	0.001	93.57	124.07
313009	8.60	515.3	0.35	47.29	20.69
323097	21.00	211.2	0.16	9.83	12.24

Reach 1 – 2

	Changes in Site 1 – 2			
Survey Date	**Discharge m^3/s**	**Specific Conductivity µS/cm**	**Cl^- mg/L**	**SO_4^{2-} mg/L**
6 January 2015	2.14	4.3	0.89	1.05
20 January 2015	3.51	9.2	0.89	0.91

This reach is between the Kakariki Bridge and the Bulls Bridge. On both survey days the river flow was increasing between these two sites. Specific conductivity and both chemical tracers were also increasing, suggesting groundwater discharge into this reach. During the survey on 20 January, another site was added for flow measurement between the bridges (Site 1.5 in Table 4). It shows river discharge decreasing by 0.92 m^3/s between Kakariki Bridge and the new site; though downstream from here it increases substantially by 4.43 m^3/s to the Bulls Bridge. This reach is gaining overall, but most likely gaining upstream from the Bulls Bridge.

Reach 2 – 3

	Changes in Site 2 – 3			
Survey Date	**Discharge**	**Specific Conductivity µS/cm**	**Cl^- mg/L**	**SO_4^{2-} mg/L**
6 January 2015	(0.46)	6.3	(0.12)	(0.36)
20 January 2015	(3.94)	0.4	0.20	0.01

This reach is between the Bulls Bridge and a quarry near McDonnell Road. On both survey days the river flow was decreasing between these two sites. Reasonably small fluctuations were observed for the chemical tracers, though specific conductivity was either stable (20 January) or increasing (6 January). This reach is likely losing to groundwater.

Reach 3 – 4

	Changes in Site 3 – 4			
Survey Date	**Discharge**	**Specific Conductivity µS/cm**	**Cl^- mg/L**	**SO_4^{2-} mg/L**
6 January 2015	0.48	2.4	0.45	0.54
20 January 2015	0.84	0.3	0.21	0.44

This reach is between the quarry at McDonnell Road and another quarry off Campion Road further downstream. On both survey days the river flow was increasing between the two

sites. Specific conductivity and both chemical tracers were also increasing between the two sites, suggesting groundwater discharge into this reach.

Reach 4 – 5

	Changes in Site 4 – 5			
Survey Date	**Discharge**	**Specific Conductivity µS/cm**	**Cl^- mg/L**	**SO_4^{2-} mg/L**
6 January 2015	(5.8)	-	-	-
20 January 2015	(0.31)	-	-	-

This reach is between the quarry at Campion Road and the permanent river flow monitoring station at Tangimoana (known as McKelvie's). Water samples were not taken at this site because of the incoming tide at the time of sampling. Discharge data is therefore collected via a different method from the gauging done at the previous sites. Despite these differences, it is capable of providing an estimate of the discharge between the two sites. On both the survey days river flow was decreasing between the two sites based on this information. Therefore, this reach of the river is said to be losing to groundwater.

It is clear from this analysis that the Rangitikei River has a dynamic relationship with the alluvial aquifer beneath it. The surveys were taken two weeks apart and comparing results with each other suggests a pattern where groundwater commonly seeps into the river. The analysis shows the reach between Kakariki Bridge and Bulls Bridge is gaining from groundwater, particularly just upstream from the Bulls Bridge. Downstream, Reach 2 – 3 is likely to be a losing reach for the river, as discharge decreases on both survey dates. Reach 3 – 4 is likely to be a gaining reach based on the surveys and Reach 4 – 5 is likely to be losing. These results differ with previous published results by Roygard & Carlyon (2004) (Figure 4), though could be due to seasonal differences between these surveys. In this low flow survey, discharge was found to be stable upstream of the Bulls Bridge, although the measurement points were between a much greater distance. Downstream of Bulls, the low flow survey found the reach to be gaining, in contrast to the results of this study, which found a losing reach. Groundwater specific conductivity was also much higher at the two upstream sites, reflecting higher residence times of groundwater, though it was similar to the surface water reading at 323097 (Figure 21 and Figure 22). Cl^- and SO_4^{2-} were also

higher in groundwater compared to surface water, except in 323097, where it was of a similar concentration.

Figure 23 also indicates some gaining and losing reaches of the river, particularly downstream of Bulls. As mentioned in Section 2.1, groundwater – surface water interactions can also be observed where water table contours cross surface water paths (Winter et al., 1998). Figure 5 gives examples where contour lines point upstream indicating groundwater discharge (Figure 5C), and also where contour lines point downstream, indicating groundwater recharge (Figure 5D). A comparison with Figure 23 using these examples suggests groundwater discharge is occurring downstream from Bulls because the 20 m, 30 m, and 40 m contour lines are pointing upstream as they cross the river, while the 10 m contour line is pointing slightly downstream as it crosses the river, suggesting groundwater recharge. These results show some similarity with the longitudinal river flow survey whereby some reaches downstream of Bulls were gaining, though closest to the coast the river was losing.

4.3.3 River Water Quality

Groundwater discharge into the river has now been demonstrated at several locations within the study area. This interaction could allow for the introduction of NO_3^--N to the river, potentially threatening the ecological health. Table 3 and Table 4 present the results of NO_3^--N sampled and analysed from the same locations as the river flow gauging and other tracers in the Lower Rangitikei River. The measured NO_3^--N appears relatively stable through the river reach, usually at a low concentration ranging from 0.01 to 0.03 mg/L. Horizons Regional Council has been monitoring nitrogen concentrations through the Rangitikei River at several locations for the past several years. These have been reported in the form of total oxidised nitrogen (TON), which is the total of NO_3^--N + NO_2^--N. Figure 25, Figure 26 and Figure 27 reproduce the recorded TON concentrations at several locations: Onepuhi, several km upstream from the Kakariki Bridge; the Bulls Bridge; and the McKelvie's permanent monitoring station. The average TON was measured at 0.093 mg/L at Ohepuni over eight years (from 2005 to 2013); 0.111 at the Bulls Bridge over five years (from 2008 to 2013); and 0.146 mg/L at McKelvie's over seven years (from 2006 to 2013). This indicates a

slightly increasing trend in TON concentrations moving from upstream to downstream in the Lower Rangitikei River.

The data shows a predictable spike in the TON concentration each year. During the winter months, the TON increases with higher rainfall, as potentially surface and/or subsurface drain flow increases directly into tributaries and the river itself. The TON decreases again in the summer months, as rainfall reduces and where base flow makes a higher proportion of total discharge. The TON concentrations during low flow conditions seem to be very low and approximately in line with the concentrations recorded for this survey (below 0.05 mg/L NO_3^--N). This demonstrates base flow is rarely responsible for increases in NO_3^--N concentrations in the river, despite there being some level of connection between surface water and groundwater.

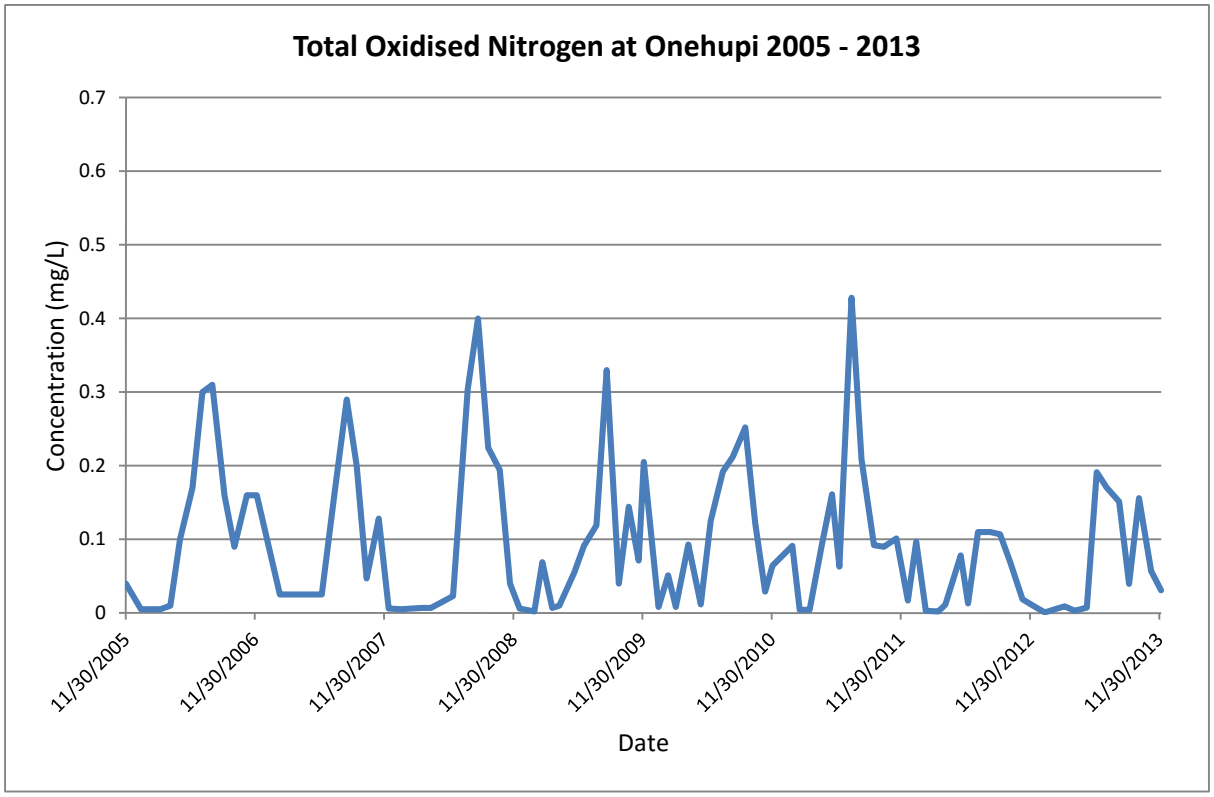

Figure 25: Total oxidised nitrogen (mg/L) at the Onepuhi site.

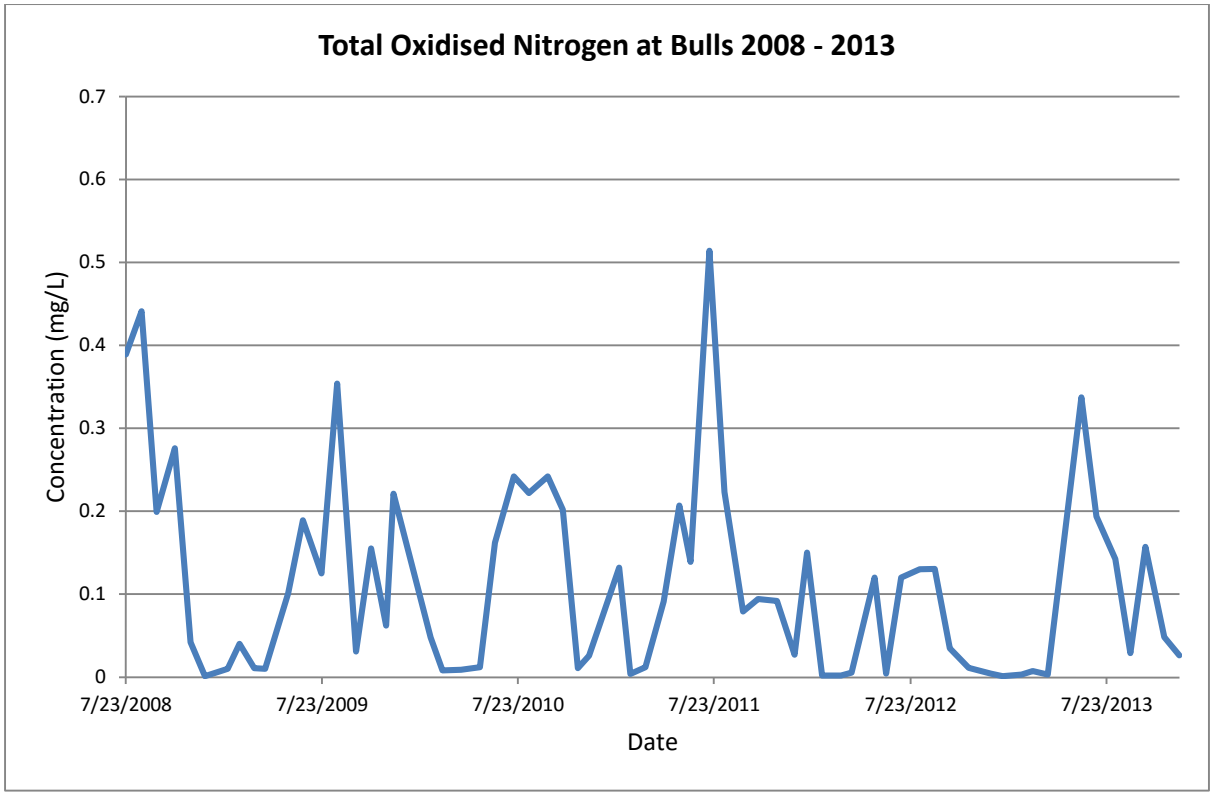

Figure 26: Total oxidised nitrogen (mg/L) at the Bulls Bridge site.

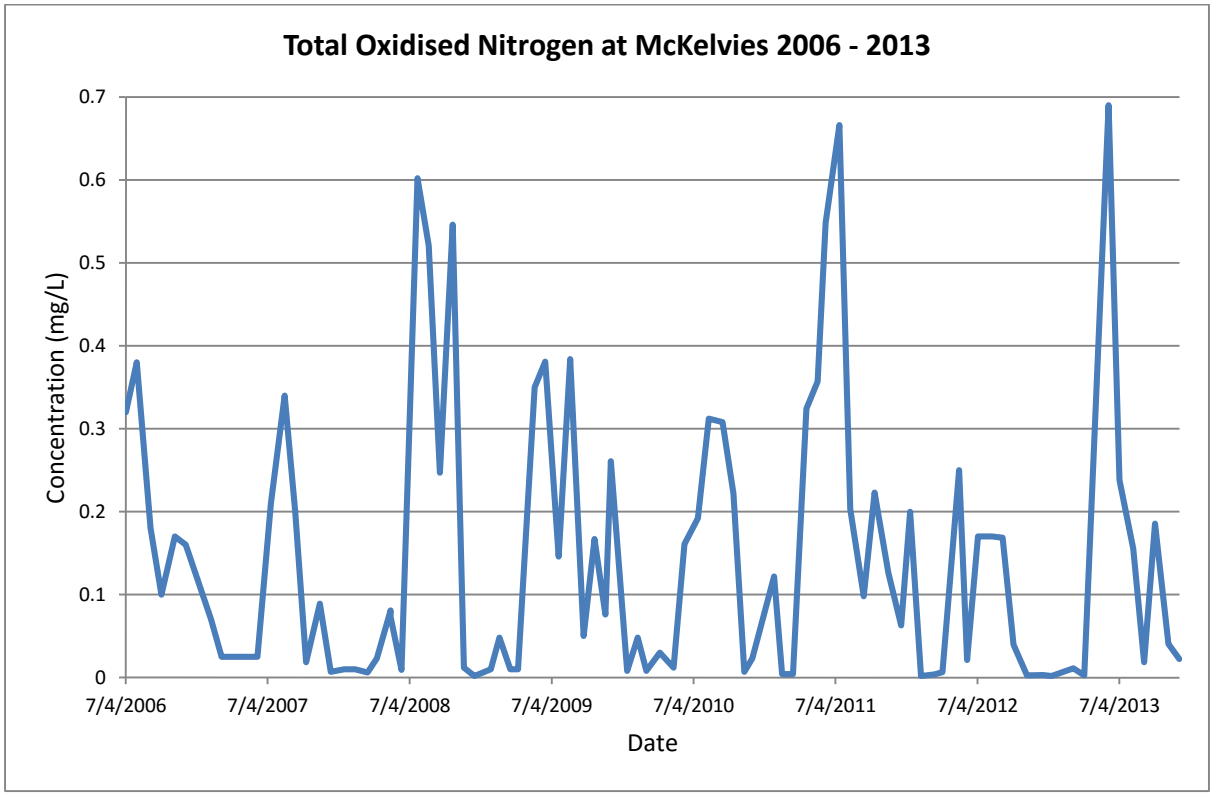

Figure 27: Total oxidised nitrogen (mg/L) at the McKelvie's site.

4.4 Conclusions

Groundwater flow within the study area reflects the wider topographic trend of the region, with groundwater flowing from the higher inland parts down to the coast. There is a negligible difference in the flow regimes of the deep and shallow groundwater, with both generally flowing in a south-west direction, similar to the Rangitikei River itself. The similar direction in which groundwater and surface water are flowing provides for interaction between the river and shallow groundwater. Two longitudinal river flow and water quality surveys (6 and 20 January 2015) during low flow conditions through the Lower Rangitikei River have revealed some interaction with the shallow groundwater beneath the river bed. The river is gaining from groundwater in several locations, but most notably upstream of the Bulls Bridge. The measured NO_3^--N levels during the surveys remain low and relatively stable throughout the entire sampled length of the river and in most cases are also lower in the river than the concentrations in some nearby groundwater wells. The NO_3^--N concentration also tends to increase from upstream to downstream, with NO_3^--N spiking during the wetter seasons when the groundwater influence is more muted. Further investigation into the transport and transformation of NO_3^--N via groundwater and its potential effects on river water quality in the catchment is needed.

5 Groundwater Chemistry and Redox Conditions

5.1 Introduction and Objectives

The redox condition of groundwater affects the transport, fate and concentration of many natural and man-made contaminants. Nitrate is one such contaminant, whose persistence depends to a large extent on the redox condition of the groundwater. Attenuation, or reduction, of NO_3^--N generally requires a low oxygen 'anoxic' environment and the availability of suitable electron donors in the groundwater system for denitrification to occur. By determining the groundwater redox conditions and its spatial distribution, a prediction can be made about the fate of chemicals and the water quality of an aquifer system (McMahon & Chapelle, 2008). This chapter uses water quality data collected in December 2014 to assess the redox condition of the groundwater in the study area and to make an estimate of the potential for NO_3^--N reduction in the Lower Rangitikei catchment.

5.2 Methods and Materials

A total of 15 existing groundwater wells in the study area were selected for a groundwater quality survey in December 2014 (Figure 28). Six of these wells were part of the state of the environment (SOE) quarterly monitoring programme by Horizons Regional Council, while nine others were additionally selected to increase the spatial resolution of the survey results. These nine additional wells were selected on the basis of a reasonably shallow depth, with a single well at 21 m and the remaining wells less than 10 m deep. Overall, the depth of all selected 15 wells ranged from 2 m to 116 m (bgl), though all but one is 30 m or shallower and single screened. The selected wells were sampled according to the National Protocol for SOE Groundwater Sampling in NZ (Daughney, 2006), in particular purging three times the volume of the well before sampling. Groundwater samples were analysed by Environmental Laboratory Services, Wellington, while standard water quality parameters, including dissolved oxygen (DO), specific electrical conductivity and redox potential (ORP) – were measured in the field. These parameters will be used to assess and interpret the groundwater redox processes within the study using a framework developed by McMahon & Chapelle (2008).

Figure 28: Location of groundwater sampling sites in the Lower Rangitikei catchment area, December 2014.

5.3 Results and Discussion

5.3.1 Groundwater Chemistry

Charge Balance Error

To ensure the analytical reliability of water samples it is usual to check the electroneutrality of the water. This is to ensure the water does not carry a net electrical charge (being positive or negative) and is electrically neutral. Most dissolved chemical species carry a charge and electroneutrality demands the sum of positively charges species matches the sum of negatively charged species (Younger, 2007). Electroneutrality can be checked by calculating the charge balance error (CBE):

$$CBE = \frac{\sum cations - \sum anions}{\sum cations + \sum anions} \times 100$$

The CBE calculation requires that all ions be converted to an 'electrical charge per volume' basis, the most appropriate for which is 'milliequivalents per litre (meq/L)'. As ions are commonly reported from laboratories in mg/L, conversion to meq/L is first necessary. Table 5 shows major ions used in the calculation, their concentrations in mg/L, and Table 6 shows their concentrations in meq/L and the calculated CBE for all 15 groundwater samples collected in this study.

If the CBE value is less than 5%, the data is considered sufficiently accurate for all uses. If the CBE lies in the range 5 – 15%, then the analysis should be used with caution, while those with a CBE greater than 15% are not regarded as being sufficiently reliable for scientific purposes (Younger, 2007). The results from Table 6 show all but one of the wells sampled in this study are within the +/-5% threshold; hence included in further analysis. Only one well, no. 313009, had a CBE of -7.99% (Table 6), though it was also considered adequate for this study.

Table 5: Ion concentrations in mg/L of wells sampled in the Lower Rangitikei catchment, December 2014.

Well ID	Ca^{2+} (mg/L)	Mg^{2+} (mg/L)	K^{+} (mg/L)	Na^{+} (mg/L)	Cl^{-} (mg/L)	SO_4^{2-} (mg/L)	NO_3^{-}-N (mg/L)	HCO_3^{-} (mg/L)
312004	30.49	22.44	4.06	19.19	27.86	0.01	0.40	207.77
312020	139.00	46.26	7.88	55.33	127.12	109.01	0.02	430.61
312001	67.62	11.64	5.63	34.01	64.44	<0.01	0.01	271.86
324067	49.67	43.72	6.50	96.04	173.04	118.55	0.02	240.18
332025	59.08	12.87	4.33	39.60	46.27	2.41	0.04	245.69
332009	49.87	16.05	5.02	28.43	28.98	<0.01	0.01	264.94
322045	106.17	11.55	12.03	40.82	58.27	43.06	1.17	301.52
322071	39.55	11.70	4.20	32.00	38.44	33.97	4.47	133.61
323097	20.71	4.19	1.94	16.55	9.83	12.24	0.16	89.34
333005	95.84	37.49	12.64	129.48	348.22	127.70	1.90	102.94
313009	32.34	11.98	4.00	26.78	47.29	20.69	0.35	168.74
343119	68.60	6.45	4.65	14.42	33.14	10.30	<0.01	215.43
323091	29.62	23.82	4.31	41.33	67.19	58.34	1.78	130.83
323077	29.42	15.56	3.18	39.68	56.00	15.18	<0.01	155.23
314065	98.62	43.24	7.46	65.56	93.57	124.07	<0.01	362.79
Minimum	20.71	4.19	1.94	14.42	9.83	<0.01	<0.01	89.34
Maximum	139.00	46.26	12.64	129.48	348.22	127.70	4.47	430.61
Mean	61.11	21.26	5.85	45.28	81.31	45.03	0.69	221.43
Standard dev.	34.77	14.37	3.05	31.24	84.86	49.67	1.23	96.48
Coefficient of variation	0.57	0.68	0.52	0.69	1.04	1.10	1.79	0.44

Table 6: Ion concentrations in meq/L with CBE results of wells sampled in the Lower Rangitikei catchment, December 2014.

Well ID	Ca^{2+} (meq/l)	Mg^{2+} (meq/l)	K^{+} (meq/l)	Na^{+} (meq/l)	Cl^{-} (meq/l)	SO_4^{2-} (meq/l)	NO_3^{-}-N (meq/l)	HCO_3^{-} (meq/l)	Total cations (meq/l)	Total anions (meq/l)	CBE %
312004	1.52	1.85	0.10	0.83	0.79	<0.01	<0.01	3.41	4.31	4.20	1.20
312020	6.93	3.81	0.20	2.41	3.58	2.27	<0.01	7.06	13.36	12.94	1.55
312001	3.37	0.96	0.14	1.48	1.82	<0.01	<0.01	4.46	5.96	6.28	-2.65
324067	2.48	3.60	0.17	4.18	4.87	2.47	<0.01	3.94	10.42	11.29	-4.00
332025	2.95	1.06	0.11	1.72	1.30	0.05	<0.01	4.03	5.84	5.39	3.99
332009	2.49	1.32	0.13	1.24	0.82	<0.01	<0.01	4.34	5.17	5.18	-0.03
322045	5.30	0.95	0.31	1.78	1.64	0.90	0.02	4.94	8.33	7.50	5.22
322071	1.97	0.96	0.11	1.39	1.08	0.71	0.07	2.19	4.44	4.05	4.49
323097	1.03	0.35	0.05	0.72	0.28	0.26	<0.01	1.46	2.15	2.00	3.55
333005	4.78	3.09	0.32	5.63	9.81	2.66	0.03	1.69	13.82	14.20	-1.35
313009	1.61	0.99	0.10	1.16	1.33	0.43	<0.01	2.77	3.87	4.54	-7.99
343119	3.42	0.53	0.12	0.63	0.93	0.22	<0.01	3.53	4.70	4.69	0.14
323091	1.48	1.96	0.11	1.80	1.89	1.22	0.03	2.14	5.35	5.28	0.59
323077	1.47	1.28	0.08	1.73	1.58	0.32	<0.01	2.54	4.56	4.44	1.26
314065	4.92	3.56	0.19	2.85	2.64	2.59	<0.01	5.95	11.52	11.18	1.52
Minimum	1.03	0.35	0.05	0.63	0.28	0.05	0.02	1.46	2.15	2.00	-7.99
Maximum	6.93	3.81	0.32	5.63	9.81	2.66	0.07	7.06	13.82	14.20	5.22
Mean	3.05	1.75	0.15	1.97	2.29	1.18	0.04	3.63	6.92	6.88	0.50
Standard dev.	1.73	1.18	0.08	1.36	2.39	1.03	0.02	1.58	3.66	3.70	3.47
Coefficient of variation	0.57	0.68	0.52	0.69	1.04	0.88	0.59	0.44	0.53	0.54	6.96

Electrical conductivity, pH and Eh

The 'specific electrical conductance' is the ability of water to conduct electricity and is directly proportional to the amount of dissolved, charged ions it contains, usually expressed as micro Siemens per centimetre (µS/cm) (Younger, 2007). Groundwater usually has a higher electrical conductivity than surface water because it has been in contact with rocks and sediments for longer, dissolving the minerals. This has given the opportunity for groundwater to dissolve soluble minerals and carry them in solution. The electrical conductivity of samples collected in this study ranged from 211.2 to 1710 µS/cm, indicating longer residence time of groundwater with a high level of dissolved minerals in solution.

pH measures the availability of hydrogen ions (H^+) in a solution. It is the most common measure of the acidity/alkalinity balance in a solution (Younger, 2007). The collected groundwater samples ranged in *pH* from 6.29 to 7.63, with eight of the wells below *pH* 7.0 suggesting groundwater at some locations in the study area is slightly acidic.

Eh is a measure of the status of redox reactions in water and is known as redox potential. It is a measure of the status of electron distribution between potentially interacting ions and is therefore usually measured in millivolts (Younger, 2007). Generally, in well-oxygenated waters, in which most cations are in their most highly charged forms (e.g. Fe^{3+} as opposed to Fe^{2+}), these waters tend to display high values of *Eh* (>100 mV). Alternatively, in waters lacking DO, in which cations are in their least charged form, *Eh* tends to be low (<100 mV), or even negative (Younger, 2007). *Eh* was not tested at all the wells sampled in this survey, but it was tested at nine of them. In these nine wells the *Eh* ranged from -121.4 to 55.6 mV, suggesting groundwater in the study area is potentially under reduced conditions.

Major Cations

Cations present in their greatest concentrations (usually greater than 1 mg/L) in groundwater are generally calcium (Ca^{2+}), magnesium (Mg^{2+}), sodium (Na^+) and potassium (K^+). These were all represented in the groundwater wells sampled. Calcium ranged from 20.71 mg/L to 139 mg/L; Mg^{2+} ranged from 4.19 mg/L to 46.26 mg/L; Na^+ ranged from 14.42 mg/L to 129.48 mg/L; and K^+ ranged from 1.94 mg/L to 12.64 mg/L (Table 5). Figure 29 displays the relative proportions of major cations in meq/L. The proportion of each cation

varied depending on the location, though Ca^{2+} was usually the largest component of cations (Figure 29). Magnesium and Na^{+} often had a similar or equal share of total cations, with K^{+} always making up the smallest proportion of the major cations (Figure 29).

Major Anions

Anions present in the greatest concentrations (usually greater than 1 mg/L) in groundwater are generally bicarbonate (HCO_3^{-}), sulphate (SO_2^{4-}) and chloride (Cl^{-}). In this study, bicarbonate was the most dominant anion in all samples ranging from 89.34 mg/L to 430.61 mg/L (Table 5). Sulphate had no or very low concentrations in several wells, but was present in concentrations of up to 127.7 mg/L; and Cl^{-} was present ranging from 9.83 mg/L to 348.22 mg/L (Table 5). Figure 30 displays the relative proportions of major anions in meq/L.

Chloride exceeds the guideline value (Ministry of Health, 2008) at only one location, at well 333005. The guideline value for chloride is 250 mg/L, which is primarily based on taste and corrosive potential, though at 333005 Cl^{-} is as high as 348.2 mg/L, therefore exceeding it. This well represents the shallowest that was sampled in the survey (2 m), so it is more likely to show any contamination. The site is an olive orchard, though it is not known whether any fertilisers or supplements are used.

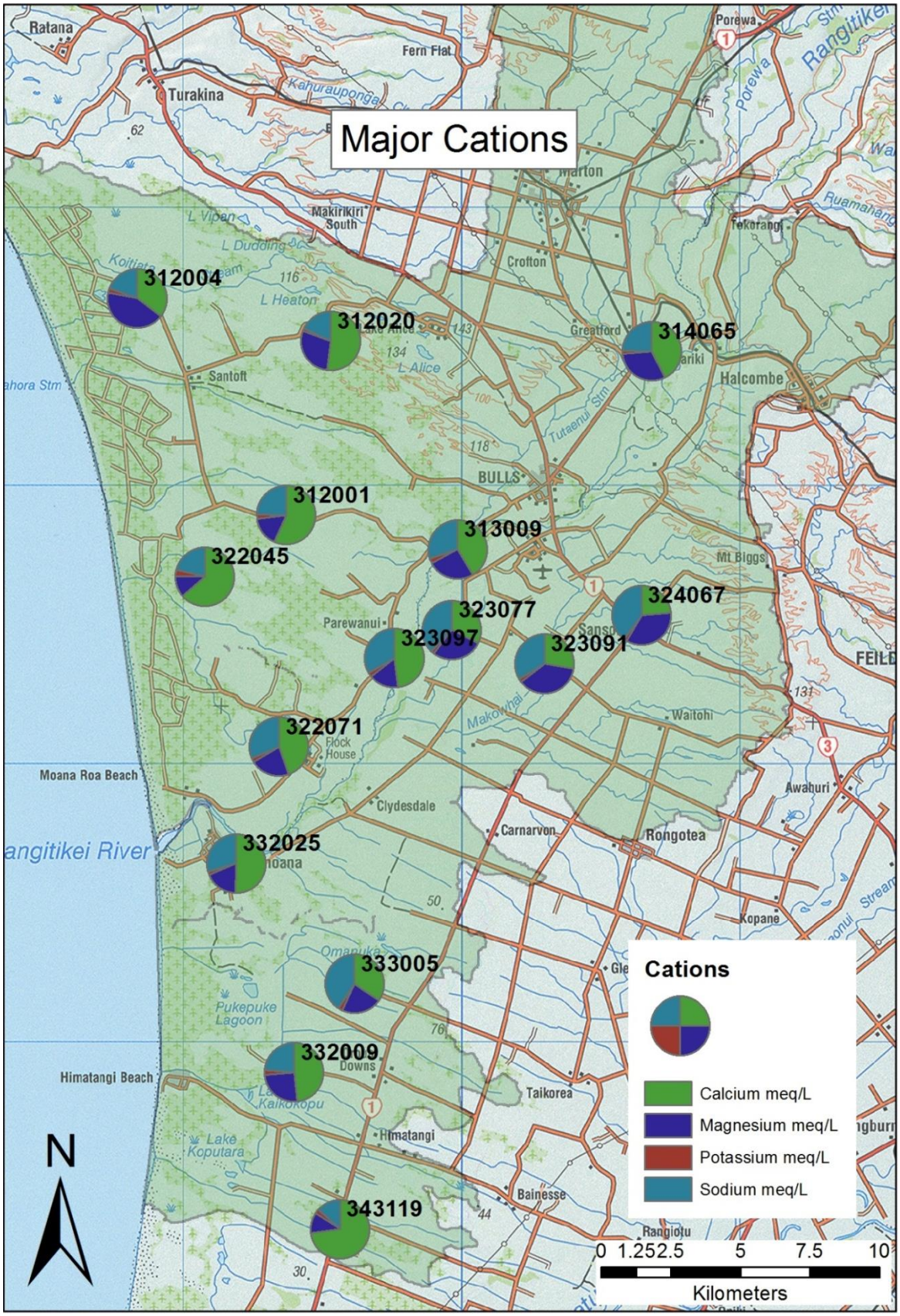

Figure 29: Distribution of major cations in groundwater in the Lower Rangitikei catchment, December 2014.

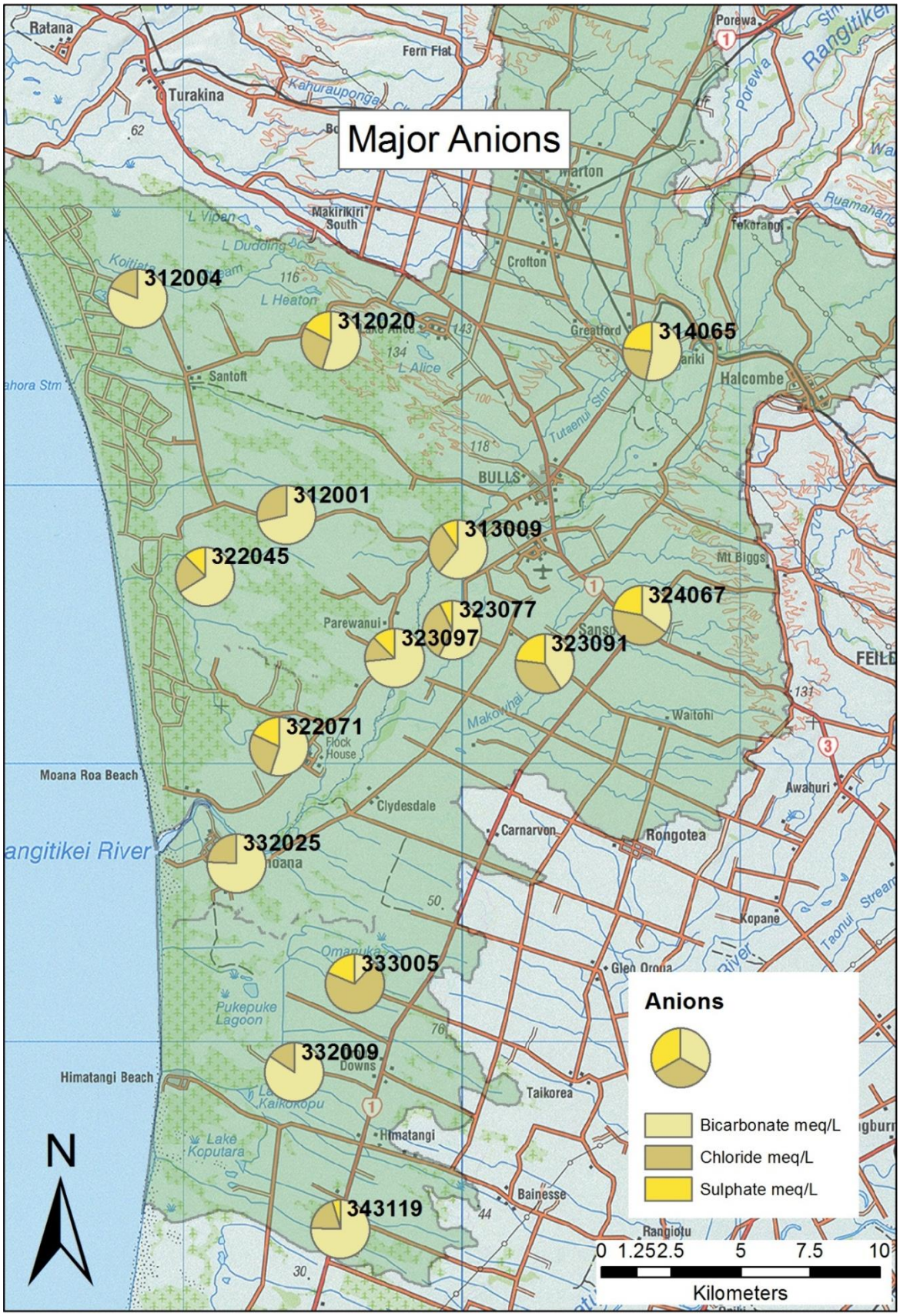

Figure 30: Distribution of major anions in groundwater in the Lower Rangitikei catchment, December 2014.

Total Dissolved Solids

Total dissolved solids (TDS) is a basic water quality measure of the overall degree of mineralisation, i.e. its content of dissolved mineral matter (Younger, 2007). TDS is determined by evaporation in a laboratory setting, though it can also be estimated by multiplying the electrical conductivity of the water by a factor in the range 0.55 – 0.75, with 0.65 commonly used (Younger, 2007). Water type can then be classed as follows in Table 7:

Table 7: Water classification based on Total Dissolved Solids (Younger, 2007).

Class	TDS
Fresh Water	<1000 mg/L
Brackish Water	1000 mg/L < TDS < 10,000 mg/L
Saline Water	10,000 mg/L < TDS < 100,000 mg/L
Hyper-saline Water	>100,000 mg/L

In this study, TDS was analysed for six samples only (Table 8) and was estimated for all samples using the measured electrical conductivity multiplied by a factor of 0.65 as described above. The actual and estimated TDS for six samples was in close agreement, validating the estimation of the TDS for other samples (Table 8, see below). These results show all samples analysed could be considered fresh water, with one at the border line between fresh water and brackish water (333005).

Table 8: Actual and estimated TDS of wells sampled in the Lower Rangitikei catchment, December 2014.

Well	TDS mg/L (actual)	TDS mg/L (estimated)
312004	298.91	263.22
312020	793.96	769.32
312001	400.52	402.54
324067	679.45	698.7
332025	357.13	355.26
332009	346.27	312.9
322045		457.2
322071		271.98
323097		126.72
333005		1026
313009		309.18

343119		302.04
323091		350.76
323077		284.64
314065		658.8

Minor Ions

A number of other minor ions were also collected, which are commonly found at lower concentrations than the major ions mentioned above. Their values for the sampled groundwater are shown in Table 9. Nitrate-nitrogen is generally low when compared to the 11.3 mg/L limit set for drinking water standards in New Zealand (Minisry of Health, 2008). No sample came close to this limit, with all samples being in the range of 0.001 – 4.47 mg/L. Most of the samples had a NO_3^--N concentration below 0.5 mg/L, with only four wells having a concentration greater than 1 mg/L. Figure 31 shows the spatial distribution of NO_3^--N in the sampled wells. The highest NO_3^--N concentration (4.47 mg/L) was recorded on a cropping property in the monitoring well (322071) installed at a depth of 10 m (bgl). The other three relatively high NO_3^--N concentrations were found on land used for cropping (322045), dairy (323091), and a residential property, though neighbouring land was used for dairying. Alternatively, there are some locations with intensive land uses that have low nitrate concentrations, including 323077 (cropping), 313009 (dairy), and 343119 (cropping).

Table 9: Concentration of minor ions collected from groundwater in the Lower Rangitikei catchment, December 2014.

Well ID	Br^- (mg/L)	As (mg/L)	B^{3+} (mg/L)	Mn^{2+} (mg/L)	Fe^{2+} (mg/L)	SiO_2 (mg/L)	NO_3^--N (mg/L)	NO_2^--N (mg/L)	NH_4^+-N (mg/L)	Land Use
312004	0.11	<0.01	0.03	0.26	9.80	60.4	0.40	<0.01	0.76	Unknown
312020	0.38	<0.01	0.03	0.19	0.39	44.6	0.02	<0.01	0.43	Golf course
312001	0.18	0.02	0.04	1.33	9.89	51.74	0.01	<0.01	2.02	Sheep/beef
324067	0.52	<0.01	0.02	0.33	20.37	67.12	0.02	<0.01	0.11	Unknown
332025	0.24	<0.01	0.04	0.70	8.87	52.45	0.04	<0.01	0.76	Grazing
332009	0.09	<0.01	0.04	0.63	0.32	54.46	0.01	<0.01	0.16	Unknown
322045	0.32		0.06	1.03	<0.01	23.71	1.17	0.01	0.09	Cropping
322071	0.15		0.04	0.11	0.51	26.65	4.47	0.01	0.04	Cropping
323097	0.04		0.04	0.24	0.02	14.1	0.16	0.01	0.01	Cropping
333005	0.38		0.02	0.02	0.86	29.9	1.90	0.09	0.02	Orchard
313009	0.11		0.03	0.42	1.38	50.67	0.35	<0.01	0.01	Dairy
343119	0.09		0.03	0.25	4.20	40.83	<0.01	<0.01	1.23	Cropping/Grazing
323091	0.24		0.07	0.46	1.29	27.05	1.78	0.02	0.07	Dairy
323077	0.22		0.03	1.1	0.31	54.48	<0.01	<0.01	0.01	Cropping
314065	0.28		0.03	0.38	0.87	41.51	<0.01	<0.01	0.31	Grazing
Minimum	0.04	0.02	0.02	0.02	0.02	14.10	0.01	0.01	0.01	
Maximum	0.52	0.02	0.07	1.33	20.37	67.12	4.47	0.09	2.02	
Mean	0.22	0.02	0.04	0.50	4.22	42.64	0.86	0.03	0.40	
Standard dev.	0.13	0.00	0.01	0.37	5.74	14.79	1.28	0.03	0.56	
Coef. of variation	0.58	0.00	0.35	0.75	1.36	0.35	1.48	1.12	1.39	

Figure 31: Distribution of NO_3^--N in groundwater in the Lower Rangitikei catchment, December 2014. The size of the dots represents the relative concentration of NO_3^--N.

5.3.2 Hydrochemical Facies and Groundwater Classification

Once the hydrochemistry of the groundwater has been established, it is possible to assign waters to a hydrochemical facies, defined as zones within a groundwater system that display distinctive combinations of cation and anion concentrations (Younger, 2007). The hydrochemical facies can be found by identifying the predominant cations and anions in a given water on the basis of percent of total meq/L for each category. To help interpret the nature of the groundwater and describe the hydrochemical facies, it is usual to present groundwater results in a graphical form, typically a Piper diagram (Piper, 1944). These diagrams present a combination of the cation and anion proportions in two triangles, the points of which are then projected on to the diamond between them as circles proportional to their TDS. The position of these points on the diagram is finally used to interpret the hydrochemical facies. Figure 32 shows the results for the December 2014 groundwater survey in the study area.

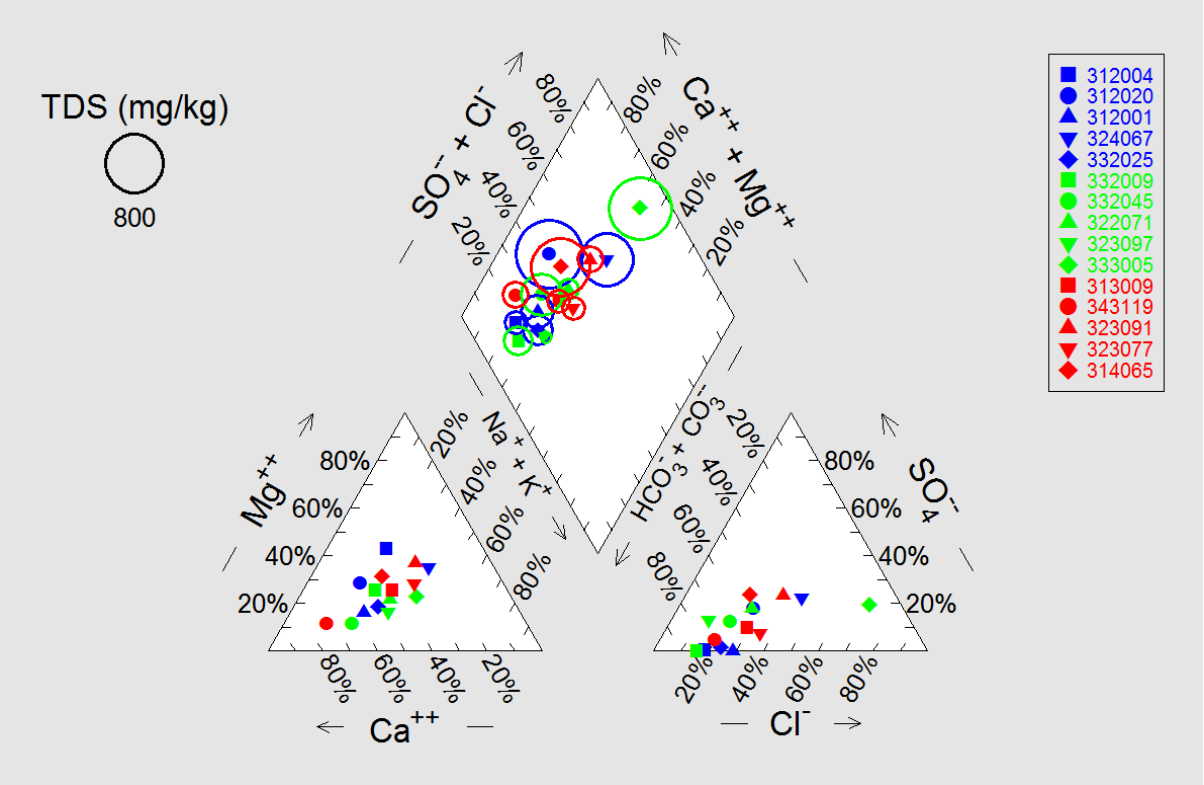

Figure 32: Piper diagram with results of the December 2014 groundwater survey. Colours are only for differentiation.

The results of the Piper diagram show some variation in the water types found in the study area. Calcium is the dominant cation at most of the locations, which has often formed ionic

bonds with the most common anion, bicarbonate, forming $CaHCO_3$. Calcium bicarbonate is a common dissolved constituent of groundwater. At some locations, other cations and anions dominate the water chemistry. Na in particular is the dominant cation at several locations which is most often combined with Cl^- creating NaCl salts.

An analysis of the SOE sampling round was undertaken in 2012, using all 21 monitored wells in the Horizons region (PDP, 2013). These results were also plotted on a Piper diagram and show the data typically plots in two clusters, highlighted as Group 1 in blue and Group 2 in brown (Figure 33). Group 2 wells indicate groundwater dominated by Ca^{2+} and HCO_3^-, whereas Group 1 wells suggest groundwater with a greater influence of Na^+ and Cl^-. There were four wells that did not fit into either of the two water-type groups defined. Group 1 wells were mostly shallow (0 – 20 m), located near the Manawatu, Mangatainoka and Ohau Rivers. While the Piper diagram suggests these wells have a Na^+ and Cl^- component, there is no obvious dominant chemical component which could be demonstrating the mixing of waters from surface water recharge and diluting the chemical composition of groundwater in these wells (PDP, 2013). Group 2, on the other hand, is generally located on the Manawatu Plains and the coastal Rangitikei lowlands. The Ca^{2+} and HCO_3^- dominant chemical component of the Group 2 wells is possibly related to the geology of underlying sediments in these locations. Groundwater dominated by Ca^{2+} and HCO_3^- can be indicative of $CaCO_3$-rich sediments such as limestone, or calcareous marine sediments (Hiscock & Bense, 2005; PDP, 2013).

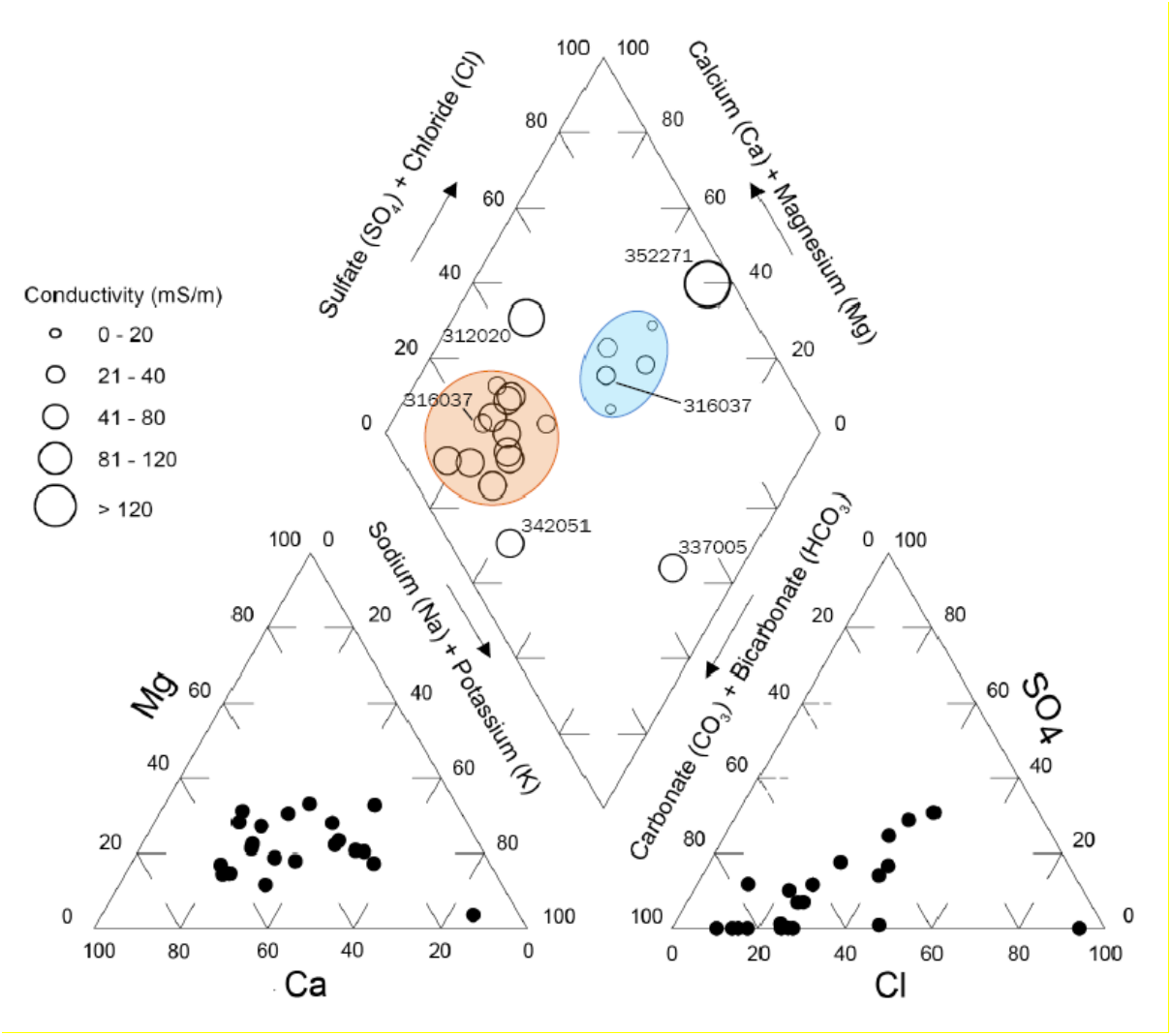

Figure 33: Piper diagram of major cation and anion data. Blue area indicates Group 1 water type and brown area indicates Group 2 water type (PDP, 2013).

When dissolved organic carbon (DOC), DO and NO_3^--N results are compared to the well depth, there are several trends that could be identified (Figure 34). In this analysis, the deepest well (116 m, well 312020) was purposefully left out to give a greater perspective on how certain groundwater variables behaved at shallow depths in the study area. DOC was collected at only nine of the sampling sites in the study area. In general, most groundwater will contain at least a few mg/L of DOC (Weight, 2008). An inverse relationship exists between the measured DOC levels and groundwater depth, where DOC decreased with the increasing depth. This is likely due to resident carbon sources (such as peat) present in the ground, or leaching from the upper layers. The same inverse relationship was found between the groundwater depth and DO and NO_3^--N, with higher DO and NO_3^--N levels at shallow depths. The three graphs in Figure 34 show a reduction in these parameters below

10 m depth. If NO_3^--N is being reduced at depths <10 m, it is likely DOC is the electron donor, though at depths >10 m, some other electron donor may be responsible.

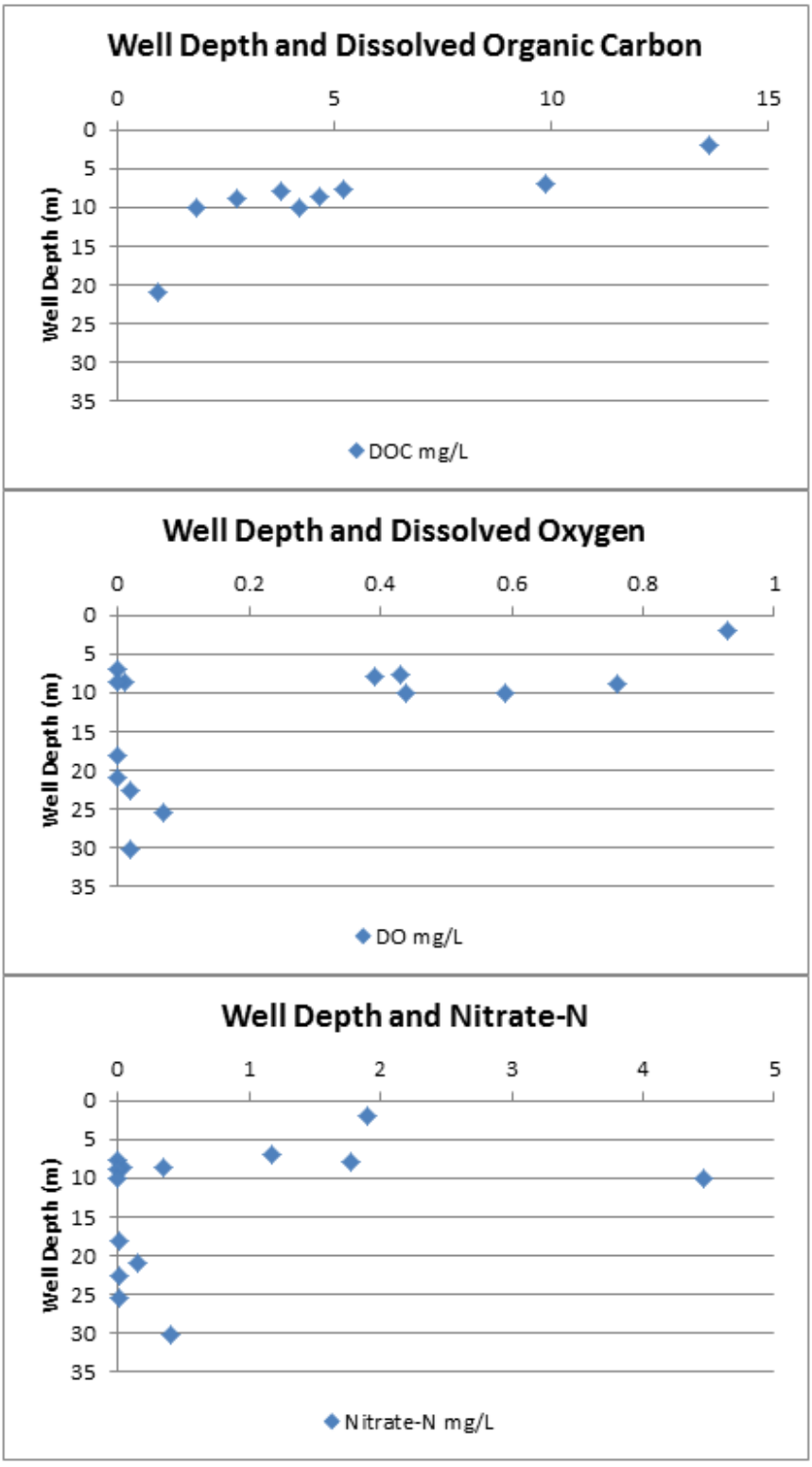

Figure 34: Concentration of selected chemical constituents relative to well depth of groundwater in the Lower Rangitikei catchment, December 2014.

5.3.3 Groundwater Redox Conditions

Oxidation-reduction (redox) reactions involve a change in the oxidation state of a chemical compound. The oxidation state (also known as the oxidation number) represents the hypothetical charge an atom would have if the ion or molecule were to dissociate. An oxidation reaction involves the loss of electrons, while reduction reactions involve the gain of electrons. Every oxidation is accompanied by a reduction and vice versa, so balance is always maintained (Hiscock & Bense, 2005). Each reaction requires an electron donor and a terminal electron acceptor. Given the major redox components of groundwater are O_2, $NO_3^-/N_2/NH_4^+$, SO_4^{2-}/HS^-, Mn^{2+}/Mn^{4+} and Fe^{2+}/Fe^{3+}, any redox reactions occurring in groundwater are able to influence the outcome of many environmental problems.

Microorganisms are responsible for catalysing these reactions in groundwater, though they are selective about which reactants they choose to metabolise and they also compete for limited resources. Dissolved organic carbon (DOC) is the most available electron donor, though reduced forms of iron and sulphur can alternatively be used as donors as well (Korom, 1992). For electron acceptors, DO produces more energy per mole of organic carbon than any other available electron acceptor and is therefore preferred by microorganisms. Under anoxic conditions, NO_3^- is the next most energetically favourable electron acceptor, followed by Mn^{4+}, Fe^{3+}, SO_4^{2-}, and lastly CO_2. This order of preferential electron acceptor utilisation is known as the ecological succession of terminal electron acceptors (Figure 7). A consequence of this ecological succession is redox processes have a tendency to segregate into zones dominated by a single electron-accepting process (McMahon & Chapelle, 2008).

By documenting the consumption of electron acceptors and the production of redox end products (such as excess N_2, H_2S, CH_4 and H_2), the redox process operating in a particular groundwater system can be determined. But these parameters are not typically measured in regional water quality assessments. To accommodate this limitation, McMahon & Chapelle (2008) have developed a framework for assessing redox processes, based on water quality parameters commonly collected in regional water quality assessments. The redox framework is based on the dissolved concentration of five commonly measured water quality parameters (dissolved O_2, NO_3^--N, Mn^{2+}, Fe^{2+}, and SO_4^{2-}). A set of threshold

concentrations for those parameters used to determine the dominant redox process for that particular water sample at a particular point in time (Table 10). As discussed in Chapter 2, the anoxic process of NO_3^--N reduction is known as denitrification and is responsible for NO_3^- attenuation in a groundwater system. The capacity for denitrification is therefore dependent on the redox condition of the groundwater. Once the dominant redox processes of an aquifer are known, predictions can be made about the fate of NO_3^--N and its subsequent transformation.

Table 10: Threshold concentrations for identifying redox processes in aquifer systems (McMahon & Chapelle, 2008).

	Water Quality Criteria (mg/L)					
Redox Process	**O_2**	**NO_3^--N**	**Mn^{2+}**	**Fe^{2+}**	**SO_4^{2-}**	**Comments**
Oxic						
O_2 reduction	≥0.5	—	<0.05	<0.1	—	—
Suboxic						
—	<0.5	<0.5	<0.05	<0.1	—	Further definition of redox processes not possible
Anoxic						
NO_3^- reduction	<0.5	≥0.5	<0.05	<0.1	—	—
Mn(IV) reduction	<0.5	<0.5	≥0.05	<0.1	—	—
Fe(III)/SO_4^{2-} reduction	<0.5	<0.5	—	≥0.1	≥0.5	—
Methanogenesis	<0.5	<0.5	—	≥0.1	<0.5	—
Mixed						
—	—	—	—	—	—	Criteria for more than one redox process are met

To make these assignments simple, McMahon & Chapelle (2008) have provided a Microsoft Excel workbook for identifying redox processes in groundwater. Data is inputted into the spreadsheet and the redox category is assigned by a process of elimination starting with DO. If the DO level is greater than 0.5 mg/L, the redox category is considered oxic until O_2 is depleted below this level. If other electron acceptors are present these will also be subsequently reduced. Combinations of redox processes can occur together if electron acceptors are present, though some species will not be reduced, no matter the concentration of that species (e.g. NO_3^--N will not be reduced if O_2 is present). In these cases, the redox category will be described as mixed. The redox process can then be identified with an examination of which electron acceptors have a high enough concentration that will succeed O_2 in the ecological succession. Table 11 displays the 15 groundwater samples with the redox variables, their concentrations, and the resulting redox

category and process according to the threshold values in Table 10. The results displayed in Table 11 show a variation in the redox category and redox processes that are active in the study area. Ten of the sites show a purely anoxic condition, where the DO concentration is less than 0.5 mg/L, and have a single redox process (or where the redox process cannot be distinguished between Fe^{3+} and SO_4^{2-} reduction, more on this below). A further two sites are classed as anoxic, but could have more than one redox process occurring. Another three sites are mixed, having both oxic and anoxic redox categories, with a range of redox processes occurring.

Table 11: Redox assignment of 15 groundwater wells surveyed in December 2014 in the Lower Rangitikei catchment.

Redox Variables	**DO**	**NO_3^--N**	**Mn^{2+}**	**Fe^{2+}**	**SO_4^{2-}**	**Redox Category**	**Redox Process**
Unit	**mg/L**	**mg/L**	**mg/L**	**mg/L**	**mg/L**		
Threshold Value	**0.5**	**0.5**	**0.05**	**0.1**	**0.5**		
312004	0.02	0.40	0.26	9.80	0.01	Anoxic	CH_4
312020	0.00	0.02	0.19	0.39	109.01	Anoxic	Fe(III)/SO_4
312001	0.00	0.01	1.33	9.90	<0.01	Anoxic	CH_4
324067	0.02	0.02	0.33	20.37	118.55	Anoxic	Fe(III)/SO_4
332025	0.01	0.04	0.70	8.87	2.41	Anoxic	Fe(III)/SO_4
332009	0.07	0.01	0.63	0.32	<0.01	Anoxic	CH_4
322045	0.00	1.17	1.03	0.01	43.10	Mixed (anoxic)	NO_3-Mn(IV)
322071	0.59	4.47	0.11	0.51	33.98	Mixed (oxic-anoxic)	O_2-Fe(III)/SO_4
323097	0.00	<0.01	0.24	0.02	12.24	Anoxic	Mn(IV)
333005	0.93	1.90	0.02	0.86	127.69	Mixed (oxic-anoxic)	O_2-Fe(III)/SO_4
313009	0.00	0.35	0.42	1.38	2.07	Anoxic	Fe(III)/SO_4
343119	0.43	<0.01	0.25	4.20	10.32	Anoxic	Fe(III)/SO_4
323091	0.39	1.78	0.46	1.29	58.34	Mixed (anoxic)	NO_3-Fe(III)/SO_4
323077	0.76	<0.01	1.10	0.31	15.18	Mixed (oxic-anoxic)	O_2-Fe(III)/SO_4
314065	0.44	<0.01	0.38	0.87	124.07	Anoxic	Fe(III)/SO_4

Aerobic respiration

Using the threshold values provided in Table 11, aerobic respiration is expected to take place at three locations: 322071, 333005, and 323077 in the study area. According to the ecological succession of terminal electron acceptors, oxygen will first be depleted before other electron acceptors, due to its higher oxidation status. Wells 322071 and 333005 have high DO levels and also have relatively high NO_3^--N levels. As expected at these sites, the NO_3^--N has remained in favour of DO being reduced, thereby preserving the NO_3^- in the shallow groundwater. However, at site 323077, DO is available in the groundwater, though there is very little NO_3^--N present. This is possibly because NO_3^--N was never present at this site despite surrounding land use being used for cropping.

Denitrification

Once DO has been depleted, NO_3^--N will become the terminal electron acceptor. This is expected to occur at 322045 and 323091, as well as those sites listed above as the DO level decreases. These two sites have the only other relatively high NO_3^--N levels, compared with the other sites sampled in December 2014. Nitrate at these two sites will be denitrified, and therefore may have lower NO_3^--N concentrations than if DO levels were higher. These two sites, as well as 322071 and 333005 (mentioned above), are the only sites with NO_3^--N levels above 1 ppm, with all other sites having less than half this level.

Manganese reduction

Once NO_3^--N has been exhausted, Mn^{4+} will become the primary electron acceptor the product of reduction is Mn^{2+}. This is expected to occur at 323097 and 322045. Mn is commonly in the form of MnO_2.

Iron/Sulphate reduction

This combination of redox category and redox process occurs at six locations: 312020; 324067; 332025; 313009; 343119; 314065. Fe^{3+} and SO_4^{2-} reduction do not actually occur simultaneously. Rather it is one limitation of the framework that it cannot distinguish between the two reduction processes. This is acknowledged by McMahon & Chapelle (2008). Ferrous iron is a reactive species and subject to mineral precipitation and sorption processes, therefore the concentration threshold may underestimate the extent of Fe^{3+}

reduction in some aquifers. Also, because the nature of Fe^{3+} reduction is partly dependent on the crystalline form of solid Fe^{3+} present in the system, it is difficult to distinguish between Fe^{3+} reduction and SO_4^{2-} reduction in groundwater systems (McMahon & Chapelle, 2008). McMahon et al. (2009) proposed a solution to this by using Fe^{2+}/H_2S ratios to distinguish between Fe^{3+} and SO_4^{2-} reduction; however, H_2S was not collected as part of this survey.

At 116 m, well 312020 is much deeper than all the other wells considered for this study. At such a depth it could not be considered representative of the shallower groundwater, though evidence of reducing conditions can still be seen in this area from the soil profile. Fe^{3+} is reduced to Fe^{2+} in wet, anoxic soils, though at the wet-dry boundary the iron is precipitated again as Fe^{3+} in the presence of oxygen. The result is a hard iron pan (Figure 35) that develops often in the topsoil and can impede drainage and rooting depth.

Figure 35: Iron pan about 30 cm from the surface, though the depth can vary. The pan shows evidence of ferrous iron being oxidised at the oxic/anoxic interface.

Methanogenesis

Methanogenesis occur at three locations in the study area: 312004, 312001, and 332009. Methanogenesis is the reduction of CO_2 by methanogens, typically occurring when all other

electron acceptors have been consumed. It is the least efficient metabolic process for converting oxygen into energy. This process implies NO_3^--N, Mn^{4+}, Fe^{3+} and SO_4^{2-} have all been reduced (or were not present in the first instance) and microbes are now only reducing the remaining electron acceptor – CO_2.

5.4 Conclusions

Groundwater in the region is dominated by the $CaHCO_3$ water type, a common hydrochemical facies which is often considered 'hard water'. Deeper groundwater generally had fewer dissolved constituents when compared with shallow groundwater, in particular dissolved organic carbon, DO and NO_3^--N. These points reinforce that shallow groundwater is always at a greater risk of pollution and often depend on the activities that are occurring on the surface. Nitrate is a redox sensitive chemical that will either persist or be reduced, depending on the presence of other certain parameters. The hydrochemical data collected from the groundwater survey was used to predict the redox condition of the groundwater and whether NO_3^- would be prone to reduction in the Lower Rangitikei catchment area. Because the redox condition of any water depends on the presence and concentration of a number of variables, 15 groundwater samples analysed for this study showed redox conditions at various stages of reduction, varying from aerobic respiration to methanogenesis. Overall, it showed generally reducing conditions in terms of NO_3^--N reduction, including low DO levels, high DOC levels and the presence of alternative electron donors including Fe^{2+}. This suggests a good potential for NO_3^--N reduction in groundwater in the Lower Rangitikei catchment. However, this needs further investigation by *in-situ* measurements of denitrification occurrence in the shallow groundwater of the study area.

6 Measuring Shallow Groundwater Denitrification

6.1 Introduction and Objectives

Shallow groundwater denitrification was estimated using a method known as the push-pull test. It is a site characterisation technique commonly applied to problems in contaminant hydrogeology to provide quantitative information about a contaminant's transport and transformation of the subsurface environment (Istok, 2013). The groundwater survey presented in Chapter 5 revealed mostly reducing conditions in the shallow groundwater, thought to be conducive to denitrification in the Lower Rangitikei catchment area. This chapter further investigates the capacity for denitrification through the shallow groundwater monitoring and *in-situ* measurements of denitrification rate at a number of selected sites in the study area. Shallow groundwater piezometers were installed at three sites within the study area on a range of soil types and land uses.

6.2 Methods and Materials

6.2.1 Site Selection and Piezometer Installation

A set of three piezometers was installed on three sites within the study area. These areas were selected based on their naturally reduced groundwater and intensive land uses providing a likelihood of NO_3^--N being present in the shallow groundwater. Site 1 (Figure 36) is a dairy farm located near Sanson on Ohakea silt loam. This site will be noted as 'Sanson Site' hereafter. A well 200 m away describes the subsurface stratigraphy of a 50 cm top soil and gravels occupying up to 8 m below this level. Site 2 (Figure 37) is a cropping dry-stock farm located near Parewanui (Bulls) on Pukepuke-Motuiti association soil. Site 2 will be noted as 'Bulls Site' hereafter. A well several metres away described the stratigraphy as 3 m of sand and gravel below this level. Site 3 (Figure 38) is a dairy farm located near Santoft also on the Pukepuke-Motuiti association. Site 3 will be noted as 'Santoft Site' hereafter. A well nearby described the stratigraphy as mostly consisting of sand in the top 6 m.

At each site, a 3 m piezometer with a 0.5 m screen; a 6 m piezometer with a 0.5 m screen; and a 6 m piezometer with a 5.5 m screen were installed. Above the ground the piezometers had an additional 30 cm of length. Piezometers were made from a 30 mm diameter PVC pipe (28 mm inner diameter). The screen was made by drilling 5 mm holes approximately 1 cm apart around the circumference of the piezometer for the required length of the screen. These holes were then covered using a 250 µm nylon mesh, with a nylon cap to close the bottom end of the piezometer.

Installation of the piezometers was done using a tractor-mounted fence post driver. A 1 m steel casing with inner steel and drive point was placed in position, with the post driver striking a plate attached to the top of the casing to ram it into the earth. The next metre of casing was then attached to the top of the now embedded casing and then rammed into the earth and repeated until the casing is at the desired depth (3 m or 6 m). Once the casing is at the appropriate depth, the inner rod is then lifted from within the outer casing using a hydraulic lift. Once removed, the piezometer slides into the space now evacuated by the inner rod. The outer casing is then removed using the hydraulic lift, while keeping the piezometer pushed down with the weight of a 1 m inner steel rod.

Sand and fine grained material were packed into the space vacated by the outer casing to complete the piezometer installation. A primary pack consisting of coarse grained quartz sand was used to pack the area around, and to 30 cm above, the screen. These plans had to be adjusted in the field as the space vacated by the outer casing often collapsed, usually between 1 to 3 metres. A secondary pack consisting of finer grained sand was then to be used to pack the area above the primary pack (or collapsed material) to 30 cm below the ground surface. About 10 cm of bentonite was added, before a 20 cm layer of concrete was poured at the top to seal the casing. Table 12 provides more detail about the piezometers. Note the screen lengths of these piezometers. Those with 0.5 m screens were used for the push-pull tests and monitoring (labelled ‘A’ and ‘B’), while those with 5.5 m screens (labelled ‘C’) were used only for monitoring purposes.

Table 12: Details of the piezometers installed at sites around the study area.

Piezometer	Depth m bgl	Screened depth m bgl
Sanson-A	3	2.5-3
Sanson-B	6	5.5-6
Sanson-C	6	0.5-6
Bulls-A	3	2.5-3
Bulls-B	6	5.5-6
Bulls-C	6	0.5-6
Santoft-A	3	2.5-3
Santoft-B	6	5.5-6
Santoft-C	6	0.5-6

Once the piezometers were installed and completed, they were pumped with a peristaltic pump to clear any sediment that may be trapped in the piezometer during installation but also to assess how well they were functioning. Sanson-A (3 m), Sanson-B (6 m) and Bulls-B (6 m) were screened in gravel and pumped water most efficiently. This indicates a higher hydraulic conductivity. Bulls-A (3 m) and Santoft-A (3 m) were screened in sand or sand/silt and had a noticeably lower hydraulic conductivity. They were therefore not able to pump water as quickly, though were still functional for the push-pull test. Santoft-B (6 m) was also screened in sand or fine silt and had a very low hydraulic conductivity. It was not able to pump water at a reasonable rate, so was not included for the push-pull test or monitoring.

Finally, as the push-pull test requires the discharge of chemicals to groundwater, a resource consent was required before the tests could commence. A discharge permit was granted in April 2015 to carry out these tests. The assessment found the potential adverse environmental effects of the push-pull tests would be less than minor.

Figure 36: Sanson Site.

Figure 37: Bulls Site.

Figure 38: Santoft Site.

6.2.2 Shallow Groundwater Monitoring

After the piezometers were installed, several parameters were monitored over March, April and May 2015. This includes NO_3^--N, NH_4^+-N, DO, redox potential (ORP), electrical conductivity, *pH* and depth to groundwater. Protocol for sampling was the same as stated in Section 5.1, where three times the volume of the piezometer was purged before sampling. 50 mL groundwater samples were field-filtered (45-micron) and stored frozen for later analysis. Not all piezometers could be sampled as intended.

6.2.3 Push-Pull Tests

The shallow groundwater system is able to act as a sink for NO_3^--N within a high nutrient environment through the process of denitrification (Rivett et al., 2008). Several methods of estimating denitrification have been developed in the past, though one that is commonly used for such measurements is the push-pull test (Trudell et al., 1986). This method was developed by Trudell et al. (1986) to quantify denitrification rates in a shallow unconfined sand aquifer. The testing regime was later developed and expanded upon by Istok et al.

(1997) to include a range of other microbial processes. The methodology used to perform the push-pull tests for this study is closely modelled on the specifications by Istok (2013).

The test was conducted by first extracting water from the piezometer to be used as test solution the following day. A tubing and packer system was inserted down into the piezometer to just above the screen. The packer creates a seal inside the piezometer to restrict well water from moving vertically within the piezometer. The peristaltic pump and a multi-parameter water quality probe were set up and groundwater was pumped until parameters (i.e. temperature, DO, specific conductivity, *pH*) had stabilised. Groundwater was then pumped into collapsible 20 L bags that had been evacuated of as much air as possible. Groundwater was pumped into these bags slowly (approximately 0.5 - 1 L/minute). They were kept in the shade while being filled. Any air was removed once the bag had filled in order to keep the water as reduced as possible. Five bags (100 L) were endeavoured to be taken for each push-pull test. This was possible at Sanson-A, Sanson-B, Bulls-B and Santoft-A because of the high hydraulic conductivity, but only 40 L was taken at Bulls-A. The test solution volume of 100 L was based on the advice by Istok (2013) and the practicality of pushing the test solution in and sampling within one day. Once the bags were filled they were stored in a temperature controlled room as close to the ambient temperature the groundwater was pumped out at, usually within a degree or two.

The following day, 1 L of acetylene gas (C_2H_2) was injected into each bag. Acetylene inhibits the reduction of N_2O to N_2 (Yoshinari et al., 1977), thereby providing an additional easily-measured proxy of denitrification. Just prior to the test solution being pushed back into the piezometer, the bags were supplemented with KNO_3^- and KBr^- salts. KBr^- is a nonreactive tracer while the KNO_3^- is the reactive tracer to determine the *in-situ* denitrification rate. These were mixed with the test solution in the field to preserve as much of the NO_3^--N as possible. Concentrations of both tracers were made up to 10 ppm for each 20 L bag. Two samples of the test solution (for each bag) were collected to later confirm their concentration, before the test solution was pumped into the piezometer at a rate of roughly 1 L/minute. All samples were 50 mL and were filtered through a 45-micron filter. Once all the test solution had been pushed back into the formation, sampling would begin (known as the 'pull' phase).

Sampling took place over 360 minutes (6 hours) from when the final test solution had been pushed back into the formation. For the first two hours, sampling took place every 30 minutes and then subsequently every hour. At each sampling interval, 2 L of groundwater (approximate volume of standing water in the piezometer) would be extracted, first at a rate of 1 L/min, and discarded, before a set of three samples were taken (50 mL, 45 micron filtered). A further 180 mL sample (unfiltered) was taken in sealed and evacuated bags for later N_2O analysis. Samples were kept chilled in the field and frozen until analysis.

A distinction can be made between experiments that attempt to estimate denitrification capacity on the one hand, and denitrification potential on the other. Those experiments testing for denitrification *capacity* add only a source of NO_3^--N (as the electron acceptor) to estimate the ambient denitrification rate. Experiments testing for denitrification potential add a source of NO_3^--N and also a source C (or some other electron donor) to estimate the maximum rate of denitrification possible (Yeomans et al., 1992). In a recent assessment of denitrification in a Waikato catchment, Clague et al. (2013) used both the potential and capacity experiments to assess whether the groundwater system is substrate limited or microbe limited. Experiments for this thesis will only examine denitrification capacity, as it is most important to understand what the fate of NO_3^--N is under ambient/background conditions. This will provide an estimate of the denitrification taking place beneath agricultural land without any supplemental electron donors.

6.2.4 Analytical Methods

Analysis for monthly groundwater samples was performed in an auto-analyser for NO_3^--N and NH_4^+-N, with a detection limit of >0.01 mg/L.

Analysis of samples for push-pull tests was performed using Ion Chromatography for NO_3^--N and Br^- with a detection limit of >0.01 mg/L. Results were interpreted by plotting the NO_3^--N and Br^- concentrations over 360 minutes. The effects of dilution on the NO_3^--N concentrations were removed by plotting dilution adjusted NO_3^--N concentrations with the following equation:

$$C_{sol} * = \frac{Csol}{\left(\frac{C}{Co}\right) tr}$$

In the equation, C_{sol}^{*} is the dilution adjusted NO_3^--N concentration in an extraction phase sample, and $(C/C_o)_{tr}$ is the relative Br^- concentration in the same sample. This data will be used to observe the progress of the NO_3^--N reduction reaction and estimate the apparent zero-order rate constant for NO_3^--N consumption (Istok, 2013).

Samples taken for N_2O analysis had 60 mL of N_2 added to them before being shaken for 90 minutes to ensure the gas exchanges with the sample water. 25 mL of gas was taken and injected into evacuated vials. These samples were then analysed using Gas Chromatography with a detection limit of >0.001 mg/L.

6.3 Results and Discussion

6.3.1 Shallow Groundwater Chemistry and Redox Conditions

After installation, the piezometers were monitored over March, April and May 2015. They were monitored to observe the background parameters of these sites and gain an understanding of the shallow groundwater chemistry and redox conditions. NO_3^--N had mostly low concentrations at all the sites monitored, with the exception of Bulls-C and Santoft-C. These piezometers showed elevated NO_3^--N concentrations in April, well above other readings, but also had elevated DO concentrations at the same time (Figure 39). NH_4^+-N was generally around 1 mg/L or less at all the sites, though it was lowest at the Bulls and Santoft sites (Figure 39). DO was also generally low at <0.5 mg/L at all sites, with the exception of Bulls-C and Santoft-C, where DO reached around 2 mg/L, with associated elevated NO_3^--N.

The redox potential throughout all locations also returned negative values over the monitoring period. This indicates a reduced groundwater environment. There was only one occasion where redox was higher, at Bulls-C in April, also where DO was high and NO_3^--N was simultaneously high as well (Figure 40). These results may be due to a rainfall event

which had the effect of mobilising nutrients and contributing to higher DO. Electrical conductivity was reasonably stable over the months with the highest results found at the Bulls site (Figure 40). A single reading at Bulls-B in March recorded the EC as 132.6 µS/cm, which is likely to be a false reading since no other results were that low. *pH* was stable across the sites, though it was lower at the Sanson site compared with the other sites (Figure 40). The water table was also stable over these months for these sites, though it was generally deeper by 0.5 m at the Bulls site (Figure 40).

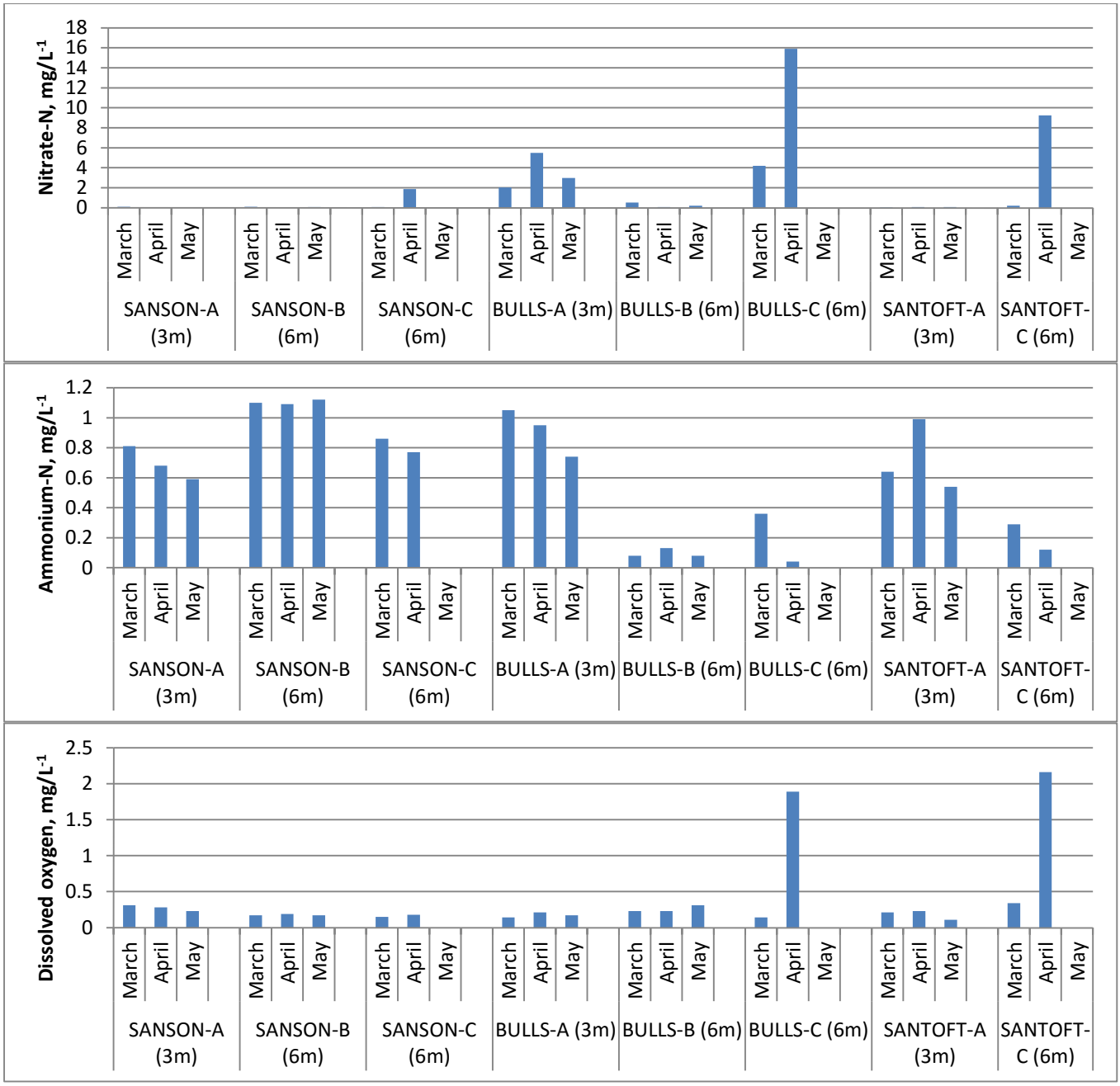

Figure 39: Shallow groundwater monitoring results over early 2015 for NO_3^--N, NH_4^+-N and dissolved oxygen at piezometers installed at Sanson, Bulls and Santoft.

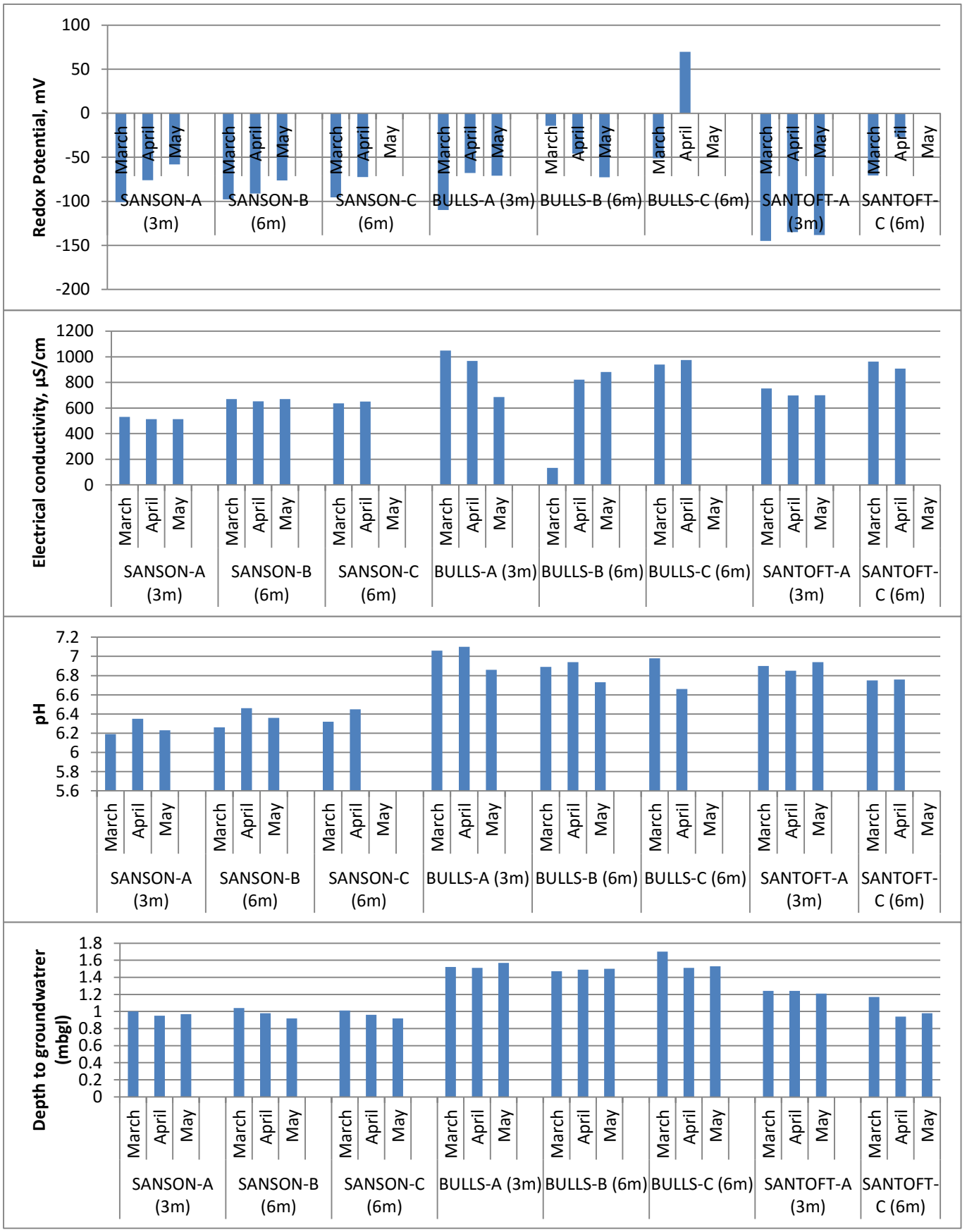

Figure 40: Shallow groundwater monitoring results over early 2015 for redox potential, pH, electrical conductivity and groundwater level at piezometers installed at Sanson, Bulls and Santoft.

6.3.2 Shallow Groundwater Denitrification

The push-pull tests were conducted to measure *in-situ* denitrification rates in selected piezometers. This section outlines the test solution and background concentrations before detailing the results of the push-pull tests.

6.3.2.1 Test Solution and Background Concentrations

As part of the push-pull tests, groundwater for preparing the test solution was pumped and stored the day before the test. Up to 100 L of groundwater was taken for these purposes, though as little as 40 L was taken at Bulls-A, because of low hydraulic conductivity. At the same time, groundwater samples were taken for analysis of background conditions of NO_3^--N and Br^-. This was necessary to accurately estimate the fate of the test solution that will be injected into the formation. Test solution and background concentration results are outlined in Table 13 to Table 17.

Table 13: Test solution and background concentrations for Sanson-A (3 m)

	Br^- mg/L	**NO_3^--N mg/L**
Test Solution 1	11.23	10.76
Test Solution 2	10.85	10.30
Test Solution 3	11.21	10.78
Test Solution 4	10.38	9.72
Test Solution 5	11.72	11.28
Background	0.18	0.03
Test solution average	11.08	10.57
Test solution average minus background	10.90	10.54

Table 14: Test solution and background concentrations for Sanson-B (6 m)

	Br^- mg/L	**NO_3^--N mg/L**
Test Solution 1	10.33	9.82
Test Solution 2	10.84	10.38
Test Solution 3	10.25	9.76
Test Solution 4	9.63	9.68
Test Solution 5	10.28	9.92
Background	0.17	<0.01
Test solution average	10.27	9.91
Test solution average minus background	10.10	9.91

Table 15: Test solution and background concentrations for Bulls-A (3 m)

	Br^- mg/L	**NO_3^--N mg/L**
Test Solution 1	10.69	11.55
Test Solution 2	10.66	11.25
Background	0.66	1.55
Test solution average	10.67	11.40
Test solution average minus background	10.02	9.85

Table 16: Test solution and background concentrations for Bulls-B (6 m)

	Br^- mg/L	NO_3^--N mg/L
Test Solution 1	11.01	10.67
Test Solution 2	9.38	8.90
Test Solution 3	9.14	8.74
Test Solution 4	6.45	5.95
Test Solution 5	7.38	6.81
Background	0.47	0.11
Test solution average	8.67	8.21
Test solution average minus background	8.21	8.10

Table 17: Test solution and background concentrations for Santoft-A (3 m)

	Br^- mg/L	NO_3^--N mg/L
Test Solution 1	10.56	10.17
Test Solution 2	10.77	10.26
Test Solution 3	10.61	10.23
Test Solution 4	10.70	10.26
Background	0.18	0.013
Test solution average	10.66	10.23
Test solution average minus background	10.48	10.21

Background Br^- concentration ranged from 0.17 to 0.66 mg/L, while NO_3^- ranged from <0.01 to 1.55 mg/L. At the Sanson and Bulls sites, NO_3^--N had lower concentrations, at 6 m, compared with 3 m. From this observation it is possible NO_3^--N is being reduced between 3 and 6 m below ground level. The test solutions (with the background concentrations subtracted) ranged from 8.21 to 10.90 mg/L for Br^-, and 8.10 to 10.54 mg/L for NO_3^--N. These concentrations are supposed to be approximately 10 mg/L. The test solutions around 8 mg/L are low. This is because two of the 20 L bags had a low concentration when the KBr^- and KNO_3^- were added (Bulls-B, Table 16).

6.3.2.2 Denitrification Rates

The denitrification rate is calculated based on how the NO_3^--N tracer declines over several hours relative to the decline in the Br^- tracer. It is expected both tracers will naturally decline over time due to dispersion and advection influences (dilution) in the subsurface (Istok, 2013). Once these dilution effects are taken into account, the difference between the two tracers could be attributed to microbial denitrification.

Figure 41 shows the dilution of both NO_3^--N and bromide over the course of the test, with NO_3^--N usually showing a greater decline as the time progressed. The NO_3^--N/Br^- ratio is a

more visual guide to the decline in NO_3^--N relative to Br^-, with a decreasing trend showing a widening gap between the two tracers. The dilution-corrected NO_3^--N concentration shows the reduction of NO_3^--N after dilution effects have been taken into account. It is the slope of this line that gives the zero-order reaction rate for NO_3^--N reduction. The red value in bold is the estimated rate of denitrification per hour. Figure 42 shows how N_2O concentrations changed over time as the test progressed. The N_2O concentrations provide a supplementary indication of denitrification as NO_3^--N is denitrified.

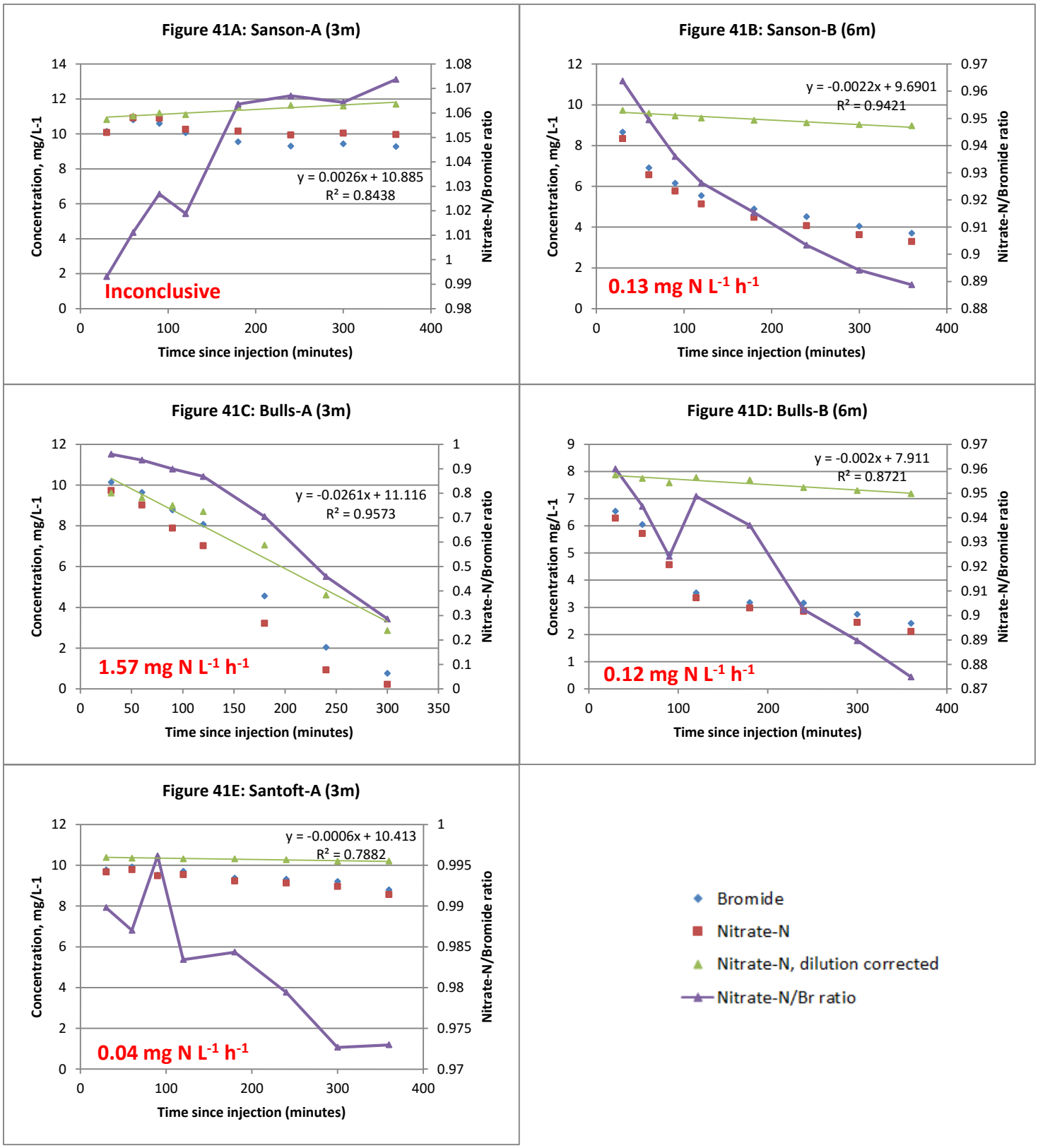

Figure 41: Results of push-pull tests showing Bromide and Nitrate-N concentrations, the dilution corrected Nitrate-N concentration and the Nitrate-N/Bromide ratio. The denitrification rate is shown in red.

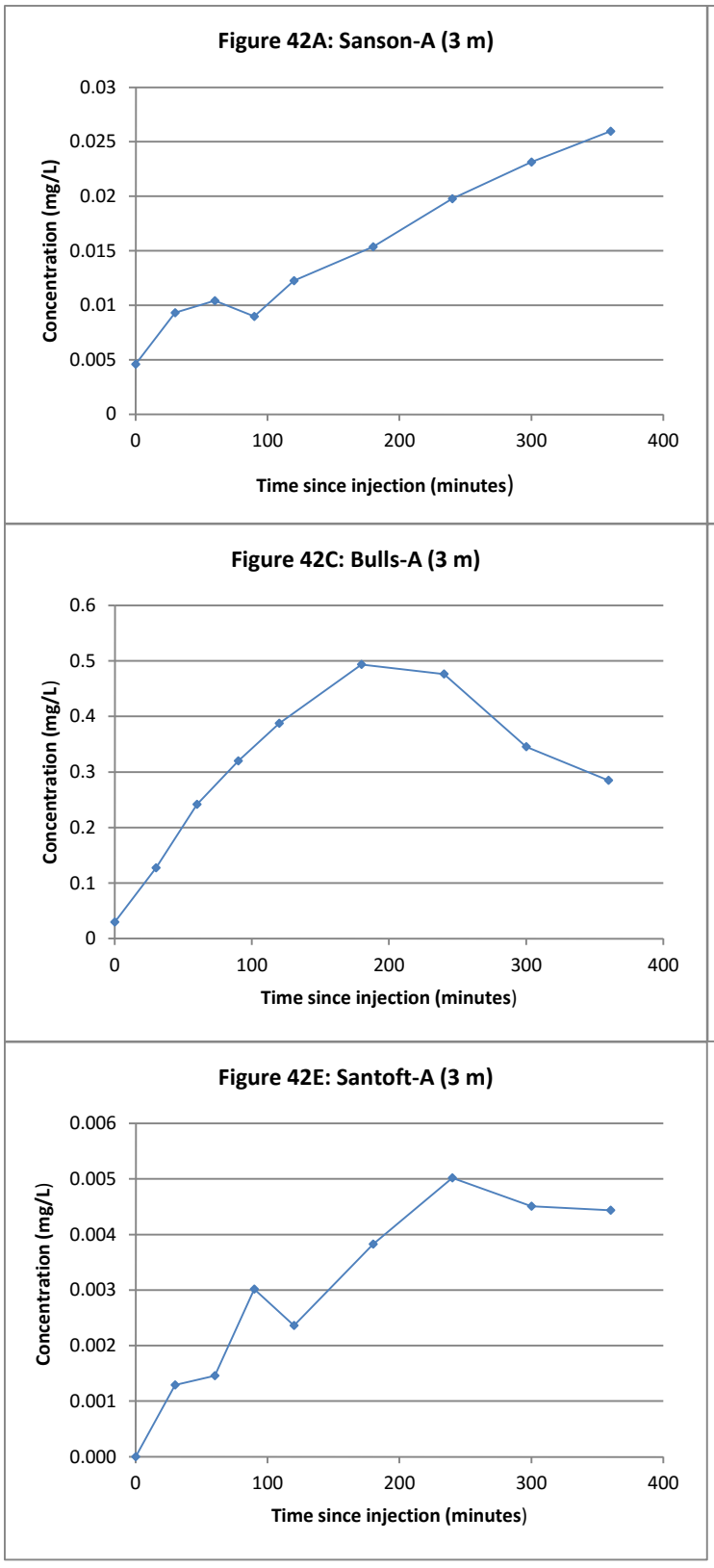

Figure 42: Concentration of N_2O-N during the push-pull test.

Site 1 (Figure 36, Sanson-A and Sanson-B) is a dairy farm near Sanson. The soil at this location is characterised by an imperfectly to poorly drained soil, the Ohakea silt loam. Infrequent flooding occurs from a nearby stream and the land use is primarily dairy farming, including neighbouring properties. The redox assessment in Chapter 5 identified this area (323091, Table 11) as mixed (anoxic), where the likely redox processes were NO_3^-, Fe^{3+} and SO_4^{2-} reduction. Sanson-A is screened in gravels and therefore has a relatively high hydraulic conductivity. During the pull phase of the push-pull test conducted at this site, at time zero 'T0', the NO_3^--N and Br^- concentrations were 8.73 and 9.08 mg/L respectively. Both increased until T60, an unexpected result as typically the tracers would begin dilution after the injection. After T60, the tracers began to dilute, but as the graph shows (Figure 41A), the Br^- concentration decreased faster than NO_3^--N and remained lower for the rest of the observation period. From T180, the tracers remained relatively stable, and by T360 NO_3^--N and Br^- had concentrations of 9.96 and 9.28 mg/L respectively. Once the NO_3^--N concentration is corrected for dilution (Figure 41A), it shows an increasing trend relative to Br^-. The NO_3^--N concentration is actually increasing at a rate of 0.16 mg N L^{-1} hr^{-1}, based on the regression line of the dilution corrected NO_3^--N. Clague (2013) also reported a similar unusual C/C_o trend during a push-pull denitrification capacity test where NO_3^--N concentration stayed consistently above the Br^- tracer concentration, though there was no increase in NO_3^--N and Br^-, as observed in this push-pull test. The N_2O concentration (Figure 42A) increases over time at a constant rate from T90, indicating to some extent denitrification is taking place. This is not, however, reflected in the largely stable NO_3^--N concentration. This test is described as inconclusive and a repeat of the push-pull test would be needed to confirm and explain the results for this site.

At 6m (Sanson-B), the dilution of the tracers followed a more predictable path during the test. At T0, the NO_3^--N and Br^- tracer concentrations were 9.31 and 9.53 mg/L respectively. As the test progressed, the tracers dilute at a steady rate, with their concentrations falling to 3.70 and 3.29 mg/L respectively by T360 (Figure 41B). Once the NO_3^--N has been dilution corrected, its concentration declined at a steady rate of 0.13 mg N L^{-1} hr^{-1} based on the regression curve (Figure 41B). NO_3^--N background concentrations at 3 m are 0.03 mg/L, while at 6 m they are <0.01 mg/L. Based on these results it is likely NO_3^--N is being reduced as it leaches through the soil profile and into the shallow groundwater. There is also steady

growth in the accumulation of N_2O over time as well (Figure 42B), though surprisingly in smaller amounts than at 3 m (Figure 42A).

Site 2 (Figure 37, Bulls-A and Bulls-B) is a cropping farm near Parewanui. The piezometers on this property are positioned next to a cropping field, which is also irrigated at certain times during the year. The redox assessment in Chapter 5 identified this area (322045, Table 11) as mixed (anoxic), where the likely redox processes were NO_3^--N and Mn^{4+} reduction. Bulls-A (3 m) is screened in sand deposits, though still has a relatively high hydraulic conductivity. At T0, NO_3^--N and Br^- concentrations were 10.55 and 10.24 mg/L respectively, after the background concentrations are subtracted. For the following two hours, both tracers diluted at a steady rate, with NO_3^--N decreasing at a faster rate than Br^- (Figure 41C). After T120, both tracers diluted at an even faster rate until they eased back to background levels. At T360, the NO_3^--N and Br^- concentrations were virtually back to background levels at 0.41 and 0.20 mg/L respectively. These values are with the background concentrations subtracted so the tracers have almost been completely diluted. The dilution corrected curve (Figure 41C) shows a strong reduction in NO_3^--N. Relative to Br^-, NO_3^--N is denitrifying at a rate of 1.57 mg N L^{-1} hr^{-1}, based on the dilution-corrected curve. The production of N_2O had a very fast and steep response from T0 (Figure 42C), with a continued steady rise to T180 and then slight decrease as the test progressed (Figure 42C). The growth in N_2O at this site (Figure 42C) was several times larger compared with the other sites, but was also significant for noting a decrease in the N_2O accumulation after T180. The drop in N_2O at this stage may indicate that NO_3^--N was exhausted by this stage (Figure 42C), probably reflecting an efficient environment for denitrification.

Bulls-B (6 m) is screened in gravel and also has a relatively high hydraulic conductivity. It presents a similar dilution curve to Bulls-B (3 m). At T0, the NO_3^--N and Br^- concentrations were 7.03 and 7.29 mg/L respectively, after the background concentrations were subtracted. Up to T120, both tracers diluted steadily, but began to ease after this point and diluted at a slower rate. At T360, the tracers were still above the background levels at 2.11 and 2.41 mg/L of NO_3^--N and Br^- respectively, and were therefore taking longer to dilute than at Bulls-A (3 m), possibly reflecting a slower groundwater movement. Once the NO_3^--N has been dilution corrected (Figure 41D), the rate of denitrification was estimated at 0.12

mg N L^{-1} hr^{-1}. NO_3^--N was still being reduced at 6 m, but not in as greater quantities further up in the shallower groundwater at 3 m depth. The background NO_3^--N at 3 m was 1.55 mg/L, while at 6 m it was 0.11 mg/L, showing a decrease with the depth that could be most likely attributed to denitrification. As NO_3^--N moves through the shallow groundwater between 3 m and 6 m depth, conditions are conducive to denitrification, with DO levels below 0.5 mg/L at both depths. The growth in N_2O accumulation (Figure 42D) mirrors that of the tracer dynamics – steady growth until T120, but greater accumulation after this stage. Unlike at the 3 m depth, N_2O keeps accumulating during the test, but only a fraction of the amount that was generated at Bulls-A (Figure 42C). At 6 m, both the rate of denitrification and the rate of N_2O accumulation grow at an order of magnitude smaller than at 3 m depth.

Site 3 (Figure 38, Santoft-A), is a dairy farm near Santoft. The piezometers are located under an irrigator operating through parts of the year. The redox assessment in Chapter 5 identified this area (312004, Table 11) as anoxic, where the likely redox process was CO_2 reduction, causing methanogenesis. Only the 3 m piezometer was able to be used for the push-pull test at this location. The 6 m piezometer was probably screened in an aquitard layer of fine material, causing a low hydraulic conductivity. During the push-pull test at Santoft-A (3 m), both the NO_3^--N and Br^- concentrations at T0 were almost the same, at 9.69 and 9.79 mg/L respectively. From this point, both tracers diluted at a very steady rate, with their concentrations falling only marginally over six hours (Figure 41E). By T360, both tracers NO_3^--N and Br^- were 8.56 and 8.79 mg/L respectively and NO_3^--N appeared to be declining at a faster rate than Br^-. Once NO_3^--N has been dilution corrected (Figure 41E), it shows only a modest amount has been reduced at a rate of 0.04 mg N L^{-1} hr^{-1}. The N_2O also accumulated (Figure 42E) during the test, but only in relatively small quantities compared with some other sites. A longer push-pull test may reveal a more accurate picture of the estimated denitrification occurring at this site.

6.4 Conclusions

This chapter has investigated the extent to which the natural subsurface environment is able to attenuate NO_3^--N. NO_3^--N was found to be generally quite low at most locations and depths, though it did tend to be higher at the Bulls site, particularly at 3 m. Push-pull tests

were conducted by raising the NO_3^--N and Br^- concentrations and observing their dilution over time in the shallow groundwater at selected sites. The speed of tracer dilution, and therefore groundwater flow, was found to vary between sites. Dilution to background levels took around 6 hours at three piezometers (Sanson-B, Bulls-A, and Bulls-B), while it took significantly longer to occur at Sanson-A and Santoft-A. Assuming the NO_3^--N and Br^- face the same dilution characteristics, the difference between these two tracers at the end of the test is attributed to the occurrence of denitrification (since Br^- is a conservative tracer) in the subsurface environment. These tests showed denitrification rates varied greatly, among and within the sites. The occurrence of denitrification was inconclusive at only one piezometer (Sanson-A), while all other test piezometers experienced some level of denitrification. According to these results, the rate ranged from 0.04 mg N L^{-1} hr^{-1} to 1.57 mg N L^{-1} hr^{-1}. Depth did not seem to be an indicator of the rate of denitrification, with the fastest and slowest rates (Bulls-A and Santoft-A respectively) occurring at the 3 m depth. Though at the Bulls site NO_3^--N was consistently observed at a higher concentration at 3 m, compared with 6 m, suggesting NO_3^--N is being reduced as it percolates down through the subsurface environment. The accumulation of N_2O has also provided a further indication of denitrification occurring and seems to accumulate in proportion to the rate of denitrification. Overall, these observations provide field-based evidence of denitrification, i.e. NO_3^--N reduction in the shallow groundwater of the Lower Rangitikei catchment. However, more detailed field surveys and *in-situ* measurements will be required to further assess this denitrification potential and its effects on transport and attenuation of NO_3^--N from farms to rivers and coastal lakes in the study area.

7 Summary and Conclusions

This thesis aims to assess the transport and fate of NO_3^--N as it moves from farms to river in the Rangitikei catchment. Each aspect of this study has been addressed separately in the preceding chapters, though not in the context of addressing the greater question. This chapter provides the opportunity to bring these individual strands together and will be discussed under their respective topics, first the transport of NO_3^--N and, secondly, the fate of NO_3^--N within the study area.

Transport of nitrate in shallow groundwater

Understanding the transport pathways of groundwater within a catchment is necessary if there is any concern about NO_3^--N reaching surface waters. NO_3^--N from the surface can be leached down through the soil profile, eventually coming into contact with the shallow groundwater. Once the NO_3^--N comes into contact with, and becomes dissolved within the groundwater, it may be diluted to a low concentration, or may be transformed in some way. If preserved, the NO_3^--N will be carried along the flow pathway, where it will eventually discharge at some point, possibly in surface waters. Groundwater flow in the coastal Rangitikei catchment was investigated by dipping approximately 100 wells in the region to map the water table and create a piezometric surface. The great range in well depths in this area meant flow systems may differ between the shallow and deep ranges. To minimise any issues, flow was mapped for both the deep and shallow wells, with a depth of 30 m providing the separation between the shallow and deep groundwater flow systems.

Both the shallow and deep systems had similar flow patterns, though there is greater topographic influence occurring on the shallow groundwater. The deep groundwater flows from the NE to the coast and most likely discharges out at sea. Shallow groundwater, on the other hand, is influenced more by the Marton anticline, with groundwater flowing along its axis from the highest elevations in Marton down to Bulls (see Figure 13 and Figure 23). Once groundwater reaches the lower elevations, it then follows the path of the deeper groundwater and flows towards the coast. The piezometric maps demonstrate groundwater is generally flowing in the same direction as the Rangitikei River, essentially

providing shallow groundwater opportunity for NO_3^--N from upstream areas to enter the river and its tributaries.

Groundwater interaction with the river was estimated using two longitudinal river flow and water quality surveys, as well as an examination of the water table contour lines as they cross the river. These techniques give an estimate of where groundwater is influxing into the river and where NO_3^--N could be predicted to inflow. The longitudinal river flow measurements showed how flow varied among different reaches of the river. On the first survey (6 January 2015), river flow varied between 16.81 and 22.61 m^3/s; while on the second survey (20 January 2015), the river flow showed less variation and a generally lower discharge between 13.49 and 17.98 m^3/s. These readings were taken two weeks apart, with little rainfall between these dates. The varying discharges cannot be entirely attributed to groundwater – surface water interactions, as it may be due to evaporation, abstraction, discharges and other reasons. River specific conductivity increases at each stage downstream, being generally higher on the second survey, with the lower discharge. The Cl^- and SO_4^{2-} tracers had almost the same behaviour between each reach as the discharge measurements, providing supplementary indications of interaction.

These longitudinal river flow and water quality results show where groundwater is estimated to be influxing into the river and shows consistent results for both survey dates. Groundwater seepage seems to be occurring at reaches upstream of the Bulls Bridge (Reach 1.5 to Reach 2, Figure 22) and also between the two aggregate quarries downstream (Reach 3 to Reach 4, Figure 21 and Figure 22). These locations provide opportunity for any nutrients dissolved in groundwater to be introduced into the surface water environment. On both sampling days, however, the NO_3^--N concentration was low and did not make any perceptible increase, even at locations where groundwater is predicted to be discharging into the river. Groundwater contour lines were also used to infer groundwater – surface water interactions. Figure 23 shows how the 20 m, 30 m, and 40 m contour lines are pointing upstream as they cross the river, suggesting groundwater is discharging through this reach. On the other hand, the 10 m contour line is pointing slightly downstream as it crosses the river, suggesting groundwater recharge at this point. These results show some

similarity with the longitudinal river flow survey, whereby some reaches downstream of Bulls were gaining, though closest to the coast was losing.

Water quality was also analysed at river monitoring sites at the Bulls Bridge, and upstream and downstream of the Bridge using long-term monitoring data (Figure 25, Figure 26 and Figure 27). On average, NO_3^--N concentrations increase from upstream, to downstream but the low flow concentrations are similar to the concentration recorded on the January 2015 surveys. River NO_3^--N concentrations do regularly spike from time to time, but this seems to have more to do with seasonal changes than any input from groundwater. Where river NO_3^--N concentrations spike, it is most likely related to the wetter seasons (winter/spring), when rainfall potentially mobilises NO_3^--N via surface or subsurface drains and is then carried into tributaries and, eventually, the river. Moreover, several neighbouring wells adjacent to the Rangitikei River have NO_3^--N concentrations the same as, or higher than, the river itself (e.g. 313009, 323097, 322071, 332025; see Table 9 and Figure 31). These elevated NO_3^--N concentrations are either not reaching the river, are being diluted as it reaches the river, or are being transformed during transit. It is this last possibility that defines the second half of the thesis.

Fate of nitrate in shallow groundwater

The potential for NO_3^--N to be reduced in shallow groundwater depends on a number of factors, the most important of which is the redox condition of the groundwater. The study area was assessed for redox potential by way of a groundwater survey, at mostly shallow wells, by collecting data on DO, *pH*, DOC and a range of cations and anions. The most common cation was Ca^{2+}, while the most common anion was HCO_3^-, forming a $CaHCO_3$ hydrochemical facies, a common groundwater type. Shallower bores had a higher possibility of contamination with Na^+ and Cl^- ions, having a greater concentration compared to deeper bores. Other water quality parameters, such as DO, DOC and NO_3^--N, were also more highly concentrated at shallower depths. This shows the potential impact land use activities may have on the quality of shallow groundwater, but also the potential for NO_3^--N to be reduced, given the appropriate conditions. At a few locations, NO_3^--N tended to persist at the shallow depths where DO was observed at higher concentrations. This is predicted because NO_3^--N will not be reduced in the presence of sufficient dissolved oxygen.

At a number of locations, DO concentrations drop with increasing depth and the NO_3^--N concentrations also decrease, indicating either greater dilution or denitrification. Up until about 10 m depth, DOC is present in high enough concentrations (>1-2 mg/L) to facilitate the denitrification process. Below 10 m, all of DO, DOC and NO_3^--N have relatively low concentrations (Figure 34).

Using a range of common groundwater quality measures (DO, NO_3^--N, Mn^{2+}, Fe^{2+} and SO_4^{2-}), the redox condition of groundwater can be understood, therefore revealing which chemical species are likely to be undergoing reduction. Depending on the concentration of these constituents, it can be predicted which redox category is likely (either oxic or anoxic) and which redox process or combination of processes is likely (aerobic oxidation, denitrification etc.). Of the 15 groundwater wells sampled, three were found to be oxic (322071, 333005, 323077, see Figure 28), where DO was greater than 0.5 mg/L. The 0.5 mg/L of DO threshold is based on the framework developed by McMahon & Chapelle (2008), though there are different estimates on the DO concentration required for NO_3^--N reduction. Some researchers have reported a lower threshold of 0.2 – 0.3 mg/L-O_2 (e.g. Tiedje, 1988; Seitzinger et al., 2006; Trudell, Gillham, & Cherry, 1986), while others have reported a higher threshold of 1 – 2 mg/L-O_2 (e.g. Puckett & Cowdry, 2002; Bolke et al., 2002; Gillham, 1991). It seems like the 0.5 mg/L threshold is likely a compromise, though it seems a conservative one. Had the DO threshold been set at 1 mg/L, none of the 15 groundwater samples would be considered oxic and potentially most of them will be undergoing denitrification.

These groundwater survey results point toward a generally favourable environment for NO_3^--N reduction to take place in the shallow groundwater in the study area. Not only is DO generally quite low in the area, providing no initial barrier or delay to NO_3^--N reduction, but suitable electron donors seem to be available in the form of DOC and, potentially Mn^{4+} and Fe^{3+}. NO_3^--N is reasonably low at most sites (Table 9), particularly where DO is low (Table 11). This either means any NO_3^--N that was present at most sites has now been reduced, or NO_3^--N was never present at these locations in appreciable concentrations anyway.

Having assessed the redox status of groundwater in the study area, actual shallow groundwater denitrification was tested using the single-well push-pull tests. Piezometers were installed at three locations (two dairy and one cropping farm) to observe how NO_3^--N behaves in shallow groundwater relative to a conservative tracer, Br^-. The piezometers were installed at different depths to detect any differences that might be apparent at different stages in the profile. NO_3^--N concentrations were collected over March, April and May 2015, showing usually low concentrations at the Sanson and Santoft sites - both dairy farming sites. The Bulls site (cropping) had generally higher and more variable concentrations over these months, but a large difference could be seen between the NO_3^--N at 3 m and at 6 m. At 3 m, NO_3^--N was relatively high and varied between 2.02 and 5.5 mg/L, while at 6 m, NO_3^--N varied between 0.06 and 0.52 mg/L. The Sanson site did not show as much variation, nor high levels of NO_3^--N. At the Santoft site, NO_3^--N was low at 3 m, similar to the Sanson site. The Bulls example might be significant because it shows a clear reduction in the NO_3^--N concentration from 3 m to 6 m.

The push-pull tests were conducted at each site - five in total (with only one at the Santoft site). While one of the tests showed inconclusive results (Sanson-A), the other tests showed denitrification occurring, although at different rates. Under the test conditions, NO_3^--N was reduced at a rate between 0.04 mg N L^{-1} hr^{-1} to 1.57 mg N L^{-1} hr^{-1}. The intermediate product N_2O was also measured during the extraction phase. N_2O was found to increase at all sites, consistent with what is expected during denitrification, though interestingly N_2O also increased where results seemed inconclusive at Sanson-A.

The results of this study are good in comparison to other similar tests. The rate of denitrification observed in the coastal Rangitikei catchment is within, or higher than, results of other denitrification tests. The test at Bulls-A (3 m) that recorded 1.57 mg N L^{-1} hr^{-1} was higher than any other results, though interestingly NO_3^--N also remained the highest at this location (ranging between 2.02 and 5.5 mg/L over several months). It is possible NO_3^--N would be even higher if not for the efficient denitrification that seems to be occurring at this location.

Conclusion and further areas of study

This thesis has provided an overview of the nature of hydrogeology in the Lower Rangitikei catchment; an analysis of groundwater flow and surface water interactions; a description of the local groundwater hydrochemistry and redox conditions; and an estimate of the amount of NO_3^--N attenuated in shallow groundwater. The main findings of this work are that:

- groundwater in the coastal Rangitikei is abstracted from primarily young, mostly marine sediments, and that marine and terrestrial deposits are not generally layered contrary to some assumptions;
- there is some groundwater interaction with the Lower Rangitikei River, particularly upstream of Bulls, where groundwater is likely seeping into the river, while downstream the river mostly provides for groundwater recharge;
- the redox condition of shallow groundwater is generally conducive to NO_3^--N reduction, whereby DO tends to be low and electron donors seem to be readily available; and
- field tests have shown denitrification is occurring in the shallow groundwater in the region.

These findings demonstrate how NO_3^--N can be attenuated in the shallow groundwater, a vital land quality if farming operations are considered intensive, as dairy often is. Potential exists for this type of information to be used as a planning tool, by delineating catchments according to their natural NO_3^--N attenuation capacity. If these characteristics are known about the land, decisions could be made about the degree of intensification, land use, stocking rates etc. that could be allowable – similar to how the Land Resource Inventory is used. Another item to consider would be the interaction shallow groundwater has with local waterways. If groundwater with a high NO_3^--N load is seeping into waterways, deterioration of water quality is likely to occur, however as this study has shown, if nitrate concentrations are low due to denitrification then discharge of shallow groundwater will have much less impact on surface water quality. Though, alternatively, if the nature of the interaction is groundwater recharge there will be less concern for surface water quality.

In light of these few considerations, further areas of study could be related to the better assessment and use of denitrification and/or redox status of groundwater and better understanding of groundwater – surface water interactions. Specifically, this includes:

- further investigating the spatial variation of denitrification occurrence and whether the redox condition of groundwater is truly a predictor of denitrification, and potentially investigating more practical methods for denitrification measurements;
- investigating whether denitrification and/or redox condition could be reliably used as a land use planning tool, and if this information could be integrated into the nutrient budgeting software such as OVERSEER;
- investigating the nature of groundwater – surface water interactions in greater detail, probably through the use of environmental tracers, such as Rn, to better understand where NO_3^--N is being introduced into surface waters.

References

Anderton, P. W. (1981). New Zealand Journal of Geology and Geophysics Structure and evolution of the South Wanganui Basin , New Zealand. *New Zealand Journal of Geology and Geophysics*, *24*, 39–63. doi:10.1080/00288306.1981.10422697

Barkle, G., Clough, T., & Stenger, R. (2007). Denitrification capacity in the vadose zone at three sites in the Lake Taupo catchment, New Zealand. *Australian Journal of Soil Research*, *45*(2), 91–99.

Barthold, F. K., Tyralla, C., Schneider, K., Vaché, K. B., Frede, H. G., & Breuer, L. (2011). How many tracers do we need for end member mixing analysis (EMMA)? A sensitivity analysis. *Water Resources Research*, *47*(8), 1–14. doi:10.1029/2011WR010604

Bates, H. K., & Spalding, R. F. (1998). Aquifer denitrification as interpreted from in situ microcosm experiments. *Journal of Environment Quality*, *27*(1), 174–182.

Begg, J. G., Palmer, A., & Gyopari, M. (2005). Geological synopsis of the Manawatu-Horowhenua area for a review of the region's hydrogeology, *GNS Science Consultancy Report* 2005/172. 36p.

Bekele, M. D., & Rawlinson, Z. J. (2014). Review of the Hydrogeology of the Rangitikei and Turakina Groundwater Management Zones, *GNS Science Consultancy Report* 2014/155. 53p.

Beu, A. G. (1999). Fossil records of the cold-water scallop Zygochlamys delicatula (Mollusca: Bivalvia) off northernmost New Zealand: How cold was the Last Glacial maximum? *New Zealand Journal of Geology and Geophysics*, *42*(4), 543–550. doi:10.1080/00288306.1999.9514860

Bolke, J. K., Wanty, R., Tuttle, M., Delin, G., & Landon, M. (2002). Denitrification in the recharge area and discharge area of a transient agricultural nitrate plume in a glacial outwash sand aquifer, Minnesota. *Water Resources Research*, *38*(7), 10.1–10.26.

Bouchard, D. C., Williams, M. K., & Rao, Y. S. (1992). Nitrate contamination of groundwater: sources and potential health effects. *American Water Works Association*, *84*(9), 85–90.

Bourodim, E. L., & Michna, L. (1972). Potential contribution of fertilizers to groundwater pollution. *Transcations – American Geophysical Union*, *53*(4), 638.

Burbery, L. F., Flintoft, M. J., & Close, M. E. (2013). Application of the re-circulating tracer well test method to determine nitrate reaction rates in shallow unconfined aquifers. *Journal of Contaminant Hydrology*, *145*, 1–9.

Burbery, L. F., & Wang, F. L. (2010). A Re-Circulating Tracer Well Test method for measuring reaction rates in fast-flowing aquifers: Conceptual and mathematical model. *Journal of*

Hydrology, *382*(1-4), 163–173.

Burgess, S. M. (1988). The climate and weather of Manawatu and Horowhenua. *New Zealand Meterological Service Miscellaneous Publications*, *115*(18), 47.

Campbell, I. B. (1978). *Soils of the Rangitikei County, North Island, New Zealand*. New Zealand Soil Bureau 38. Wellington, New Zealand: Department of Scientific and Industrial Research.

Capel, P. D., McCarthy, K. A., & Barbash, J. E. (2008). National, holistic, watershed-scale approach to understand the sources, transport, and fate of agricultural chemicals. *Journal of Environmental Quality*, *37*(3), 983–93. doi:10.2134/jeq2007.0226

Carter, R. M., Abbott, S. T., & Naish, T. R. (1999). Plio-Pleistocene Cyclothems from Wanganui Basin , New Zealand: Type Locality for an Astrochronologic Time-Scale, or Template for Recognizing Ancient Glacio-Eustasy? *The Royal Society*, *357*(1757), 1861–1872.

Carter, R. M., & Naish, T. R. (1998). A review of Wanganui Basin, New Zealand: global reference section for shallow marine, Plio–Pleistocene (2.5–0 Ma) cyclostratigraphy. *Sedimentary Geology*, *122*(1-4), 37–52. doi:10.1016/S0037-0738(98)00097-9

Christensen, T. H., Bjerg, P. L., Banwart, S. A., Jakobson, R., Heron, G., & Albrechtsen, H. J. (2000). Characterisation of redox conditions in groundwater contaminant plumes. *Journal of Contaminant Hydrology*, *45*(3-4), 165–241.

Clague, J. (2013). *Denitrification in the shallow groundwater system of two agricultural catchments in the Waikato, New Zealand* (Unpublished PhD thesis). Lincoln, New Zealand: Lincoln University.

Clague, J., Stenger, R., & Clough, T. (2013). The impact of relict organic materials on the denitrification capacity in the unsaturated-saturated zone continuum of three volcanic profiles. *Journal of Environment Quality*, *42*, 145–154.

Clark, M., & Roygard, J. (2008). *Land Use Capability in the Manawatu-Wanganui Region*. Palmerston North.

Clement, A. J. H. (2011). *Holocene sea-level change in the New Zealand archipelago and the geomorphic evolution of the Holocene coastal plain incised-valley system: The Lower Manawatu valley, North Island, New Zealand* (Unpublished PhD thesis). Palmerston North, New Zealand: Massey University.

Cowie, J. D. (1963). Dune-building phases in the Manawatu district, New Zealand. *New Zealand Journal of Geology and Geophysics*, *6*, 268–280.

Cowie, J. D., Fitzgerald, P., & Owers, W. (1967). *Soils of the Manawatu-Rangitikei sand country, North Island, New Zealand Sheet 1*. New Zealand Soil Bureau Bulletin, 29.

Wellington, New Zealand: Department of Scientific and Industrial Research.

Cowie, J. D., & Rijkse, W. C. (1977). *Extended legend of soil map Manawatu County, North Island, New Zealand*. Wellington, New Zealand: Department of Scientific and Industrial Research.

Daughney, C. J. (2006). *A National Protocol for State of the Environment Groundwater Sampling in New Zealand*. Wellington, New Zealand: Ministry for the Environment.

Di, H. J., & Cameron, K. C. (2002). Nitrate leaching in temperate agroecosystems: Sources, factors and mitigating strategies. *Nutrient Cycling in Agroecosystems*, *64*(3), 237–256.

Di, H. J., Cameron, K. C., Moore, S., & Smith, N. P. (1998a). Nitrate leaching and pasture yields following the application of dairy shed effluent or ammonium fertilizer under spray or flood irrigation: results of a lysimeter study. *Soil Use and Management*, *14*(4), 209–214.

Di, H. J., Cameron, K. C., Moore, S., & Smith, N. P. (1998b). Nitrate leaching from dairy shed effluent and ammonium fertiliser applied to a free-draining pasture soil under spray or flood irrigation. *New Zealand Journal of Agricultural Research*, *41*(2), 263–270. doi:10.1080/00288233.1998.9513310

Elwan, A., Singh, R., Horne, D., Roygard, J., & Clothier, B. (2015). Nitrogen attenuation factor: can it tell a story about nutrients in different subsurface environments? In: *Moving farm systems to improved attenuation*. (Eds L.D. Currie and L.L Burkitt). http://flrc.massey.ac.nz/publications.html. Occasional Report No. 28. Fertilizer and Lime Research Centre, Massey University, Palmerston North, New Zealand.

Erisman, J. W., Sutton, M. A., Galloway, J. N., Klimont, Z., & Winiwarter, W. (2008). How a century of ammonia synthesis changed the world. *Nature Geoscience*, *1*(10), 636–639.

Fleming, C. A. (1953). *Geology of the Wanganui Subdivision; Waverley and Wanganui sheet districts (N137 and N138).* Wellington, New Zealand: Department of Scientific and Industrial Research.

Gibbard, P. L., Head, M. J., & Walker, M. J. C. (2010). Formal ratification of the Quaternary System/Period and the Pleistocene Series/Epoch with a base at 2 . 58 Ma. *Journal of Quaternary Science*, *25*(2), 96–102. doi:10.1002/jqs

Gillham, R. W. (1991). Nitrate contamination of groundwater in southern Ontario and the evidence for denitrification. In I. Bogardi & R. D. Kuzelka (Eds.), *Nitrate Contamination* (NATO ASI S., pp. 86–92). Berlin: Springer-Verlag.

Hadfield, J. C., Morgenstern, U., & Piper, J. J. (2007). Delayed impacts of land-use via groundwater on Lake Taupo, New Zealand. *Transcations on Ecology and the Environment*, *103*, 293–303.

Hantush, M. H., Kalin, L., & Govindaraju, R. (2011). Subsurface and surface water flow interactions. In M. Aral & S. Taylor (Eds.), *Groundwater Quantity and Quality Management* (p. 573). Reston, VA: American Society of Civil Engineers.

Harter, T., Rosenstock, T. S., Liptzin, D., Dzurella, K., Fryjoff-Hung, A., Hollander, A., … Tomich, T. P. (2014). Agriculture's contribution to nitrate contamination of Californian groundwater (1945–2005). *Journal of Environment Quality*, *43*(3), 895–907. doi:10.2134/jeq2013.10.0411

Haynes, R. J., & Williams, P. H. (1993). Nutrient cycling and soil fertility in the grazed pasture ecosystem. *Advanced Agronomy*, *46*, 119–199.

Hewitt, A. E. (1998). *New Zealand Soil Classification* (2nd Ed.). Lincoln, New Zealand: Manaaki Whenua Press.

Hiscock, K., & Bense, V. F. (2005). *Hydrogeology, Principles and Practice* (2nd Ed.). Malden, MA: Blackwell Publishing.

Howard, J. B., & Rees, D. C. (1996). Structural Basis of Biological Nitrogen Fixation. *Chemical Reviews*, *96*(7), 2965–2982.

Istok, J. D. (2013). *Push-Pull Tests for Site Characterisation*. Berlin, Germany: Springer-Verlag.

Istok, J. D., Humphrey, M. D., Schroth, M. H., Hyman, M. R., & O'Reilly, K. T. O. (1997). Single well, push pull test for in situ determination of microbial activities. *Ground Water*, *35*(4), 619–631.

Jackson, J., van Dissen, R., & Berryman, K. (1998). Tilting of active folds and faults in the Manawatu region, New Zealand: evidence from surface drainage patterns. *New Zealand Journal of Geology and Geophysics*, *41*, 377–385.

Jarvis, S. C., Scholefield, D., & Pain, B. (1995). Nitrogen cycling in grazing systems. In P. E. Bacon (Ed.), *Nitrogen cycling in grazing systems*. New York: NY, Marcel Dekker.

Journeaux, T. D., Kamp, P. J. J., & Naish, T. (1996). Middle Pliocene cyclothems, Mangaweka region, Wanganui Basin, New Zealand: A lithostratigraphic framework. *New Zealand Journal of Geology and Geophysics*, *39*(1), 135–149. doi:10.1080/00288306.1996.9514700

Kalbus, E., Reinstorf, F., & Schirmer, M. (2006). Measuring methods for groundwater – surface water interactions: a review. *Environmental Research*, 873–887.

Kamp, P. J. J., Vonk, A. J., Bland, K. J., Hansen, R. J., Hendy, A. J. W., McIntyre, A. P., … Nelson, C. S. (2004). Neogene stratigraphic architecture and tectonic evolution of Wanganui, King Country, and eastern Taranaki Basins, New Zealand. *New Zealand Journal of Geology and Geophysics*, *47*(4), 625–644.

doi:10.1080/00288306.2004.9515080

Korom, S. F. (1992). Natural denitrification in the saturated zone: a review. *Water Resources Research*, *28*(6), 1657–1668.

Lieffering, R. E. (1990). *Hydrogeological investigation of the Palmerston North region* (Unpublished Master's thesis). Palmerston North, New Zealand: Massey University.

MacLeod, C. J., & Moller, H. (2006). Intensification and diversification of New Zealand agriculture since 1960: An evaluation of current indicators of land use change. *Agriculture, Ecosystems and Environment*, *115*(1-4), 201–218. doi:doi:10.1016/j.agee.2006.01.003

Martley, P. R. (2001). *Hydrogeology of the Feilding District, Manawatu* (Unpublished Master's thesis). Christchurch, New Zealand: University of Canterbury.

McMahon, P. B., & Chapelle, F. H. (2008). Redox processes and water quality of selected principal aquifer systems. *Ground Water*, *46*(2), 259–71. doi:10.1111/j.1745-6584.2007.00385.x

McMahon, P. B., Cowdry, T. K., Chapelle, F. H., & Jurgens, B. C. (2009). *Redox Conditions in Selected Principal Aquifers of the United States*. USGS Fact Sheet 2009-3041. Denver, CO.

Michna, L., & Bourodim, E. L. (1973). Seepage flows – Field data measurements for evaluation of potential contribution of fertilizers to groundwater pollution. *Soil Science*, *115*(6), 401–408.

Ministry of Health. (2008). *Drinking Water Standards for New Zealand 2005 (Revised 2008)*. Wellington, New Zealand.

Moore, J. E. (2012). *Field Hydrogeology* (2nd Ed.). Boca Raton, FL: CRC Press.

Mortimer, N., Tulloch, A. J., & Ireland, T. R. (1997). Basement geology of Taranaki and Wanganui Basins, New Zealand. *New Zealand Journal of Geology and Geophysics*, *40*(2), 223–236. doi:10.1080/00288306.1997.9514754

Naish, T., & Kamp, P. J. J. (1995). Pliocene-Pleistocene marine cyclothems , Wanganui Basin , New Zealand : a lithostratigraphic framework. *New Zealand Journal of Geology and Geophysics*, *38*(8), 223–243.

Naish, T., & Kamp, P. J. J. (1997). Sequence stratigraphy of sixth-order (41 k.y.) Pliocene–Pleistocene cyclothems, Wanganui basin, New Zealand: A case for the regressive systems tract. *Geological Society of America Bulletin*, *109*(8), 978–999. doi:10.1130/0016-7606(1997)109<0978:SSOSOK>2.3.CO;2

Nichols, G. (2009). *Sedimentology and Stratigraphy* (2nd Ed..). West Sussex, UK: Wiley-

Blackwell.

Ottley, C. J., Davison, W., & Edmunds, W. M. (1997). Chemical catalysis of nitrate reduction by iron (II). *Geochimica et Cosmochimica Acta*, *61*(9), 1819–1828.

Parfitt, R., Schipper, L., Baisden, W., & Elliott, A. (2006). Nitrogen inputs and outputs for New Zealand in 2001 at national and regional scales. *Biogeochemistry*, *80*(1), 71–88. doi:10.1007/s10533-006-0002-y

PDP (2013). *Report on Horizons Groundwater Quality Monitoring Network*. Prepared for Pattle Delamore Partners Ltd for Horizons Regional Council. Christchurch, NZ: Horizons Report 2013/EXT/1318.

Petricevich, M. (1970). *Preliminary report on the water resources of the Manawatu Region*. Palmerston North, New Zealand: Manawatu Catchment Board.

Pillans, B., Alloway, B., Naish, T., Westgate, J., Abbott, S., & Palmer, A. (2005). Silicic tephras in Pleistocene shallow-marine sediments of Wanganui Basin, New Zealand. *Journal of the Royal Society of New Zealand*, *35*(1-2), 43–90. doi:10.1080/03014223.2005.9517777

Pillans, B. J. (1990). Late Quaternary marine terraces, South Taranaki-Wanganui. Scale 1:100,000. *New Zealand Geological Survey miscellaneous series map 18*. Lower Hutt, New Zealand Geological Survey.

Piper, A. M. (1944). A graphic procedure in the geochemical interpretation of water-analyses. *American Geophysical Union, Transactions*, *25*, 914–923.

Prado, B., Duwig, C., Escudey, M., & Esteves, M. (2006). Nitrate sorption in a Mexican Allophanic Andisol using intact and packed columns. *Communications in Soil Science and Plant Analysis*, *37*(15-20), 2911–2925. doi:10.1080/00103620600833017

Proust, J.-N., Lamarche, G., Nodder, S., & Kamp, P. J. J. (2005). Sedimentary architecture of a Plio-Pleistocene proto-back-arc basin: Wanganui Basin, New Zealand. *Sedimentary Geology*, *181*(2005), 107–145.

Puckett, L. J., & Cowdry, T. K. (2002). Transport and fate of nitrate in glacial outwash aquifer in relation to groundwater age, land use practices, and redox processes. *Journal of Environment Quality*, *34*(6), 2278–1241.

Quinn, J. M., Wilcock, R. J., Monaghan, R. M., McDowell, R. W., & Journeaux, P. R. (2009). Grassland farming and water quality in New Zealand. *Irish Journal of Agri-Environmental Research*, *7*, 69–88.

Rabalais, N. N. (2002). Nitrogen in Aquatic Ecosystems. *Royal Swedish Academy of Sciences*, *31*(2), 102–112.

Rivas, A., Singh, R., Bishop, P., Horne, D., Roygard, J., & Hedley, M. (2014). Measuring denitrification in the subsurface environment of the Manawatu River catchment. In: *Nutrient management for the farm, catchment and community*. (Eds L.D. Currie and C L. Christensen). http://flrc.massey.ac.nz/publications.html. Occasional Report No. 27. Fertilizer and Lime Research Centre, Massey University, Palmerston North, New Zealand.

Rivett, M. O., Buss, S. R., Morgan, P., Smith, J. W. N., & Bemment, C. D. (2008). Nitrate attenuation in groundwater: A review of biogeochemical controlling processes. *Water Research*, *42*(16), 4215–4232. doi:10.1016/j.watres.2008.07.020

Rivett, M. O., Smith, J. W. N., Buss, S. R., & Morgan, P. (2007). Nitrate occurrence and attenuation in the major aquifers of England and Wales. *Quarterly Journal of Engineering Geology & Hydrogeology*, *40*(4), 335–352.

Roygard, J., & Carlyon, G. (2004). *Water Allocation Project Rangitikei River*. Palmerston North, New Zealand: Horizons Regional Council.

Rust, C. M., Aelion, C. M., & Flora, J. R. V. (2000). Control of pH during denitrification in sub-surface sediment microcosms using encapsulated phosphate buffer. *Water Research*, *34*(5), 1447–1454.

Sánchez-Pérez, J. M., Bouey, C., Sauvage, S., Teissier, S., Antiguedad, I., & Vervier, P. (2003). A standardised method for measuring in situ denitrification in shallow aquifers: numerical validation and measurements in riparian wetlands. *Hydrology and Earth System Sciences*, *7*(1), 87–96. doi:10.5194/hess-7-87-2003

Seitzinger, S., Harrison, J. K., Bohlke, J. K., Bouwman, A. F., Lowrance, R., Peterson, B., … Van Drecht, G. (2006). Denitrification across landscapes and waterscapes: A synthesis. *Ecological Applications*, *16*(6), 2064–2090.

Silva, R. G., Cameron, K. C., Di, H. J., & Hendry, T. (1999). A lysimeter study of the impact of cow urine, dairy shed effluent, and nitrogen fertiliser on nitrate leaching. *Australian Journal of Soil Research*, *37*, 357–69.

Singh, B. (1976). Nitrate pollution of groundwater from nitrogen fertilizers and animal wastes in the Punjab India. *Agriculture and Environment*, *3*(1), 57–67.

Singh, B. (1979). Nitrate pollution of groundwater from farm use of nitrogen fertilizers – Review. *Agriculture and Environment*, *4*(3), 207–225.

Smith, V. H., Tilman, G. D., & Nekola, J. C. (1999). Eutrophication: impacts of excess nutrient inputs on freshwater, marine, and terrestrial ecosystems. *Environmental Pollution*, *100*, 179–196.

Stenger, R., Barkle, G., Burgess, C., Wall, A., & Clague, J. (2008). Low nitrate contamination

of shallow groundwater in spite of intensive dairying: The effect of reducing conditions in the vadose zone-aquifer continuum. *Journal of Hydrology (New Zealand)*, *47*(1), 1–24.

Stenger, R., Clague, J., Woodward, S., Moorhead, B., Burbery, L. F., & Canard, H. (2012). Groundwater assimilative capacity - an untapped opportunity for catchment-scale nitrogen management? In: *Advanced Nutrient Management: Gains from the Past - Goals for the Future*. (Eds L.D. Currie and C L. Christensen). http://flrc.massey.ac.nz/publications.html. Occasional Report No. 25. Fertilizer and Lime Research Centre, Massey University, Palmerston North, New Zealand.

Stenger, R., Clague, J., Woodward, S., Moorhead, B., Wilson, S., Shokri, A., … Canard, H. (2013). Denitrification - the key component of a groundwater system's assimilative capacity for nitrate. In: *Accurate and efficient use of nutrients on farms*. (Eds L.D. Currie and C L. Christensen). http://flrc.massey.ac.nz/publications.html. Occasional Report No. 26. Fertilizer and Lime Research Centre, Massey University, Palmerston North, New Zealand.

Te Punga, M. T. (1953). *The geology of Rangitikei Valley*. Wellington, New Zealand: Department of Scientific and Industrial Research.

Tesoriero, A. J., Liebscher, H., & Cox, S. (2000). Mechanism and rate of denitrification in an agricultural watershed: electron and mass balance along groundwater flow paths. *Water Resources Research*, *36*(6), 1545–1559.

Tiedje, J. M. (1988). *Ecology of denitrification and dissimilatory nitrate reduction to ammonium*. (A. J. B. Zehnder, Ed.) *Biology of Anaerobic Microorganisms*. New York, NY: John Wiley & Sons.

Townsend, D., Vonk, A., & Kamp, P. J. J. (2008). *Geology of the Taranaki Area*. Institute of Geological and Nucliear Sciences 1:250,000 geological map 7. 1 sheet + 77p. Lower Hutt, New Zealand: GNS Science.

Trudell, M. R. R., Gillham, R. W. W., & Cherry, J. A. (1986). An in-situ study of the occurrence and rate of denitrification in a shallow unconfined sand aquifer. *Journal of Hydrology*, *83*(3-4), 251–268. doi:10.1016/0022-1694(86)90155-1

van der Perk, M. (2012). *Soil and Water Contamination*. Leiden, The Netherlands: CRC Press/Balkema.

Verloop, J., Boumans, L. J. M., Van Keulen, H., Oenema, J., Hilhorst, G. J., Aarts, H. F. M., & Sebek, L. B. J. (2006). Reducing nitrate leaching to groundwater in an intensive dairy farming system. *Nutrient Cycling in Agroecosystems*, *74*(1), 59–74. doi:10.1007/s10705-005-6241-9

Vonk, A. J., & Kamp, P. J. J. (2004). Late Miocene-Early Pliocene Matemateaonga Formation in eastern Taranaki Peninsula: A new 1:50,000 geological map and stratigraphic framework. In *2004 New Zealand Petroleum Conference proceedings* (pp. 1–9). Wellington: Crown Minerals, Ministry of Economic Development.

Weight, W. D. (2008). *Hydrogeology Field Manual* (2nd Ed.). New York, NY: McGraw Hill.

Wilcock, R. J., Nash, D., Schmidt, J., Larned, S. T., Rivers, M. R., & Feehan, P. (2011). Inputs of nutrients and fecal bacteria to freshwaters from irrigated agriculture: Case studies in Australia and New Zealand. *Environmental Management*, *48*(1), 198–211. doi:10.1007/s00267-011-9644-1

Wilson, S. (2007). *Reconnaissance Vertical Electrical Sounding Survey of the Rangitikei-Manawatu-Horowhenua Area*. Palmerston North, New Zealand: Horizons Regional Council.

Winter, T. C., Harvey, J. W., Franke, O. L., & Alley, W. M. (1998). *Groundwater and Surface Water: a Single Resource*. Retrieved from http://pubs.usgs.gov/circ/circ1139/

Yeomans, J. C., Bremner, J. M., & McCarty, G. W. (1992). Denitrification capacity and denitrification potential of subsurface soils. *Communications in Soil Science and Plant Analysis*, *23*(9-10), 919–927. doi:10.1080/00103629209368639

Yoshinari, T., Hynes, R., & Knowles, R. (1977). Acetylene inhibition of nitrous oxide reduction and measurement of denitrification and nitrogen fixation in soil. *Soil Biology and Biochemistry*, *9*, 177–183.

Younger, P. L. (2007). *Groundwater in the Environment*. Malden, MA: Blackwell Publishing.

Zarour, H. (2008). *Groundwater Resources in the Manawatu-Wanganui Region*. Palmerston North, New Zealand: Horizons Regional Council.

Appendix: Well Log Descriptions

312007

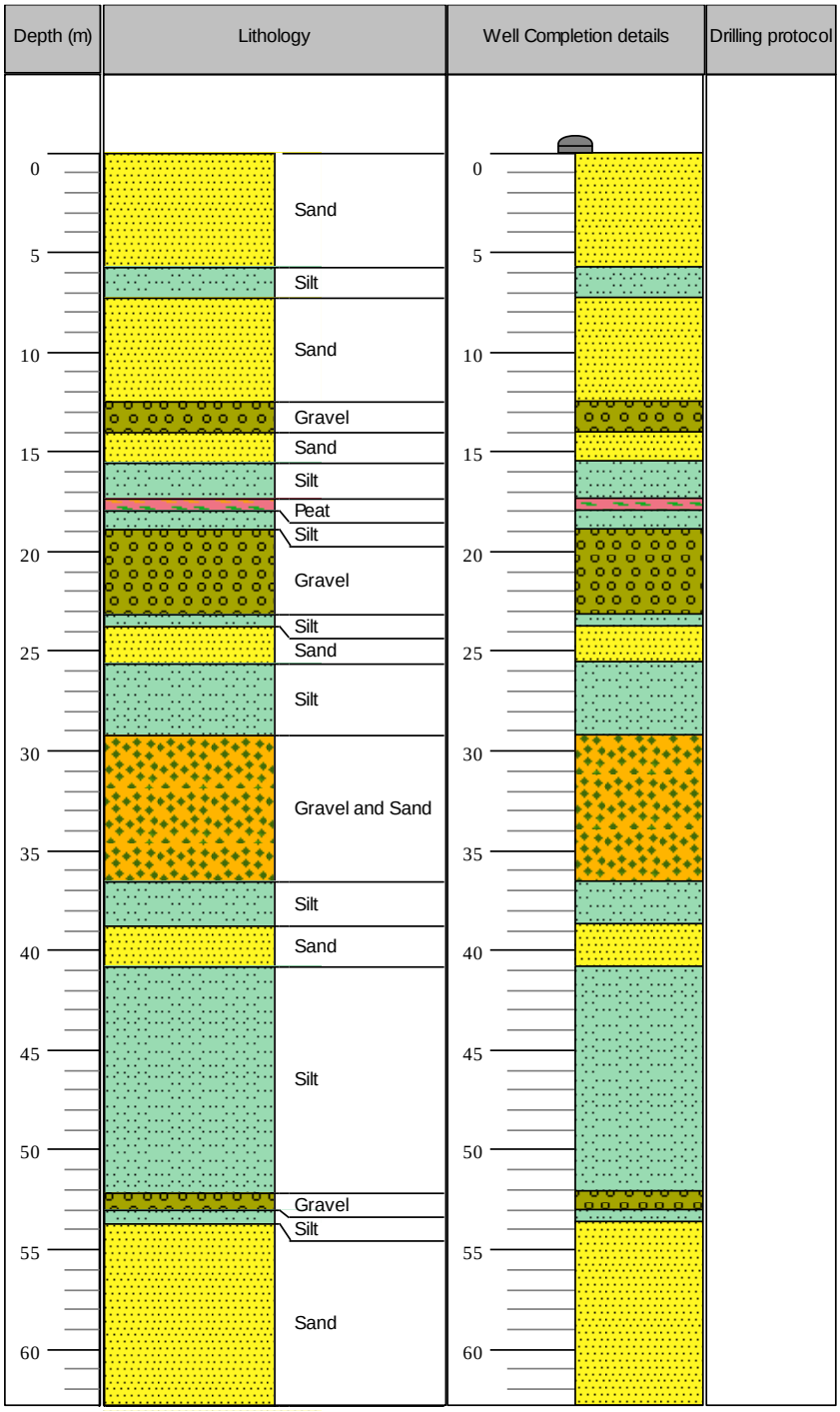

312010

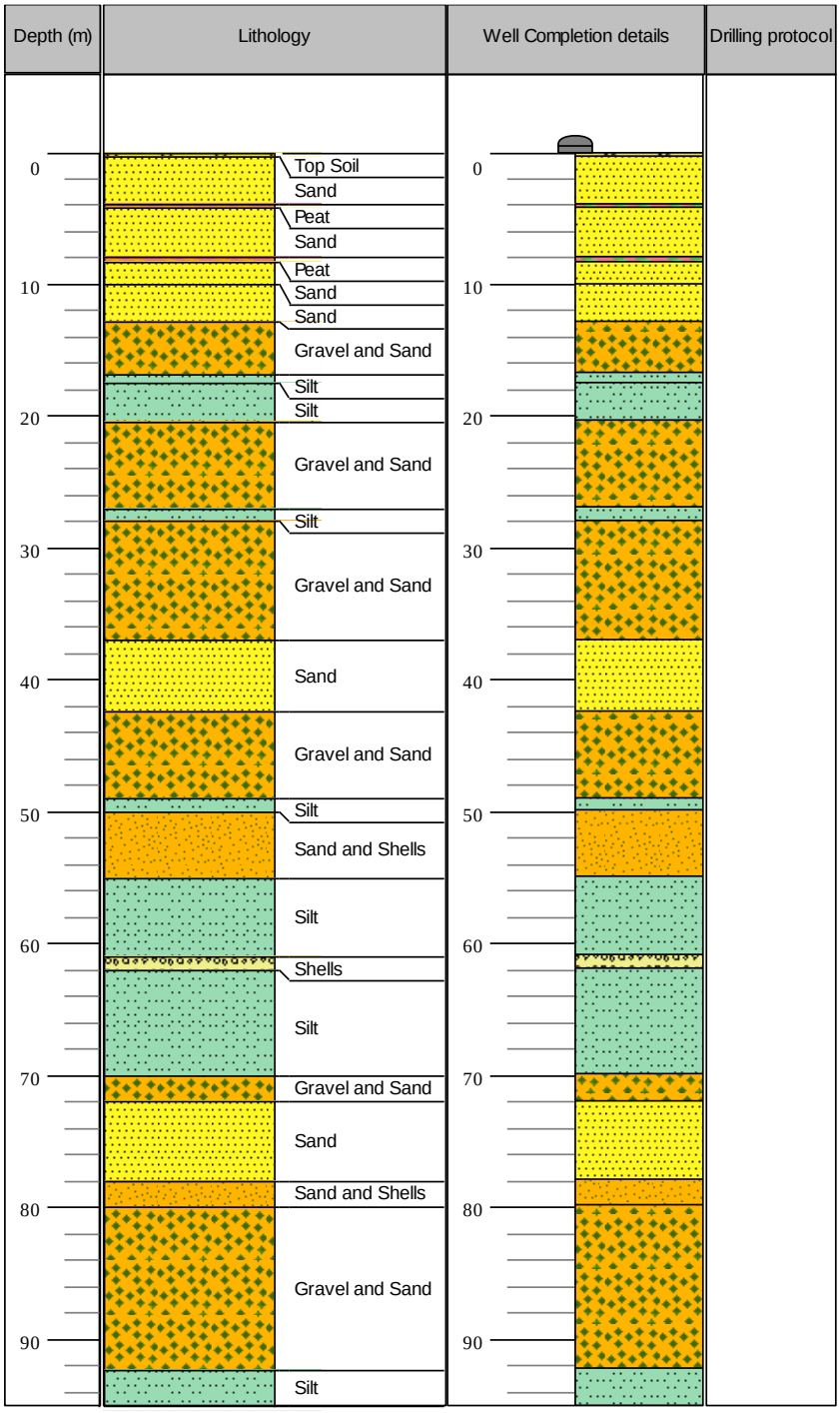
Depth (m)
Lithology
Well Completion details
Drilling protocol
0
10
20
30
40
50
60
70
80
90
Top Soil
Sand
Peat
Sand
Peat
Sand
Sand
Gravel and Sand
Silt
Silt
Gravel and Sand
Silt
Gravel and Sand
Sand
Gravel and Sand
Silt
Sand and Shells
Silt
Shells
Silt
Gravel and Sand
Sand
Sand and Shells
Gravel and Sand
Silt

312022

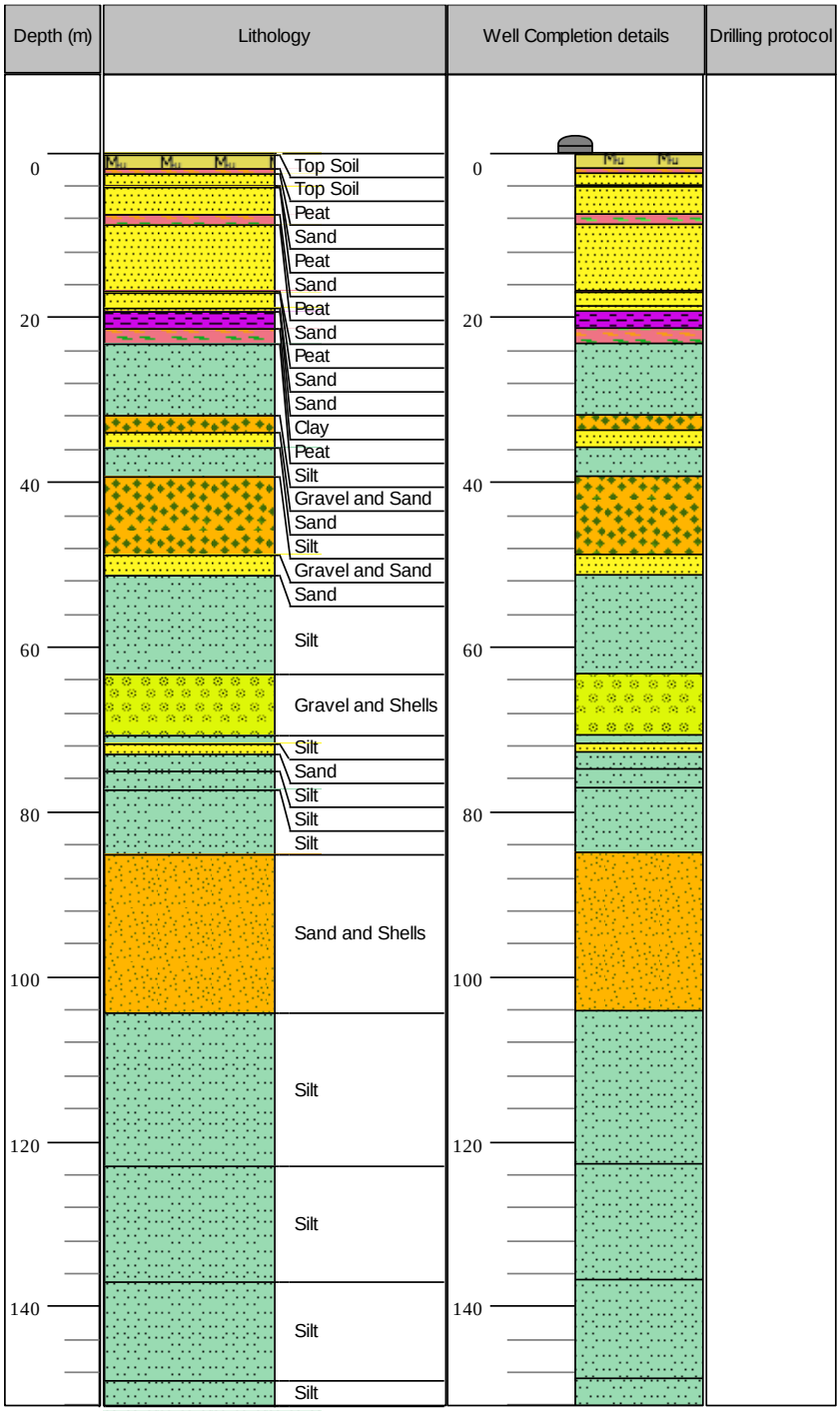
Depth (m)
Lithology
Well Completion details
Drilling protocol
0
20
40
60
80
100
120
140
Top Soil
Top Soil
Peat
Sand
Peat
Sand
Peat
Sand
Peat
Sand
Sand
Clay
Peat
Silt
Gravel and Sand
Sand
Silt
Gravel and Sand
Sand
Silt
Gravel and Shells
Silt
Sand
Silt
Silt
Silt
Sand and Shells
Silt
Silt
Silt

312024

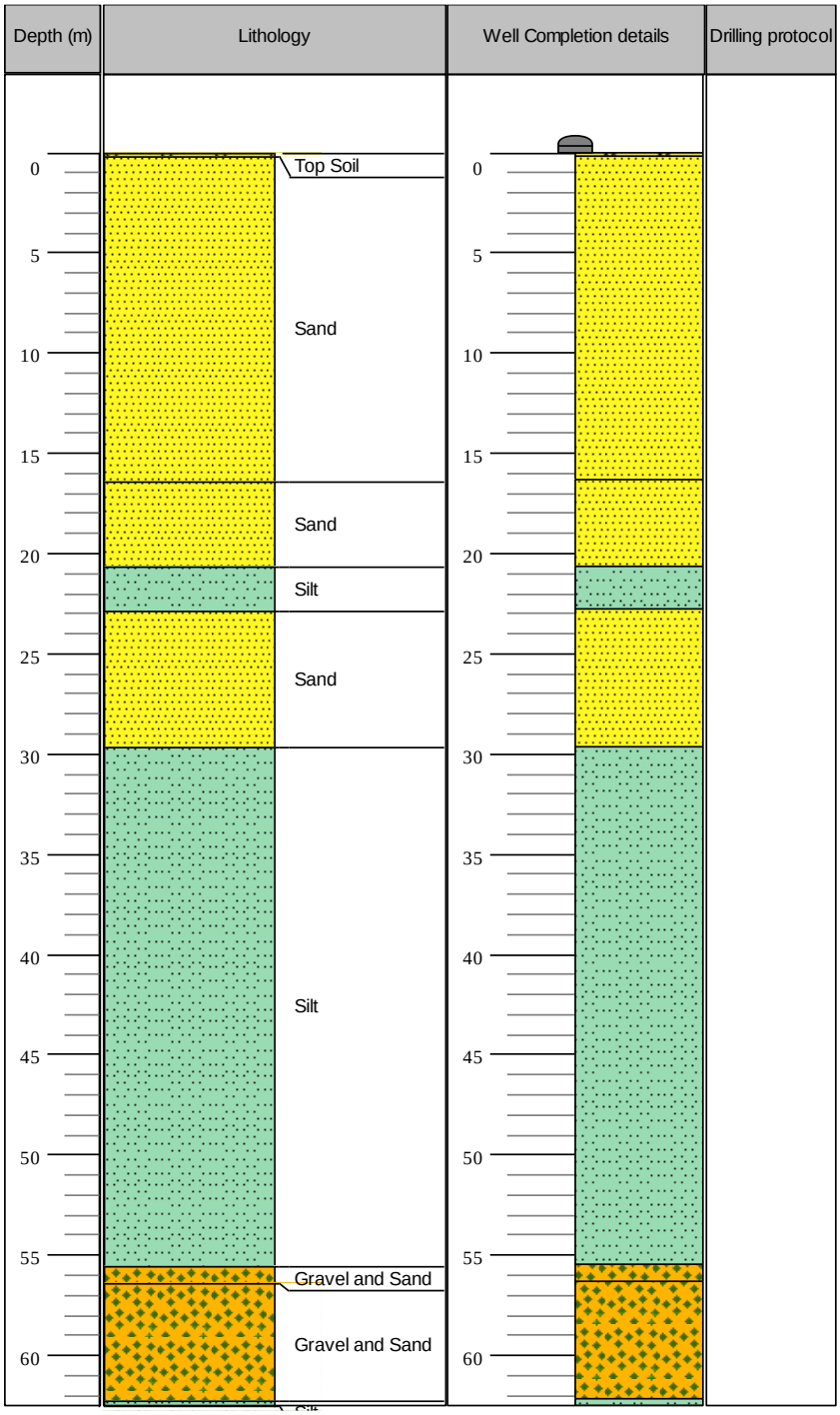
Depth (m)
Lithology
Well Completion details
Drilling protocol
0
5
10
15
20
25
30
35
40
45
50
55
60
Top Soil
Sand
Sand
Silt
Sand
Silt
Gravel and Sand
Gravel and Sand

312033

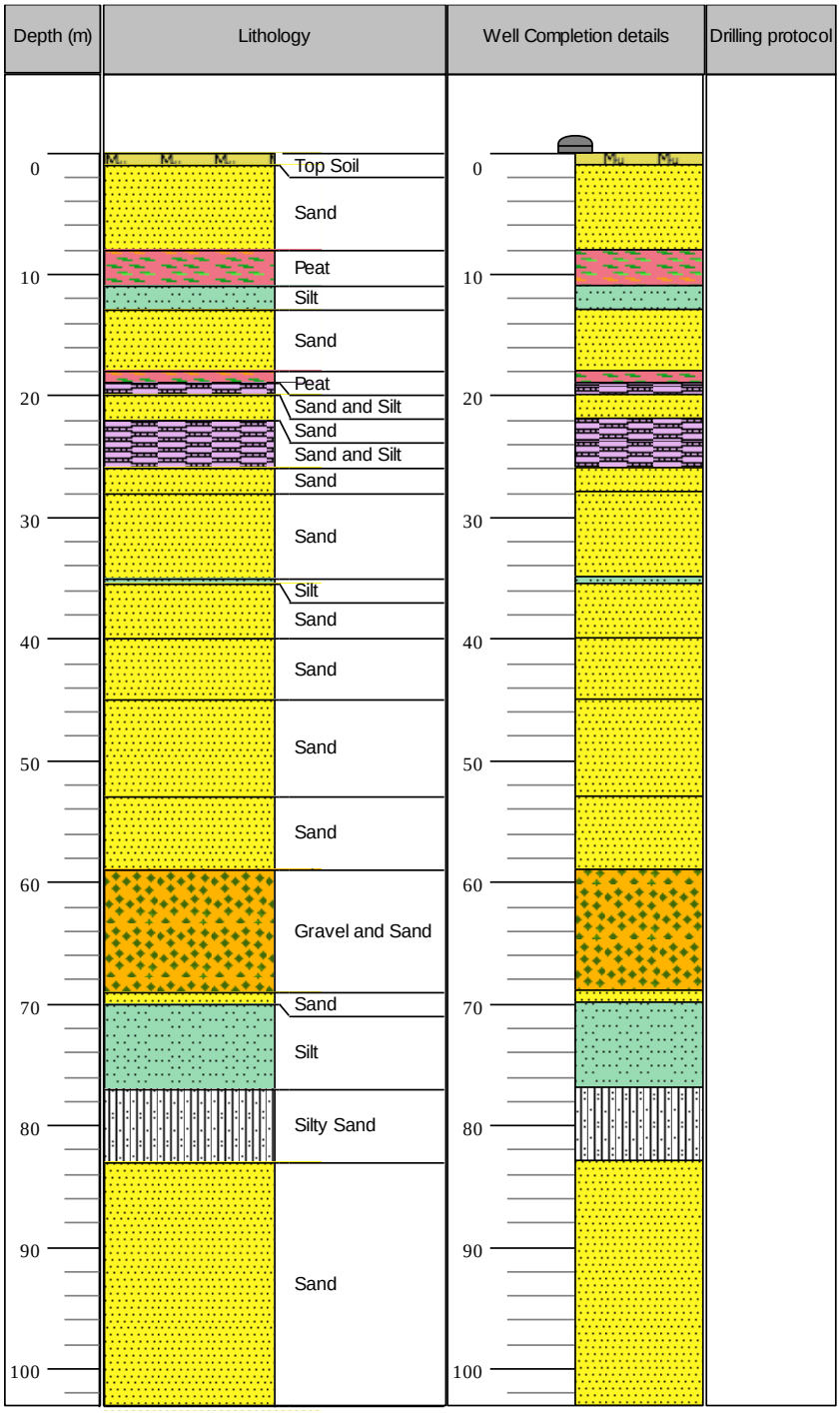
Depth (m)
Lithology
Well Completion details
Drilling protocol
0
10
20
30
40
50
60
70
80
90
100
Top Soil
Sand
Peat
Silt
Sand
Peat
Sand and Silt
Sand
Sand and Silt
Sand
Sand
Silt
Sand
Sand
Sand
Sand
Gravel and Sand
Sand
Silt
Silty Sand
Sand

312034

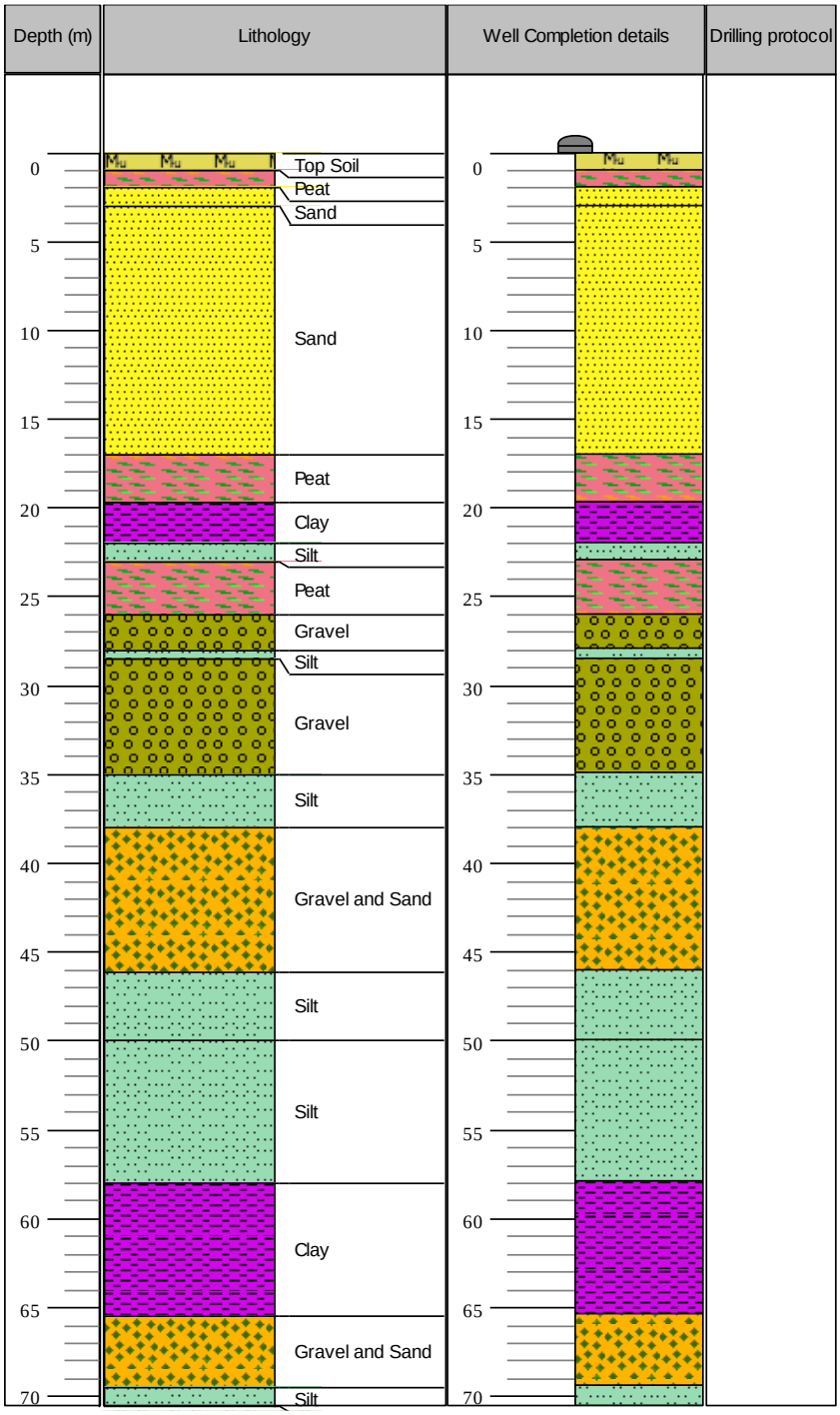
Depth (m)
Lithology
Well Completion details
Drilling protocol
0
5
10
15
20
25
30
35
40
45
50
55
60
65
70
Top Soil
Peat
Sand
Sand
Peat
Clay
Silt
Peat
Gravel
Silt
Gravel
Silt
Gravel and Sand
Silt
Silt
Clay
Gravel and Sand
Silt

313009

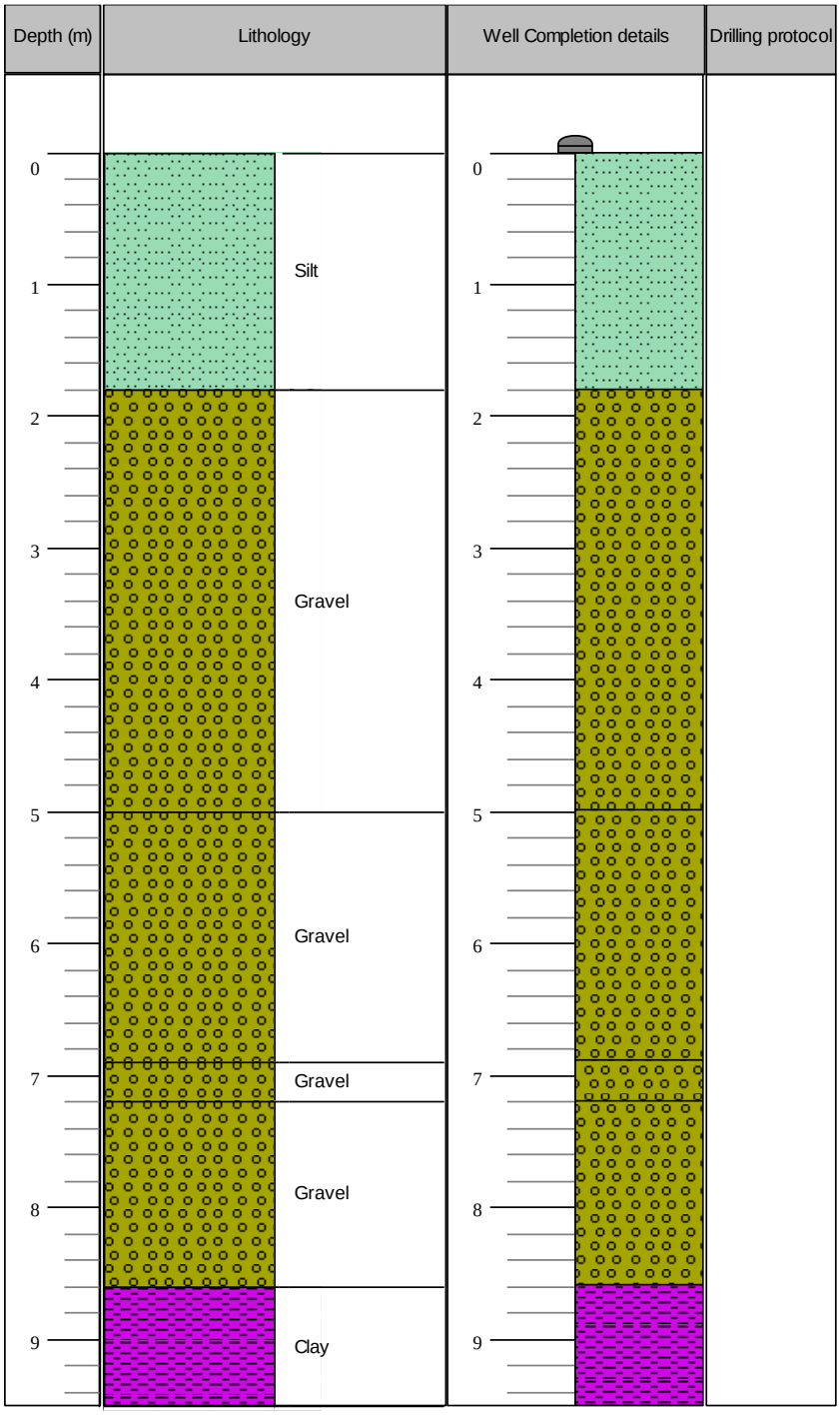
Depth (m)
Lithology
Well Completion details
Drilling protocol
0
1
2
3
4
5
6
7
8
9
Silt
Gravel
Gravel
Gravel
Gravel
Clay

313035

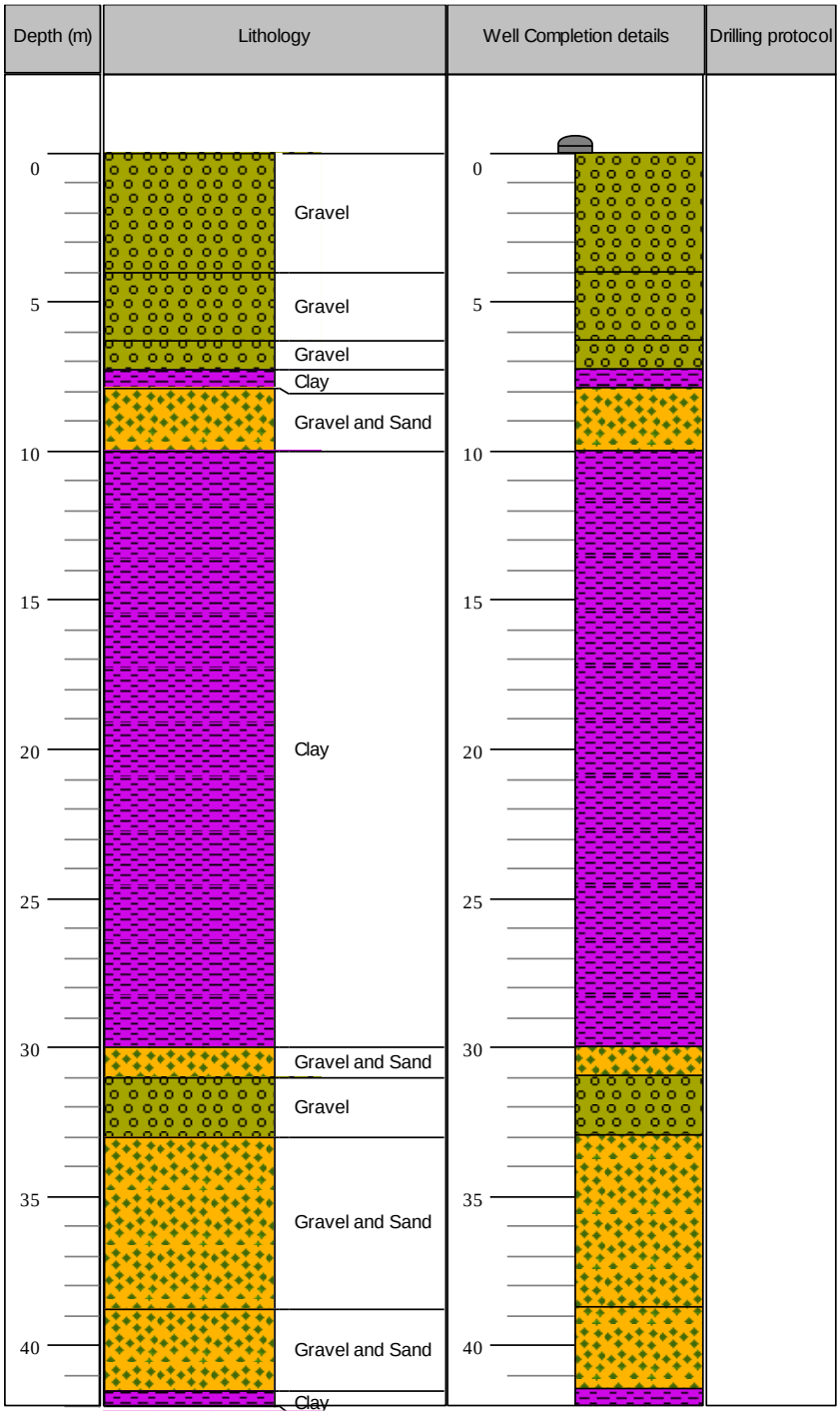
Depth (m)
Lithology
Well Completion details
Drilling protocol
0
5
10
15
20
25
30
35
40
Gravel
Gravel
Gravel
Clay
Gravel and Sand
Clay
Gravel and Sand
Gravel
Gravel and Sand
Gravel and Sand
Clay

313059

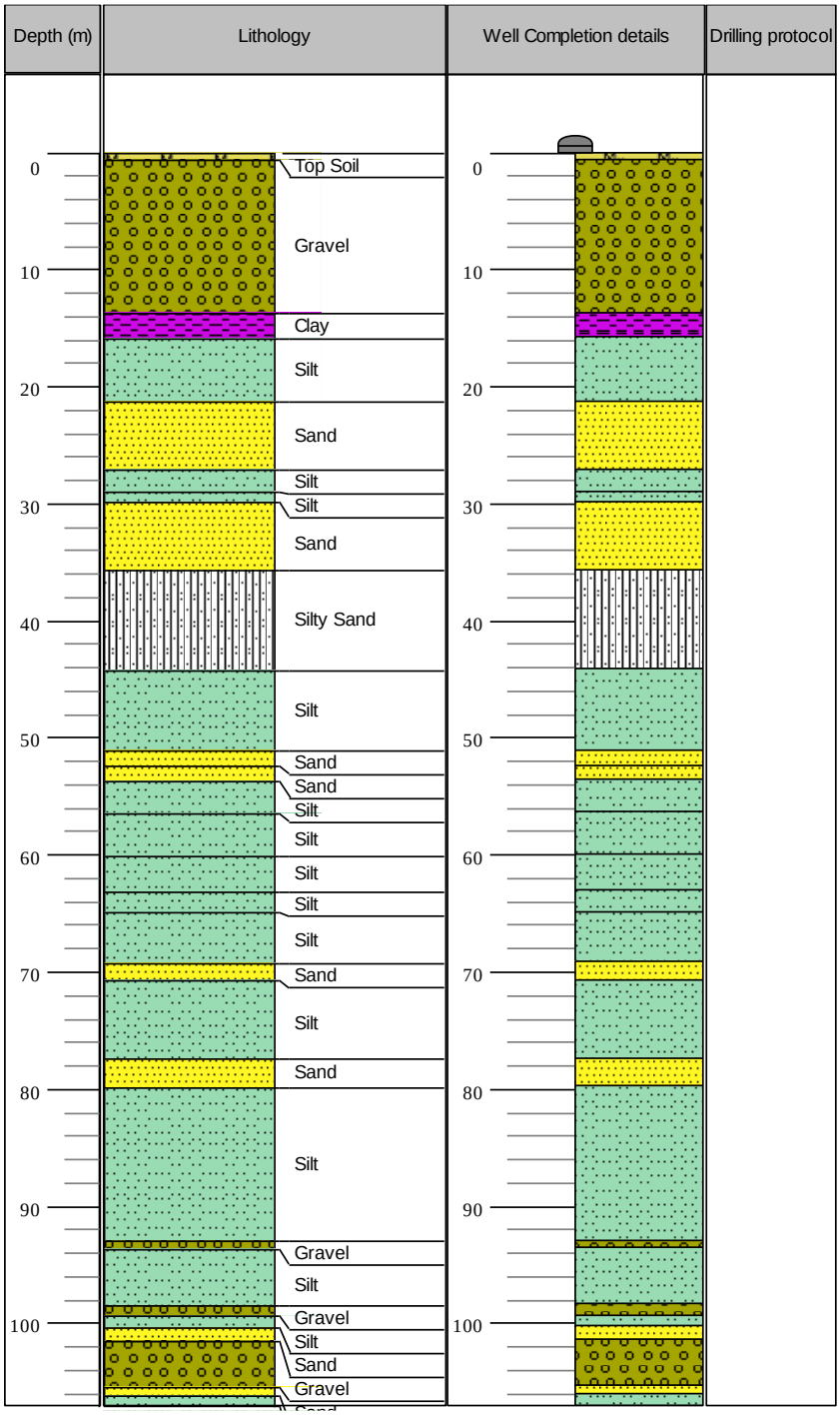
Depth (m)
Lithology
Well Completion details
Drilling protocol
0
10
20
30
40
50
60
70
80
90
100
Top Soil
Gravel
Clay
Silt
Sand
Silt
Silt
Sand
Silty Sand
Silt
Sand
Sand
Silt
Silt
Silt
Silt
Silt
Sand
Silt
Sand
Silt
Gravel
Silt
Gravel
Silt
Sand
Gravel

313087

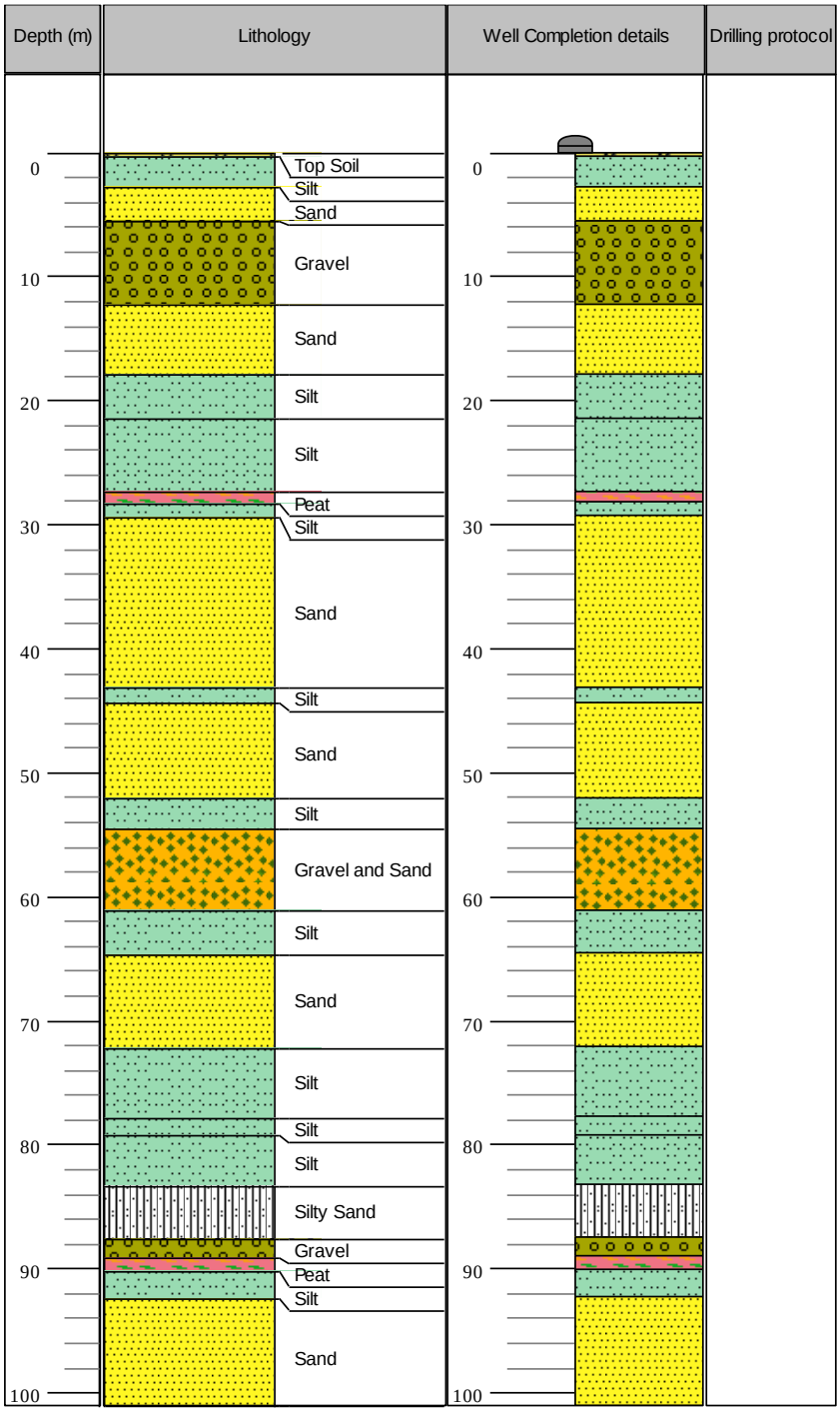
Depth (m)
Lithology
Well Completion details
Drilling protocol
0
10
20
30
40
50
60
70
80
90
100
Top Soil
Silt
Sand
Gravel
Sand
Silt
Silt
Peat
Silt
Sand
Silt
Sand
Silt
Gravel and Sand
Silt
Sand
Silt
Silt
Silt
Silty Sand
Gravel
Peat
Silt
Sand

322015

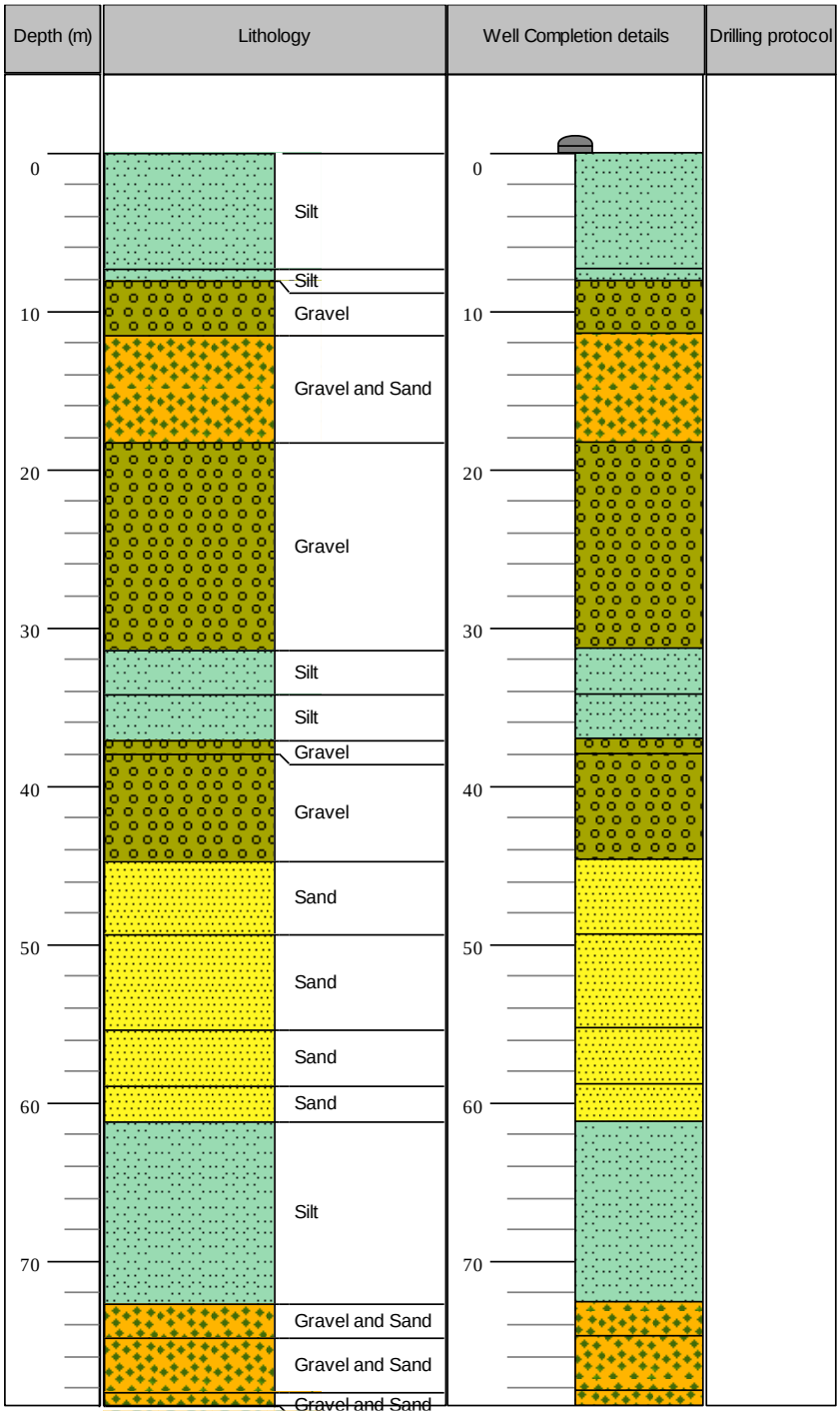
Depth (m)
Lithology
Well Completion details
Drilling protocol
0
10
20
30
40
50
60
70
Silt
Silt
Gravel
Gravel and Sand
Gravel
Silt
Silt
Gravel
Gravel
Sand
Sand
Sand
Sand
Silt
Gravel and Sand
Gravel and Sand
Gravel and Sand

322017

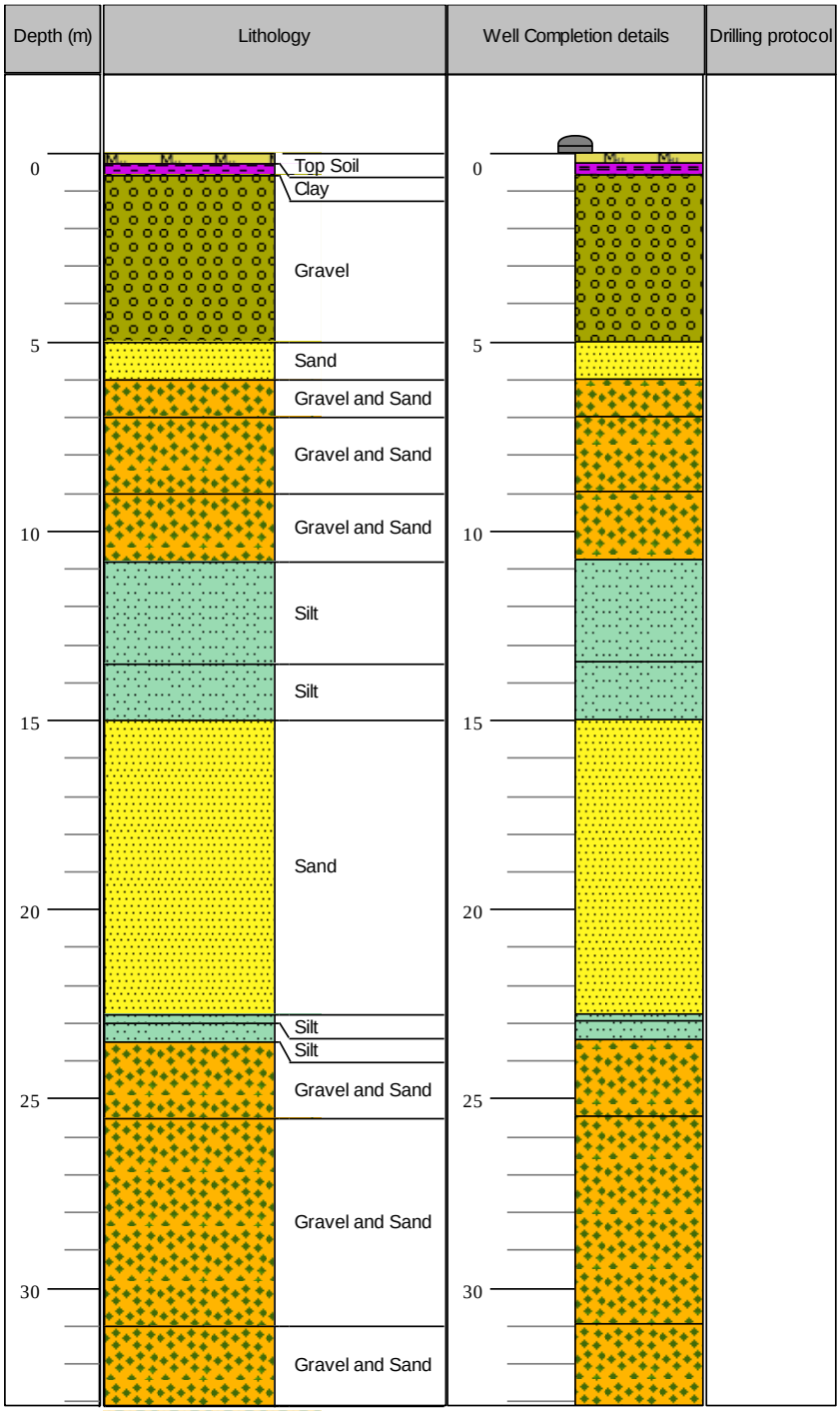
Depth (m)
Lithology
Well Completion details
Drilling protocol
0
5
10
15
20
25
30
Top Soil
Clay
Gravel
Sand
Gravel and Sand
Gravel and Sand
Gravel and Sand
Silt
Silt
Sand
Silt
Silt
Gravel and Sand
Gravel and Sand
Gravel and Sand

322023

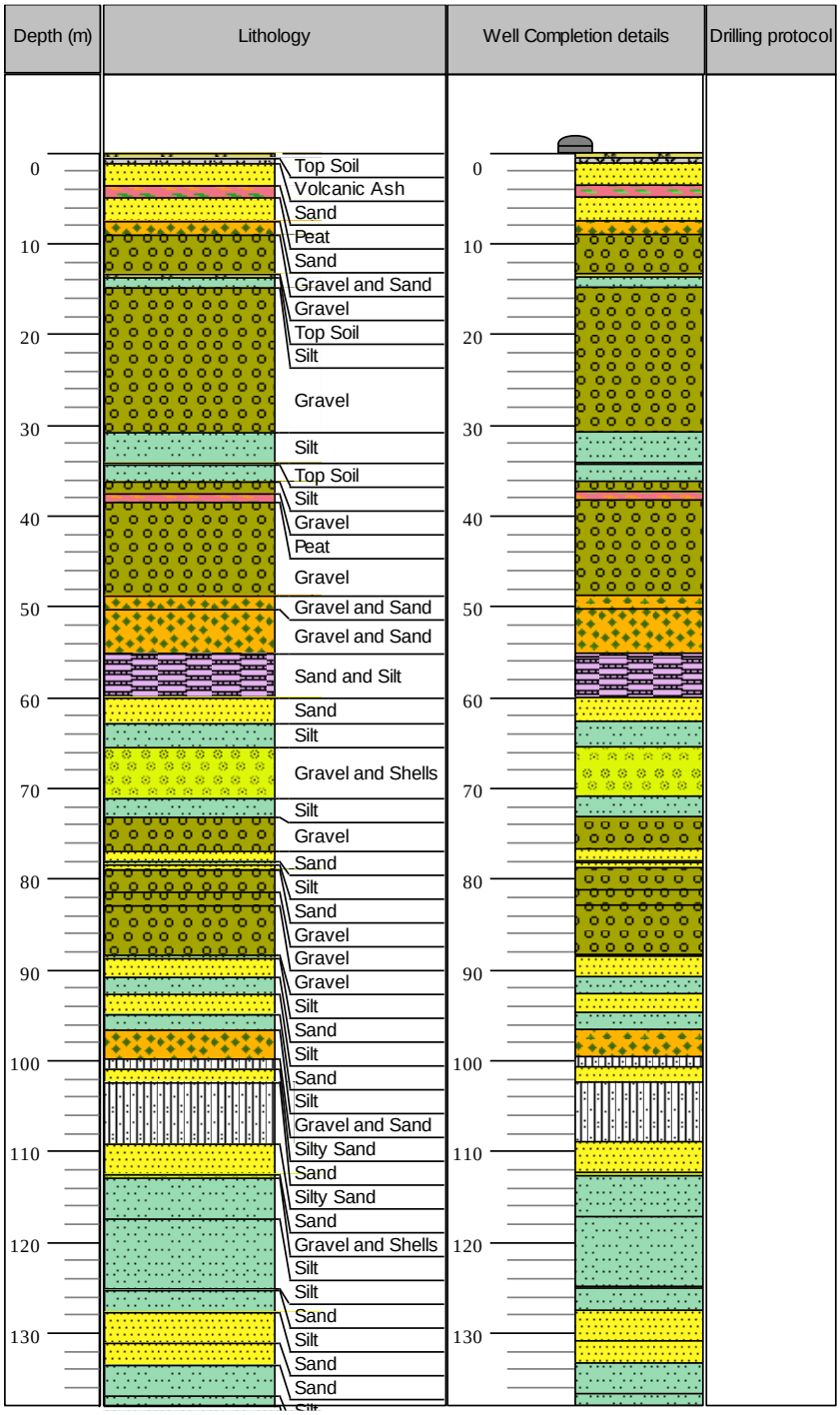
Depth (m)
Lithology
Well Completion details
Drilling protocol
0
10
20
30
40
50
60
70
80
90
100
110
120
130
Top Soil
Volcanic Ash
Sand
Peat
Sand
Gravel and Sand
Gravel
Top Soil
Silt
Gravel
Silt
Top Soil
Silt
Gravel
Peat
Gravel
Gravel and Sand
Gravel and Sand
Sand and Silt
Sand
Silt
Gravel and Shells
Silt
Gravel
Sand
Silt
Sand
Gravel
Gravel
Gravel
Silt
Sand
Silt
Sand
Silt
Gravel and Sand
Silty Sand
Sand
Silty Sand
Sand
Gravel and Shells
Silt
Silt
Sand
Silt
Sand
Sand

322041

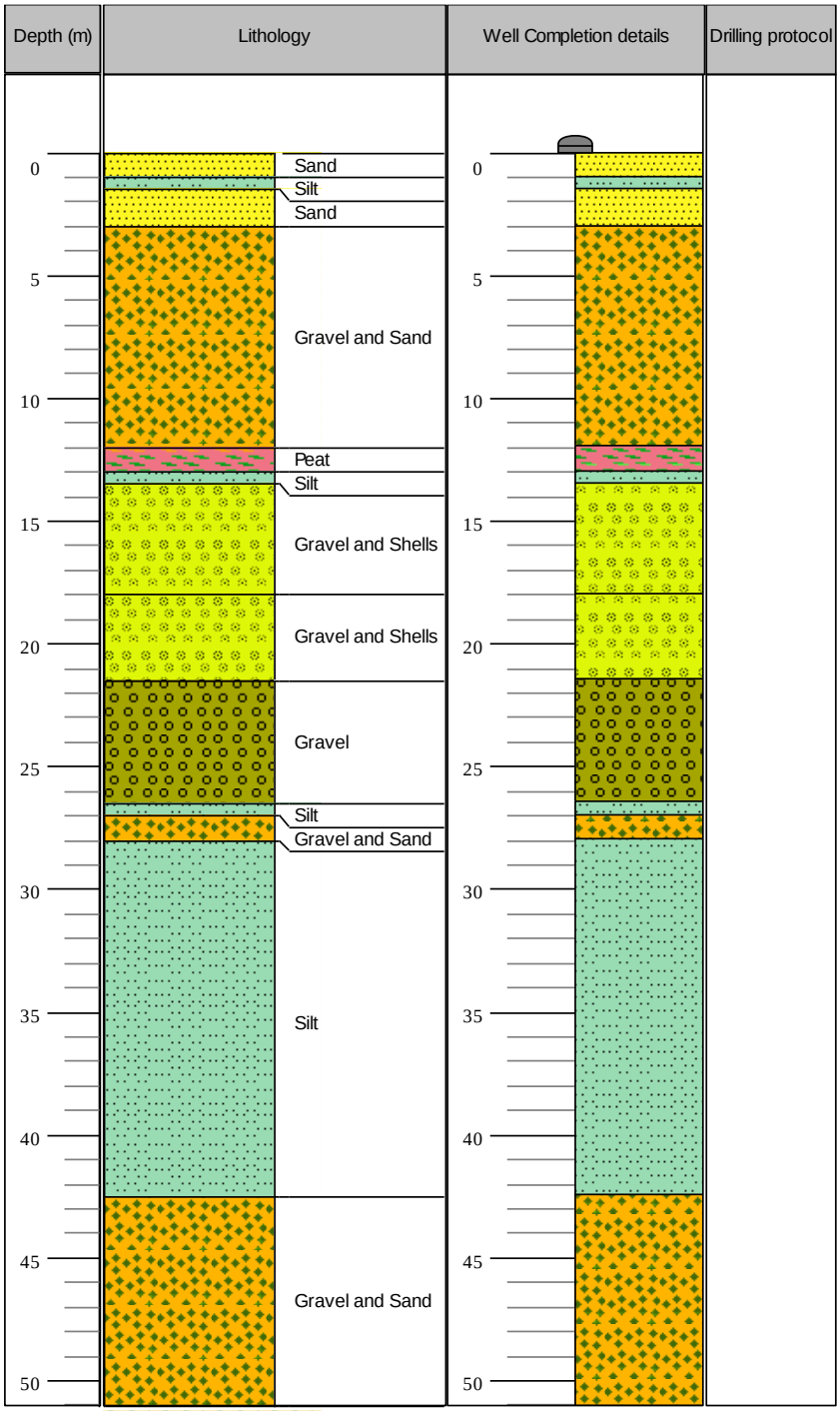
Depth (m)
Lithology
Well Completion details
Drilling protocol
0
5
10
15
20
25
30
35
40
45
50
Sand
Silt
Sand
Gravel and Sand
Peat
Silt
Gravel and Shells
Gravel and Shells
Gravel
Silt
Gravel and Sand
Silt
Gravel and Sand

322059

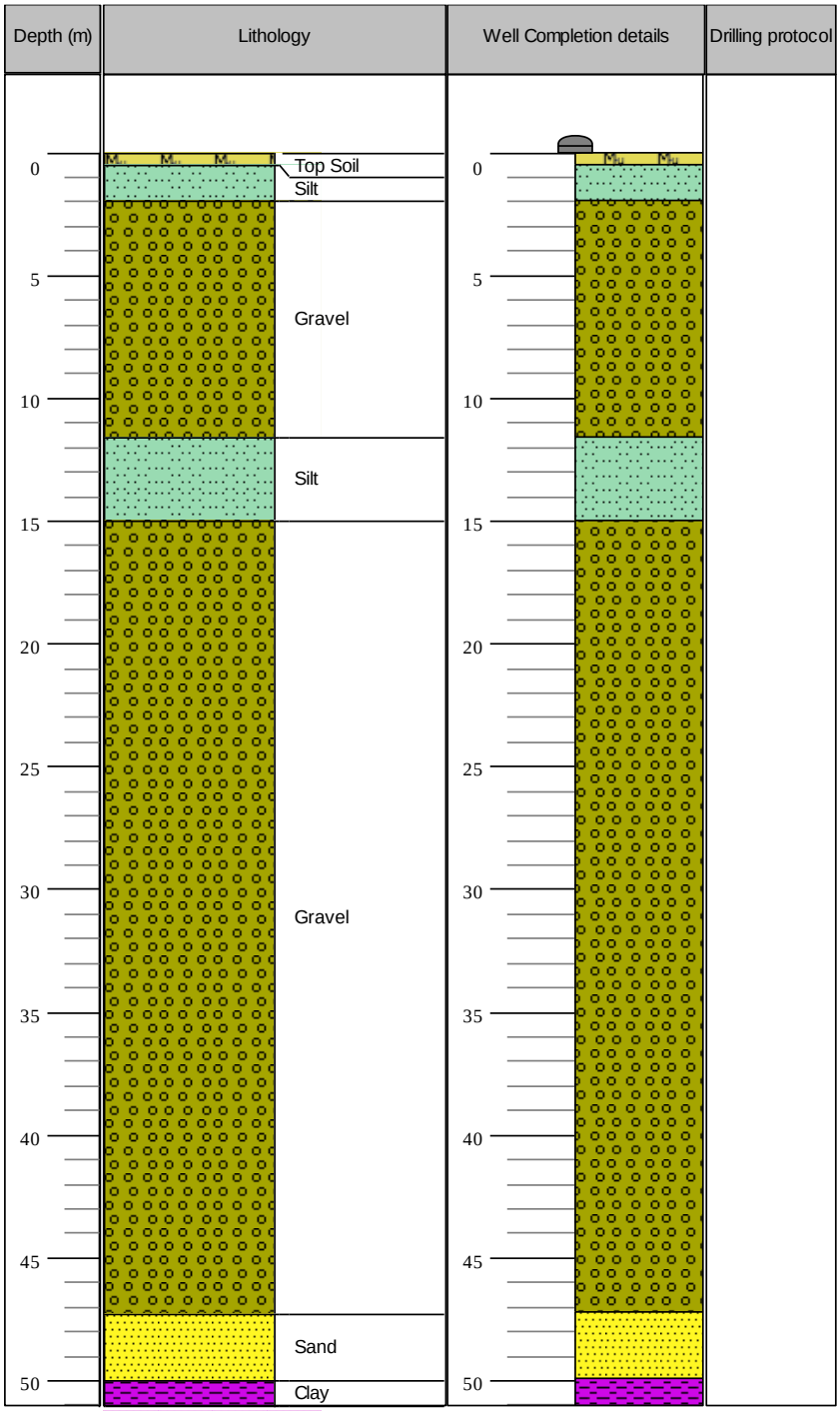
Depth (m)
Lithology
Well Completion details
Drilling protocol
0
5
10
15
20
25
30
35
40
45
50
Top Soil
Silt
Gravel
Silt
Gravel
Sand
Clay

323015

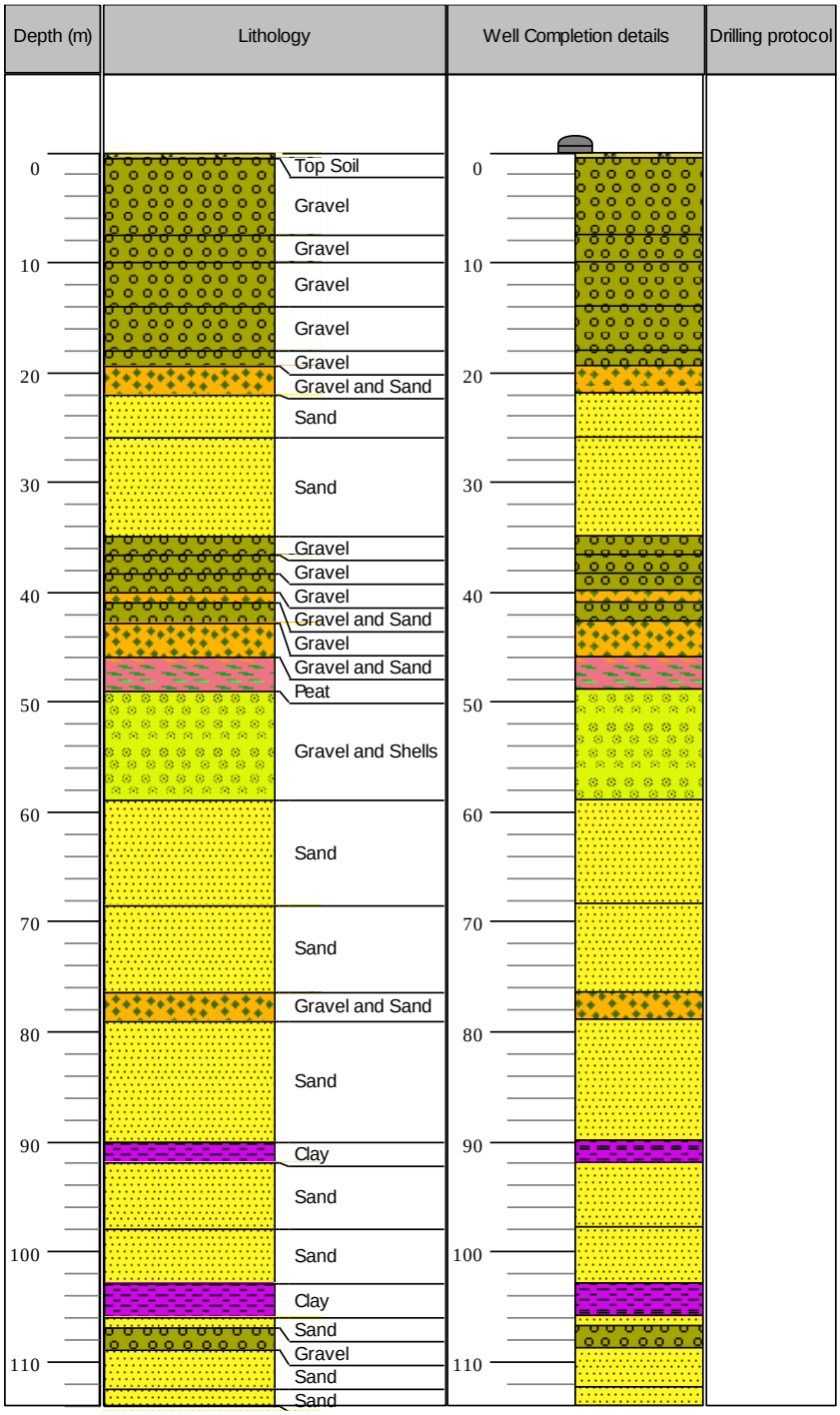
Depth (m)
Lithology
Well Completion details
Drilling protocol
0
10
20
30
40
50
60
70
80
90
100
110
Top Soil
Gravel
Gravel
Gravel
Gravel
Gravel
Gravel and Sand
Sand
Sand
Gravel
Gravel
Gravel
Gravel and Sand
Gravel
Gravel and Sand
Peat
Gravel and Shells
Sand
Sand
Gravel and Sand
Sand
Clay
Sand
Sand
Clay
Sand
Gravel
Sand
Sand

323067

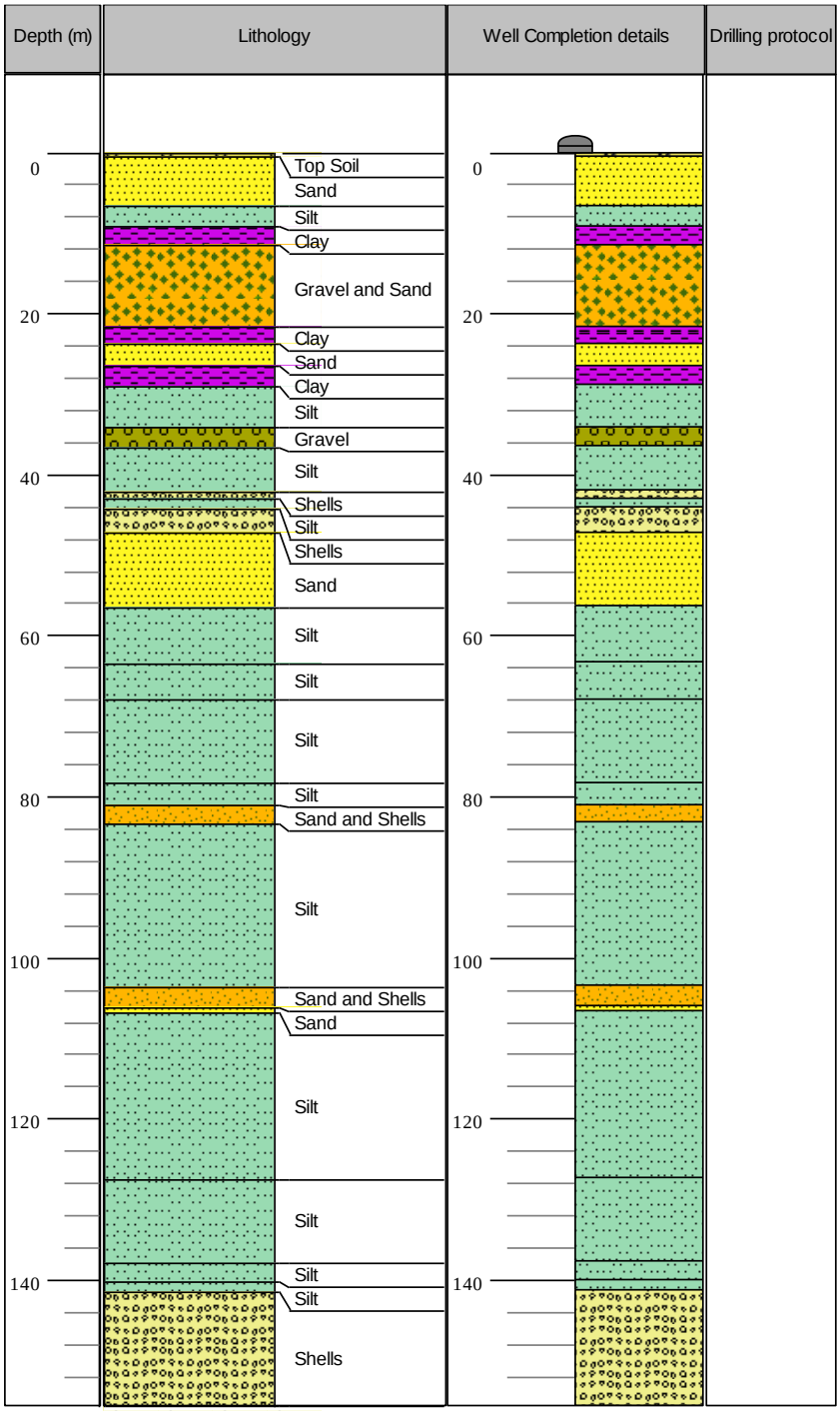
Depth (m)
Lithology
Well Completion details
Drilling protocol
0
20
40
60
80
100
120
140
Top Soil
Sand
Silt
Clay
Gravel and Sand
Clay
Sand
Clay
Silt
Gravel
Silt
Shells
Silt
Shells
Sand
Silt
Silt
Silt
Silt
Sand and Shells
Silt
Sand and Shells
Sand
Silt
Silt
Silt
Silt
Shells

323352

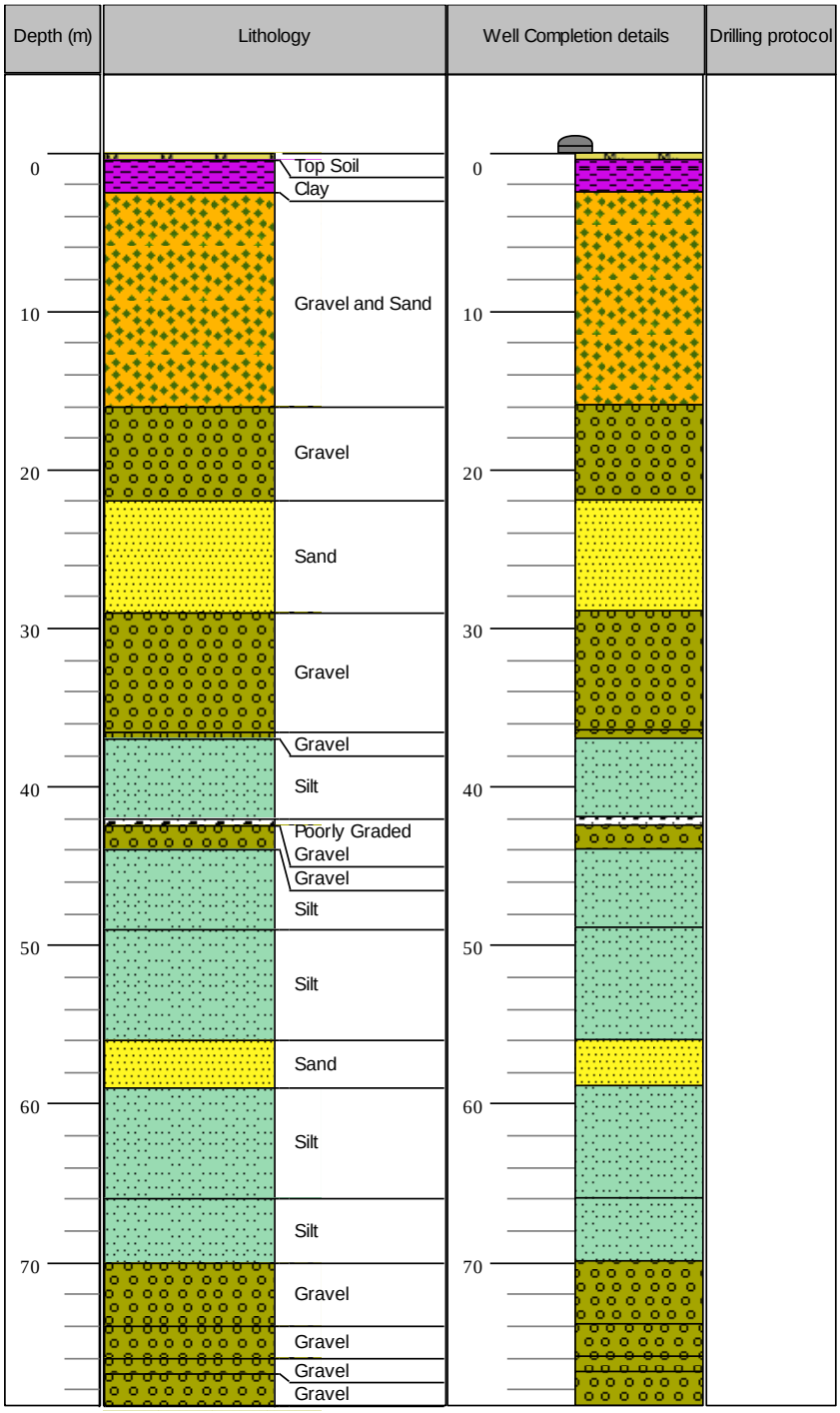
Depth (m)
Lithology
Well Completion details
Drilling protocol
0
10
20
30
40
50
60
70
Top Soil
Clay
Gravel and Sand
Gravel
Sand
Gravel
Gravel
Silt
Poorly Graded Gravel
Gravel
Silt
Silt
Sand
Silt
Silt
Gravel
Gravel
Gravel
Gravel

344213

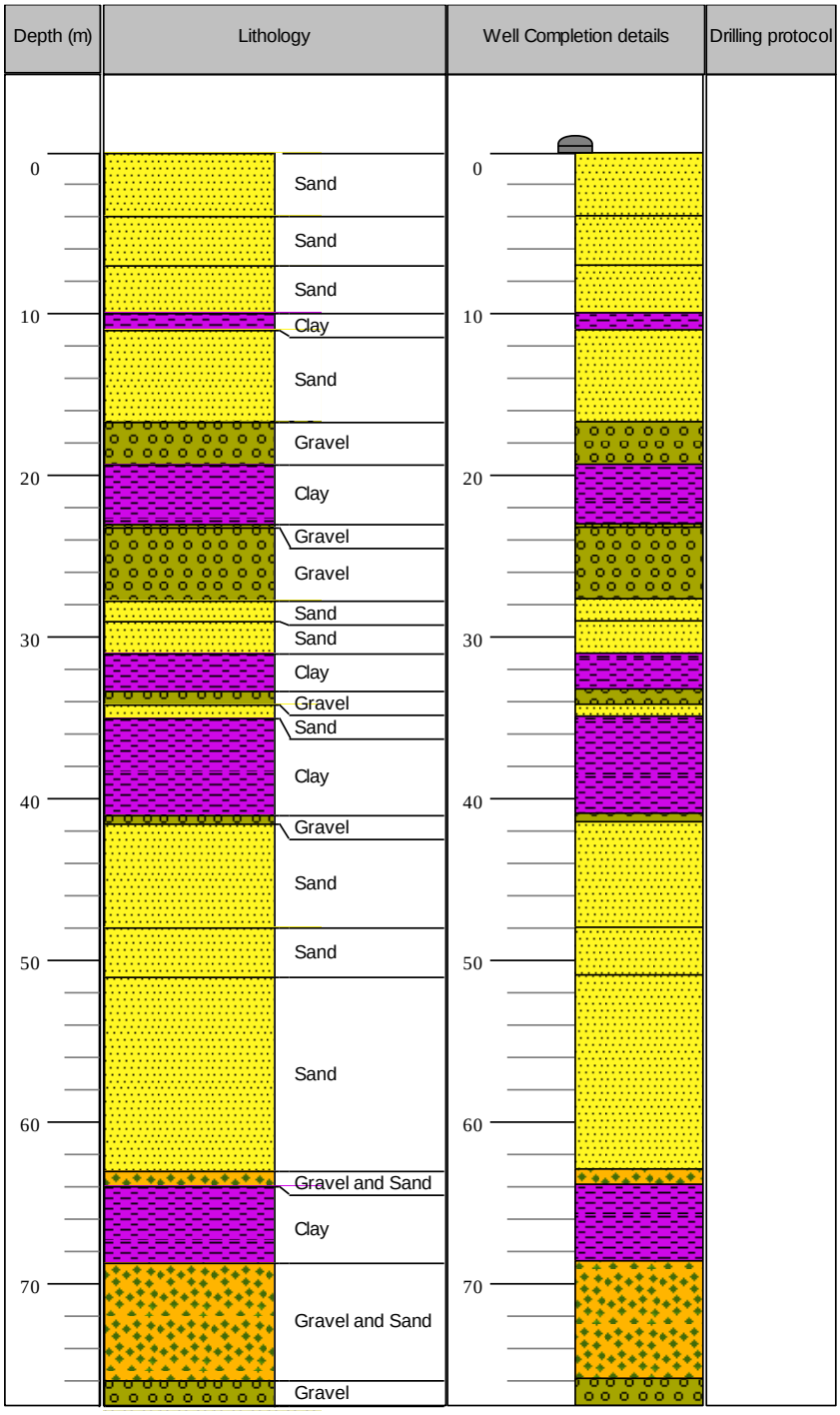
Depth (m)
Lithology
Well Completion details
Drilling protocol
0
10
20
30
40
50
60
70
Sand
Sand
Sand
Clay
Sand
Gravel
Clay
Gravel
Gravel
Sand
Sand
Clay
Gravel
Sand
Clay
Gravel
Sand
Sand
Sand
Gravel and Sand
Clay
Gravel and Sand
Gravel